Mechanisms of Extracellular Vesicle Cargo Delivery

Shaghayegh Askarian Amiri

THÈSE

Pour obtenir le grade de

DOCTEUR DE L'UNIVERSITÉ GRENOBLE ALPES

École doctorale : CSV- Chimie et Sciences du Vivant
Spécialité : Biologie Structurale et Nanobiologie
Unité de recherche : Institut de Biologie Structurale

Mécanismes de livraison de la cargaison des vésicules extracellulaires

Mechanisms of Extracellular Vesicle Cargo Delivery

Présentée par :

Shaghayegh ASKARIAN AMIRI

Direction de thèse :

Rémy SADOUL Prof des Universités, Université Grenoble Alpes	Directeur de thèse
Marie-odile FAUVARQUE Ingénieur-chercheur CEA, Université Grenoble Alpes	Co-directrice de thèse

Rapporteurs :

Pascal LEBLANC
CHARGE DE RECHERCHE HDR, CNRS délégation Rhône-Auvergne
Delphine MURIAUX
DIRECTRICE DE RECHERCHE, CNRS délégation Occitanie Est

Thèse soutenue publiquement le **6 octobre 2023**, devant le jury composé de :

Rémy SADOUL PROFESSEUR DES UNIVERSITES, Université Grenoble Alpes	Directeur de thèse
Pascal LEBLANC CHARGE DE RECHERCHE HDR, CNRS délégation Rhône-Auvergne	Rapporteur
Delphine MURIAUX DIRECTRICE DE RECHERCHE, CNRS délégation Occitanie Est	Rapporteure
Pascal DOURNAUD DIRECTEUR DE RECHERCHE, INSERM délégationParis Ile-de-France Centre Nord	Examinateur
Mireille ALBRIEUX PROFESSEUR DES UNIVERSITES, Université Grenoble Alpes	Présidente

Invités :

Marie-odile fauvarque
Grenoble Alpes University

Dedicated to my parents

Mina and Masoud

ACKNOWLEDGMENTS

First, I would like to thank all the members of the jury: Dr. **Pascal Leblanc**, Dr. **Dephine Muriaux**, Dr. **Sandrine Fraboulet**, Dr. **Pascal Dournaud**, and Prof. **Mireille Albrieux,** for agreeing to be part of my thesis committee. It is of great value to me that you have taken this time to evaluate my thesis.

I would like to express my sincerest gratitude to my thesis supervisor, Prof. **Rémy Sadoul,** for your confidence, empathy, and willingness to address my inquiries. I am grateful for the trust you placed in me by entrusting me with this remarkable project. I am deeply thankful for your kindness and generosity. You have been a source of support, especially during the challenging times of the Covid-19 lockdown. Your reassuring words, "whenever you need to discuss the project, I will be there" have provided me with the encouragement I needed throughout my journey. **Christine**, you are the symbol of kindness and grace. I am grateful for the valuable knowledge and practical techniques I have learned from you. Words cannot express my gratitude for your help and support, as you have been by my side, listening to my concerns throughout this journey. Thank you for everything.

I would also like to extend my thanks to my co-supervisor, Dr. **Marie-Odile Fauvarque,** your support in providing guidance, even in a more indirect manner, has played a significant role in shaping my research experience.

This thesis has been financed by the **GRAL** (Grenoble Alliance for integrated Structural and Cell Biology, **Labex GRAL and CBH-EUR-GS (ANR-17-EURE-0003)**). I would like to express my sincere gratitude to the GRAL manager, **Anne-Mathilde Thierry**, for her exceptional kindness and support from the very beginning. Thank you for always listening to me and helped me with any challenges, even when they fell outside your responsibilities. You are the one I will greatly miss. I would like to express my heartfelt gratitude to Dr. **Winfried Weissenhorn** for fostering a positive and scientific atmosphere within the group. Your wisdom and guidance have been invaluable in creating a scientific and friendly environment.

To all the members of the EBEV group, **Delphine**, thank you for your help and willingness to assist with any issues I faced in the lab. I greatly admire your motivation and dedication throughout the experiment. Your energy as you walk and run in the lab are truly inspiring. **Nolwenn**, your understanding of the stress I experienced during the past year meant the world to me. I am deeply grateful for your presence in the lab for me, even when you were not feeling well. **Cécile**, thank you for your insightful questions during lab meetings, which have enriched my thinking about the project, and thank you for your kindness and hospitality. **Kimi** and **Guidenn**, my heartfelt thanks to both of you for generously sharing your experiences with me. I truly cherish the memories of our lunches together, walking through the campus, and engaging in conversations. Thank you for your companionship and the meaningful connections we have formed. **Haiyan,** my dear lunch buddy, having you by my side during these years has been a true blessing. Our conversations have been a way for me to release my stress. I cannot imagine how challenging it would have been without your presence. Thank you for being there for me,

and I am grateful to have you as a dear friend. And you **Borys**, you already know how much you have teased me, don't you? Your load laugh and sneezes, frequent coffee break… oh my goodness! I cannot believe I will miss them soon. Thank you, my hardworking friend, for bringing such incredible energy to our office. **Hamida,** you have been like a supportive sister to me. Thank you for all your guidance and encouragement you have provided throughout our journey together.

This would not have been possible without my friends! My Grenoble family, **Azin, Ali, Mojan and Davoud,** the fun and laughter we shared really helped me get through this. You should know that your support and encouragement was worth more than I can express here.

I would like to give a special thanks to my dear aunt **Roya** and her husband **Reza** for your support and care when we arrived in France during the lockdown. You went above and beyond, taking care of us and providing the love and support of a mother. I am forever grateful for your kindness and the assistance which has been instrumental in bringing me to where I am today. And my cousins **Mehdi** and **Houman**, my childhood playmates. Since our arrival in France, your support, particularly in overcoming language barriers, has been invaluable. And Mehdi thank you for your invaluable help in finalizing my thesis manuscript.

And the most important people in my life, **my parents,** I would like to dedicate this thesis to my parents. Thank you, Maman and Baba. I owe everything I have achieved to you. Your endless support, invaluable guidance, sacrifices and love have brought me to where I am today. Thank you for allowing me to pursue my dreams. And you **Niloufar**, the kindest sister in the world, you taught me so much since we were children. I have learned how to be strong and patient like you. And your two little "eshghe khale (عشق خاله)", **Hirad** and **Rayan**, for their energy. They are my biggest reason of homesickness after moving to France.

I would also like to extend a heartfelt thanks to my **grandparents**, with whom I have lived since the age of 18 until my move to France. Their presence in my life has been an immense blessing, and I am grateful for their constant prayers and well-wishes. I am forever indebted to them for their guidance and care.

I would like to express my deepest gratitude to my second family, my parents-in-law, **Maman Anna and Baba Javad,** I hold them in the same regard and love as my own parents. Thank you both for your immense kindness, unwavering support, and guidance. I am incredibly fortunate and overjoyed to be your "deter deter". **Nima and Pouya,** I owe a profound debt of gratitude to both of you for my journey to France. From the moment I began searching for a Ph.D. position until this very day, your support and assistance have been unwavering. I am incredibly fortunate to have you both as brothers in my life.

I would like to extend my final thanks to the person without whom I would not be the person I am today. **Mani**, thank you for always being there for me through the ups and downs of this challenging journey. I am grateful for the life we have built together. Our partnership, shared dreams, the countless moments we have had together, both in times of difficulty and joy… I am fortunate to have you by my side. You know I would never have embarked on this journey without you by my side…

Table of Contents

Table of Figures

Table of Tables

List of Abbreviations

AIP1	Apoptosis Interacting Protein 1
ALG-2	Apoptosis-Linked Gene 2
Alix	Alg-2 interacting protein X
ARMMs	ARRDC1-Mediated Microvesicles
ARRDC1	ARRestin Domain-Containing protein 1
CEP55	CEntrosomal Protein 55
CHMP	CHarged Multi-vesicular body Protein
Chol	Cholestrol
CIE	Clathrin-Independent Endocytosis
CIN85	Cbl-iNteracting protein of 85 kDa
dMVB	degradative MVB
DNA	DeoxyriboNucleic Acid
ECM	ExtraCellular Matrix
EE	Early Endosome
EGFR	Epidermal Growth Factor Receptor
ESCRT	Endosomal Sorting Complex Required for Transport
EVs	Extracellular Vesicles
FAK	Focal Adhesion Kinase
GAGs	GlycosAminoGlycan chains
gDNA	guide DNA
GUVs	Giant Unilamellar Vesicles
HiBit	Highe affinity NanoBit
HRS	Hepatocyte growth factor Regulated tyrosine kinase Substrate
Hsp	Heat shock protein
HSPGs	Heparan Sulfate ProteoGlycans
ILV	IntraLuminal Vesicle
KO	KnockOut
LBPA	LysoBiPhosphatidic Acid
LE	Late Endosome
LgBit	Large NanoBit
lncRNA	long non-coding RNA
MHC	Major Histocompatibility Complex
miRNA	microRNA
mRNA	messenger RNA
MSC	Mesenchymal Stem Cell
MVB	MultiVesicular Body
nSMase2	Neutral SphingoMyelinase 2

PA	PhosphatidicAcid
PC	PhosphatidylCholine
PE	PhosphatidylEthanolamine
PGs	Proteoglycans
PI	PhosphatidylInositol
PI3K	PhosphatidylInositol 3-Kinase
PK	Proteinase K
PLP	ProteoLipid Protein
PRD	Proline Rich Domain
PS	PhosphatidylSerine
PTGFRN	ProsTaGandin F2 Receptor iNhibitor
RBP	RNA-Binding Protein
SH3	Src Homology type 3
SM	SphingoMyelin
sMVB	secretory MVB
snRNA	small nuclear RNA
TM4SF	TransMembrane 4 SuperFamily
TNF	Tumor Necrosis Factor
TSG101	Tumor Susceptibility Gene 101
TSPN6	Tetraspanin-6
Vps4	Vacuolar Protein Sorting 4
VSV	Vesicular Stomatitis Virus
WT	Wild-Type

Abstract

Extracellular vesicles (EVs) are recognized to play an important role in physiological and pathological intercellular communication processes. EVs carry lipids, proteins, and microRNAs, which can be shuttled between cells, thereby allowing intercellular communications. The transfer of biologically active EVs cargoes into receiving cells begins with endocytosis of the EVs, which are thought to fuse with the endosomal membrane. This is analogous to the content delivery of some enveloped viruses, which requires their fusion with the endosomal membrane in a way dependent on acidic pH and the protein Alix.

The aim of our work is to characterize the molecular mechanisms driving the fusion of EVs with target membranes of cells or liposomes. For this, we used luciferase complementation assay to follow the fusion of EVs to membranes of receiving cells and fluorescence membrane-mixing assay to quantify EV membrane fusion to liposomes. We also intend to test if alike viruses, Alix is required for fusion of EVs with endosomal membranes.

For this, we used recipient cells expressing LgBit, an inactive subunit of nanoluciferase that activates upon binding to a small peptide, HiBit was fused to the EV cargo proteins and luminescence should only be emitted once HiBit is delivered to the cytoplasm of LgBit recipient cells. We could demonstrate the interaction of HiBit-containing EVs with LgBit-receiving cells but no increase in luminescence, suggesting that no fusion occurs. While in the presence of VSV-G protein, luminescence was enhanced, showing that our method is capable of detecting fusion of EVs to membranes of receiving cells. Importantly, the presence of Alix in recipient cells did not seem to be crucial for this fusion, as it also occurred in Alix ko cells.

However, using fluorescence membrane-mixing assay, our results demonstrated the fusion of stained EVs with unlabeled liposomes in the presence of recombinant Alix at low pH, simulating the acidic conditions found in endosomes.

Finally, we examined how Alix is associated with EVs, as the protein had been reported to be both cytosolic and extracellular suggesting that it can cross membranes. In summary, my thesis work tends to show that EV have the capacity to fuse with membrane in an Alix-dependent process in vitro. However, we were unable to establish the role of Alix in EV fusion with endosomal membrane in vivo.

Résumé

Les vésicules extracellulaires (VE) sont reconnues pour jouer un rôle important dans les processus de communication intercellulaire physiologiques et pathologiques. Les VE transportent des lipides, des protéines et des microARN, qui peuvent être transférés entre les cellules, permettant ainsi les communications intercellulaires. Le transfert de cargaisons de VE biologiquement actives dans les cellules réceptrices commence par l'endocytose des VE, qui fusionneraient avec la membrane endosomale. Ceci est analogue au transfert de contenu de certains virus enveloppés qui nécessite leur fusion avec la membrane endosomale d'une manière qui dépend du pH acide et de la protéine Alix.

Le but de notre travail est de caractériser les mécanismes moléculaires à l'origine de la fusion des VE avec les membranes cibles des cellules ou des liposomes. Pour ce faire, nous avons utilisé le test de complémentation de la luciférase pour suivre la fusion des VE avec les membranes des cellules réceptrices ainsi que des tests de transfert de fluorescence pour quantifier la fusion des membranes des VE avec les liposomes. Nous avons testé si, à l'instar des virus, Alix est nécessaire à la fusion des VE avec les membranes endosomales.

Pour ce faire, nous avons utilisé des cellules réceptrices exprimant LgBit, une sous-unité inactive de la nanoluciférase qui s'active en se liant à un petit peptide appelé HiBit. HiBit a été fusionné aux protéines cargo des EV et la luminescence mesurée qui ne devrait être émise qu'une fois HiBit délivré dans le cytoplasme des cellules réceptrices de LgBit. Nous avons pu démontrer l'interaction des EVs contenant HiBit avec les cellules réceptrices de LgBit mais aucune augmentation de la luminescence suggérant la fusion. En revanche, en présence de la protéine de fusion VSV-G, la luminescence a augmenté, ce qui montre que notre méthode est capable de détecter la fusion des EV avec les membranes des cellules réceptrices. Il est important de noter que la présence d'Alix dans les cellules réceptrices ne semble pas être cruciale pour cette fusion, puisqu'elle se produit également dans les cellules Alix ko. Cependant, en utilisant un essai in vitro nous avons démontré la fusion d'EVs avec des liposomes en présence d'Alix recombinant à faible pH, simulant les conditions acides retrouvées dans les endosomes. Enfin, nous avons examiné comment Alix est associé aux EVs, car la protéine a été signalée comme étant à la fois cytosolique et extracellulaire, ce qui suggère qu'elle peut traverser les membranes. En résumé, mon travail de thèse tend à montrer qu'in vitro les EV ont la capacité de fusionner avec la membrane dans un processus dépendant d'Alix. Cependant, nous n'avons pas pu établir le rôle d'Alix dans la fusion des EV avec la membrane endosomale in vivo.

Chapter 1 INTRODUCTION

1.1 Extracellular vesicles

Intercellular communication is essential for the development of multicellular organisms to maintain homeostasis (B. H. Sung, Parent, & Weaver, 2021). This process relies on the release of chemical mediators such as bioactive proteins and lipids into the extracellular space. These mediators bind to receptors on other cells and change their physiology through signalization cascades (Peinado et al., 2012; Valadi et al., 2007).

As well as chemical mediators, cells can also use membrane extracellular vesicles (EVs) for intercellular communication. EVs are vesicles that contain multiple biologically active cargo components, such as lipids, proteins, and microRNAs (miRNAs), and can be secreted by cells. When released, EVs can be taken up by recipient cells, transferring their cargo and thereby modifying the physiology of the recipient cells (Dolcetti et al., 2020; Raposo & Stoorvogel, 2013; Xie et al., 2019).

EVs have been used as diagnostic markers since it has been shown that they carry disease-specific markers (Melo et al., 2015; Simpson, Lim, Moritz, & Mathivanan, 2009). For example, EVs derived from cancer cells contain tumor-specific molecules, including proteins and RNAs, which hold great potential as biomarkers for evaluating tumor malignancy (Hosseini et al., 2017). Thus, exploring the role of EVs in intercellular communication within cancer cells provides an innovative approach to cancer detection (Urabe et al., 2020).

Over the course of decades, EVs were first discovered as small vesicles secreted from reticulocytes (Harding, Heuser, & Stahl, 1983; Johnstone, Adam, Hammond, Orr, & Turbide, 1987). It was first considered that cells use these vesicles to discard unnecessary molecules as a “garbage can” (Kawamoto et al., 2012). However, in 1996, Raposo et al., revealed another aspect of EV’s function by showing the impact of immune cell derived EVs on the immune system (Raposo et al., 1996). A few years later, subsequent studies showed that EVs carry microRNAs (miRNAs) and mRNAs which can be delivered to recipient cells and may exert functional effects (Kosaka et al., 2010; Valadi et al., 2007). These studies have turned many researchers’ attention to investigating the role of EVs further.

Extracellular vesicles are heterogeneous by nature, encompassing distinct populations that vary not only by their size but also by their origins and characteristics. EVs are generally classified into three main categories (Deb, Gupta, & Mazumder, 2021; Xie et al., 2019): (1) Apoptotic bodies (>1000 nm), which are released through blebbing by cells during apoptosis. (2) microvesicles (100 to 1000nm), released via budding from the plasma membranes; and (3) exosomes (50 to 150 nm) derived from endosomal compartments and released into the extracellular space upon fusion with the plasma membrane (Chivet, Hemming, Pernet-Gallay, Fraboulet, & Sadoul, 2012; Elmore, 2007; Pegtel & Gould, 2019; S, Mäger, Breakefield, &

Wood, 2013). It is important to note that, the role of EVs is different from that of apoptotic bodies, as they are released mostly from healthy cells. Various methods are currently available for characterizing EVs such as, 1) western blot, to detect specific components within EVs, like endosomal protein CD63, which are indicative of exosomes, or proteins expressed in cell membranes like CD9 or CD81 in the case of ectosomes, 2) Nanoparticle tracking analysis, to classify EVs based on their size distribution and number, 3) Electron microscopy and flow cytometry, in combination with antibodies targeting specific surface markers of large EVs. Furthermore, "omics" technologies enhance the analysis of the EV cargo like miRNA and mRNA (transcriptomics), proteins (proteomics), and lipids (lipidomics) (Ratajczak & Ratajczak, 2020). These approaches provide a comprehensive understanding of the content of EVs and enable a better insight into their characterization.

1.2 Mechanisms involved in microvesicles formation from the plasma membrane.

In recent years, mechanisms underlying microvesicle biogenesis from cell surfaces have been emerging. One intriguing mechanism involves the arrestin domain-containing protein 1 (ARRDC1), which localizes to the plasma membrane through its arrestin motif. ARRDC1 interacts with Tumor Susceptibility Gene 101 (TSG101), a component of the endosomal sorting complex required for transport (ESCRT), facilitating the formation of microvesicles known as ARRDC1-mediated microvesicles (ARMMs) (Nabhan, Hu, Oh, Cohen, & Lu, 2012). Other mechanisms involved in microvesicle biogenesis, especially in various tumor cell populations, imply cytoskeletal elements and their regulatory proteins. One critical regulator of actin dynamics is Rho GTPase and the Rho-associated protein kinase (ROCK) (B. Li, Antonyak, Zhang, & Cerione, 2012). The coordinated action of actin and myosin together with a subsequent ATP-dependent contraction, facilitates the release of microvesicles from the apical membrane (McConnell et al., 2009).

1.3 Mechanisms involved in exosome biogenesis.

Exosomes stem from endosomes, which are intracellular compartments responsible for collecting endocytosed material. Endocytosis is the principal route of entry of biomolecules into the eukaryotic cells. During endocytosis, the plasma membrane forms invaginations and buds into intracytoplasmic vesicles containing the ingested material. The ingested materials can be recycled back to the plasma membrane or targeted for degradation within lysosomes (Mukherjee, Ghosh, & Maxfield, 1997). Endocytosis plays a key role in various biological

processes such as nutrient uptake, mitosis, plasma membrane remodeling, polarity maintenance, and cell migration (Doherty & McMahon, 2009). Biologically, it facilitates the reutilization and degradation of plasma membrane components like proteins, receptors, and lipids that are essential for cell interaction with the external environment (Miaczynska & Stenmark, 2008).

Internalized cargoes from several endocytic pathways are delivered to a common early endosome (EE). EEs function as the main sorting station in the cell. Some receptors and proteins that need to be recycled back to the plasma membrane are sorted into recycling endosomes, which will fuse with the plasma membrane. EEs mature to late endosomes (LE) through significant protein and lipid remodeling. LEs eventually fuse with lysosomes leading to the degradation of their content (Figure 1). Several endosome properties are redefined as a result of this maturation process. For instance, sphingomyelin is exchanged for ceramides, Rab5 is exchanged with Rab7, and Rab4, Rab11, and Rab22 are also exchanged with Rab9 (Poteryaev, Datta, Ackema, Zerial, & Spang, 2010; Rink, Ghigo, Kalaidzidis, & Zerial, 2005; Scott & Gruenberg, 2011; Scott, Vacca, & Gruenberg, 2014). Another aspect of endosomal maturation is the gradual decrease in luminal pH. EE has a pH of about 6.8, which decreases to 6.0–4.8 in the LEs and reaches around 4.5 in lysosomes. Regulation of the luminal pH in endosomes is mediated through the V-ATPases complex, which is a large, multi-subunit proton pump. This complex consists of two domains: the V0 domain forms a transmembrane pore for protons and the V1 domain binds to and hydrolyzes ATP (Marshansky & Futai, 2008). This acidification and its regulation are important for the activation of hydrolytic enzymes, enabling the degradation of intracellular components and facilitating protein clearance (Mindell, 2012). Moreover, this reduction in pH is essential for membrane trafficking, receptor-ligand uncoupling, and internalization of pathogens (Maxfield & Yamashiro, 1987).

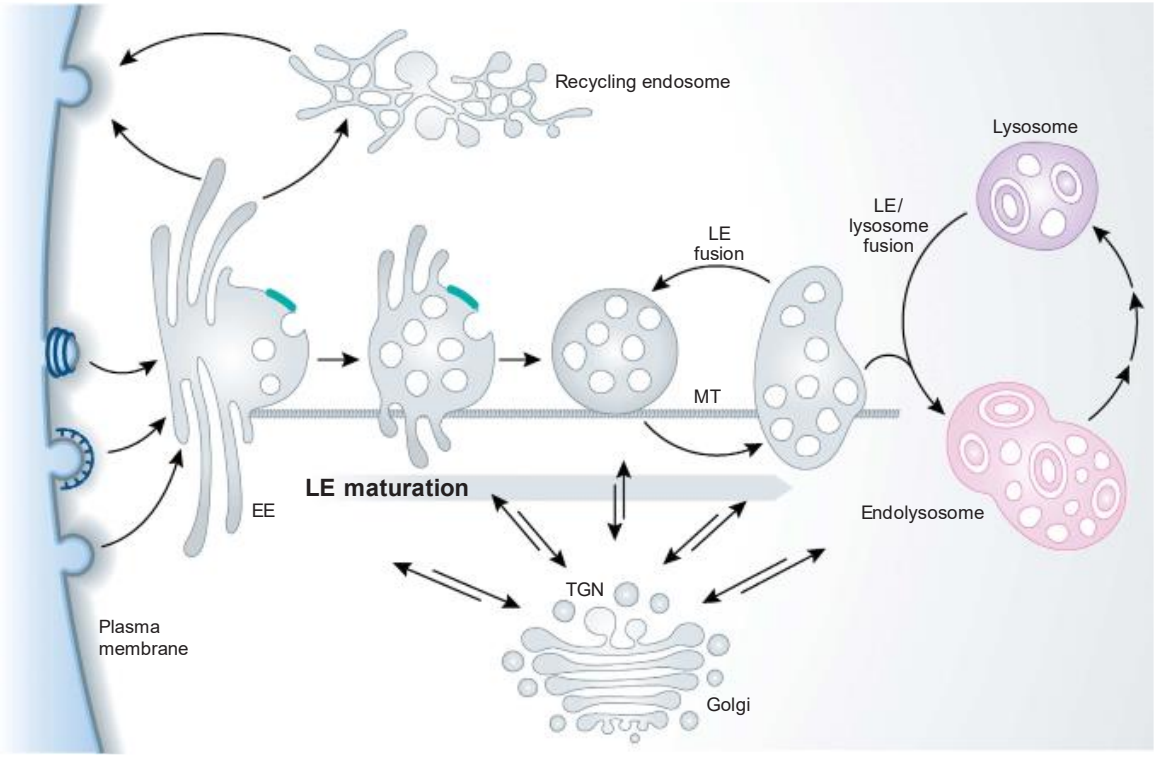

Figure 1: **The endosome/lysosome system.**
Adapted from (Huotari & Helenius, 2011)

1.4 Biogenesis of MVBs

Exosomes correspond to Intraluminal vesicles (ILVs) that accumulate within endosomes, forming the so-called multivesicular bodies (MVBs). MVBs were first observed in the early endosomal compartment in the 1980s (Gruenberg, Griffiths, & Howell, 1989). Afterward, the existence of MVBs between the early and late endosomes was discovered. It is estimated that MVBs have a diameter of 250-1000 nm and contain an average of 24 ILVs, which range in size from 50 to 100 nm (Von Bartheld & Altick, 2011) (Figure 2).

Some MVBs are transported to the plasma membrane and fuse with it, releasing their ILV content which, once outside are known as exosomes (Colombo, Raposo, & Théry, 2014; Gruenberg, 2020). Others follow a degradation pathway by fusing with the lysosomes (Kalluri & LeBleu, 2020) (Figure 3).

Several mechanisms and pathways are involved in the budding of endosomal membrane and ILVs (or future exosomes) biogenesis. In general, these mechanisms comprise ESCRT (Endosomal Sorting Complex Required for Transport)-dependent and ESCRT-independent pathways (Figure 4).

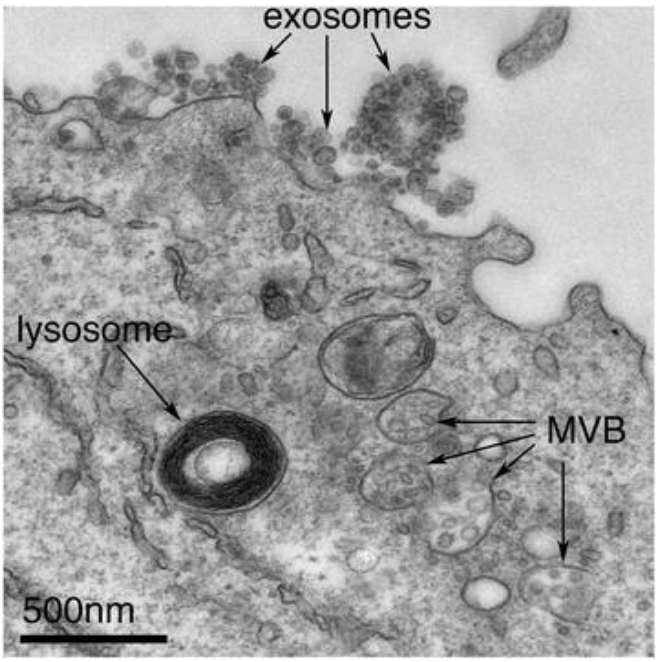

Figure 2: **Exosomes correspond to intraluminal vesicles of multivesicular bodies.**
Adapted from (Edgar, 2016)

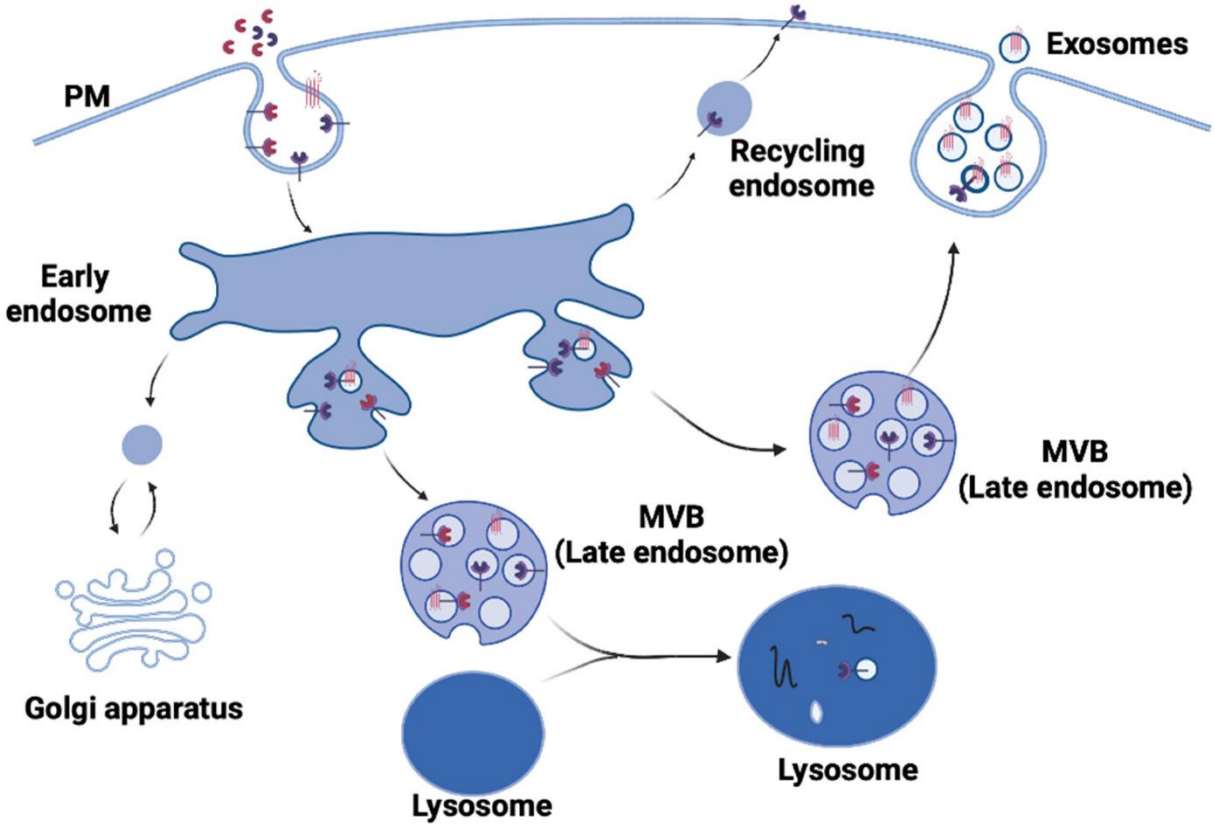

Figure 3: **Schematic of the exosome biogenesis.**
Adapted from (Krylova & Feng, 2023)

ILVs are made by invaginations and budding of the endosomal membrane called MVBs. These ILVs can be secreted into the extracellular space upon fusion of the MVBs with the plasma membranes becoming exosomes (Colombo et al., 2014; Gruenberg, 2020)

1.4.1 ESCRT-Dependent ILVs Biogenesis

The ESCRT system is a canonical pathway of ILV formation. This machinery consists of five cytosolic protein complexes ESCRT-0, -I, -II, -III, and Vps4 (vacuolar protein sorting) proteins. ESCRT recognizes cargo proteins on the limiting membrane of endosomes that are targeted for degradation, sorting them into membrane invaginations that eventually separate as ILVs inside endosomes (Vietri, Radulovic, & Stenmark, 2020). This complex is recruited to the endosome through the ubiquitin tag of membrane proteins. Ubiquitinated tag is recognized by the hepatocyte growth factor regulated tyrosine kinase substrate (HRS) subunit of the ESCRT-0. The FYVE domain of ESCRT-0 then binds to phosphatidylinositol 3-phosphate, an endosomal lipid enriched in endosomal compartments. Subsequently, ESCRT-0 recruits one component of ESCRT-I, the TSG101 subunit, followed by the ESCRT-II complexes. Their cooperation prompts curvature of the endosomal membrane around the ubiquitinated proteins, resulting in formation of ILV (Schöneberg, Lee, Iwasa, & Hurley, 2017). The charged multi-vesicular body protein 6 (CHMP6) subunit of the ESCRT-III complex binds to ESCRT-II and then recruits CHMP4. This assembly polymerizes into a filament-like coil in the neck of the two lipid bilayer sheets, bringing them together, and effectively trapping the cargoes within the ILVs. The association of CHMP3 and CHMP2, subunits of the ESCRT-III complex, facilitates the cleavage of budding ILVs following ATP hydrolysis by Vps4. As a result of this enzymatic activity, ESCRT-III proteins are unfolded and recycled into the cytosol (Krylova & Feng, 2023; O. Schmidt & Teis, 2012) (Figure 4)(Table 1).

In the ESCRT-dependent pathway, several other molecules participate in ILV generation. One such molecule is the ESCRT-associated protein Alg-2 interacting protein X (Alix), which is involved in ILV formation. The yeast homolog of mammalian Alix, known as Bro1, binds to the VPS4 subunit of ESCRT-III and contributes to the formation of ILVs (Tseng et al., 2021).

Alix facilitates the interaction between the cytosolic adaptor protein syntenin to syndecan heparan sulfate proteoglycan, a ubiquitous transmembrane protein (Baietti et al., 2012; Ghossoub et al., 2014). After Syndecan-Syntenin and Alix association, Alix recruits the ESCRT-III protein CHMP4 through its Bro1 domain. Alix recruitment is dependent on direct interaction with the late endosome lipid LBPA (lysobiphosphatidic acid) (Larios, Mercier, Roux, & Gruenberg, 2020). The cone-shaped structure of LBPA allows membrane deformation and the formation of ILVs (Matsuo et al., 2004).

These interactions drive ILV formation. Additionally, the SH3 domain of c-Src kinase in the endosome binds to the proline-rich domain (PRD) of Alix, activating ESCRT-mediated ILV formation (Hikita, Kuwahara, Watanabe, Miyata, & Oneyama, 2019; Imjeti et al., 2017)(Figure 5).

1.4.2 ESCRT-Independent ILVs Biogenesis

Aside from classical ESCRT-dependent processes, complex lipids and proteins are involved in ILV generation in an ESCRT-independent manner (Figure 4 B) (Skryabin, Komelkov, Savelyeva, & Tchevkina, 2020). While the exact mechanism of ILV formation in this pathway is less clear, several important factors have been identified.

Exosomes are known to contain cholesterol, sphingolipids, and phosphatidylserine, a composition that resembles membrane lipid rafts. Among the proteins associated with exosomes, flotillins, and caveolins, contribute to the lipid raft membrane. The assembly of lipid rafts has been implicated in ESCRT-independent ILV formation due to its involvement in membrane curvature and vesicle formation (Dawson, 2021; Skotland, Hessvik, Sandvig, & Llorente, 2019).

Flotillins and caveolin are membrane scaffolding proteins involved in various cellular processes.

Flotillin-1 has emerged as a prominent marker of exosomes over the past two decades (de Gassart, Geminard, Fevrier, Raposo, & Vidal, 2003) and Caveolin-1, an integral membrane protein with a hairpin-like structure, acts as a scaffold for the assembly of lipids and proteins on the membranes (Parton, McMahon, & Wu, 2020).

Caveolin-1 modulates the sorting of extracellular matrix cargo like Tenascin-C into ILVs. This pathway is greatly regulated by the ceramide pathway. Knocking down nSMase2 significantly affects the release of Tenascin-C-containing exosomes in MDA-MB468 breast tumor cells (Albacete-Albacete et al., 2020). On the other hand, the knockdown of flotillin-1 significantly reduced the release of caveolin-1-containing exosomes in PC-3 cells (Phuyal, Hessvik, Skotland, Sandvig, & Llorente, 2014). These observations suggest that flotillin-1 and caveolin-1 mediate ILV biogenesis and cargo sorting via the ESCRT-independent pathway, although their involvement may vary depending on the cell type.

Cholesterol is involved in late endosomal trafficking and is enriched in exosomes. It has both effects on ILV formation and exosome secretion. Among B-lymphocytes, only MVBs that contain high cholesterol level could release their ILVs as exosomes (Möbius et al., 2002). The U18666A treatment, which causes cholesterol accumulation in MVBs by inhibiting lysosomal cholesterol export, increases exosome secretion in fibroblast cells, while the ILV sorting of Tenascin-C is decreased (Albacete-Albacete et al., 2020). Strauss et al., demonstrated that cumulative levels of cholesterol not only promote flotillin endocytosis but also increase exosome secretion in Oli-neu oligodendroglial cells, while cholesterol depletion reduces the release of flotillin-containing exosomes (Strauss et al., 2010). Controversially, increasing the cellular cholesterol level has been shown to inhibit exosome release in astrocytes (Abdullah et

al., 2021). Therefore, cholesterol may have contradictory effects on ILV/exosome formation, depending on the specific cell type or cargo.

Neutral sphingomyelinase 2 (nSMase2)-ceramide is the most well-studied aspect of the ESCRT-independent pathway. Ceramide is derived from the cleavage of sphingomyelin into phosphatidylcholine and ceramide by nSMase2. Ceramide plays a vital role in organizing lipid raft microdomains on the plasma membrane, by the assembly of sphingolipids, cholesterol, and proteins. It has been shown that nSMase2 inhibition significantly decreases the secretion of the proteolipid protein (PLP) in exosomes derived from an oligodendrocyte line (Oli-neu). Thus, the PLP secretion in exosomes was found to be independent of ESCRTs but dependent on ceramides. In an experiment using giant unilamellar vesicles (GUVs) composed of phosphatidylcholine, sphingomyelin, and cholesterol, Trajkovic et al., demonstrated the budding and formation of small vesicles upon the addition of SMase and confirmed the role of ceramides in ILV formation (Trajkovic et al., 2008). Ceramides induce spontaneous negative curvature of the membrane, which could explain its role in ILV generation in an ESCRT-independent manner.

The transmembrane 4 superfamily (TM4SF), or tetraspanins, serve as important membrane scaffolds and are a highly conserved family of membrane integral proteins. It has been shown that tetraspanins play an important role in ILV sorting and biogenesis (Kummer, Steinbacher, Schwietzer, Thölmann, & Ebnet, 2020). Exosomes contain high levels of tetraspanins, especially CD63 and CD81, which are commonly used as markers (Kalluri & LeBleu, 2020).

CD63 and Tetraspanin-6 (TSPN6) promote ILV sorting and exosomal secretion in different cell types. For example, CD63 coupled with Apo-lipoprotein E regulates the ILV sorting of melanocyte protein PMEL (Han et al., 2022; van Niel et al., 2011). Various other cargoes are also proposed to be sorted into ILVs/exosomes via a CD63-dependent mechanism, including latent membrane protein 1 (LMP1), vascular endothelial growth factor (VEGF), ferritin (Ma et al., 2021; Yanatori, Richardson, Dhekne, Toyokuni, & Kishi, 2021; Yokoi et al., 2019). In addition, in Hek293 cells, the interaction of TSPN6 with syntenin induces ILV sorting and exosome release of amyloid precursor protein (Guix et al., 2017). Furthermore, growing evidence suggests that CD63 downregulation reduces ILV generation (van Niel et al., 2011).

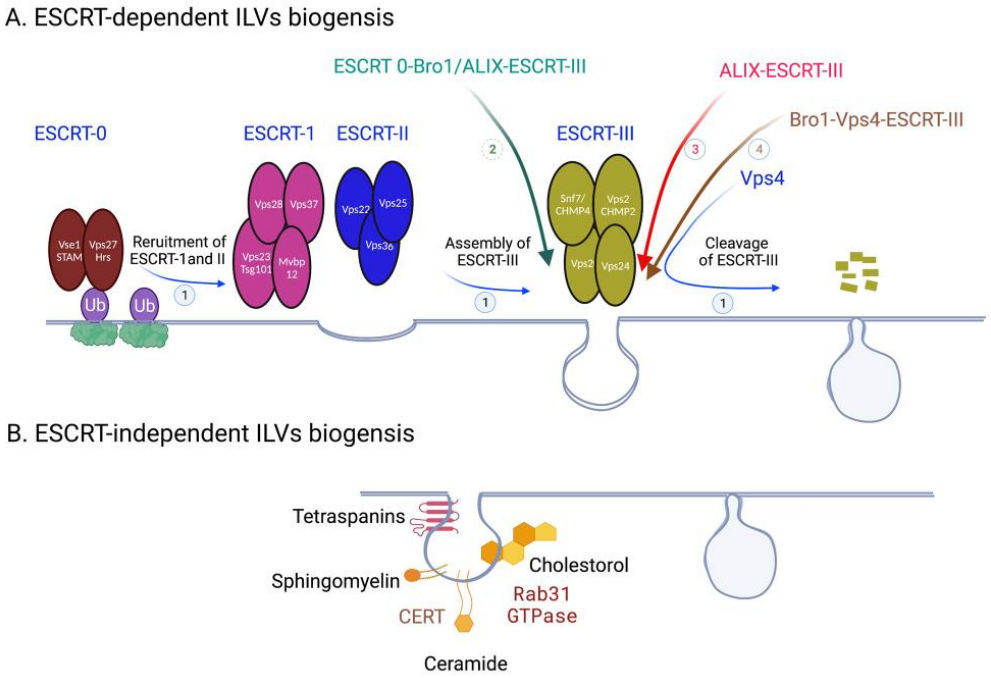

Figure 4: **Exosome biogenesis.**

Adapted from (Krylova & Feng, 2023).

A. ESCRT-dependent ILVs biogenesis.
B. ESCRT-independent ILVs biogenesis.

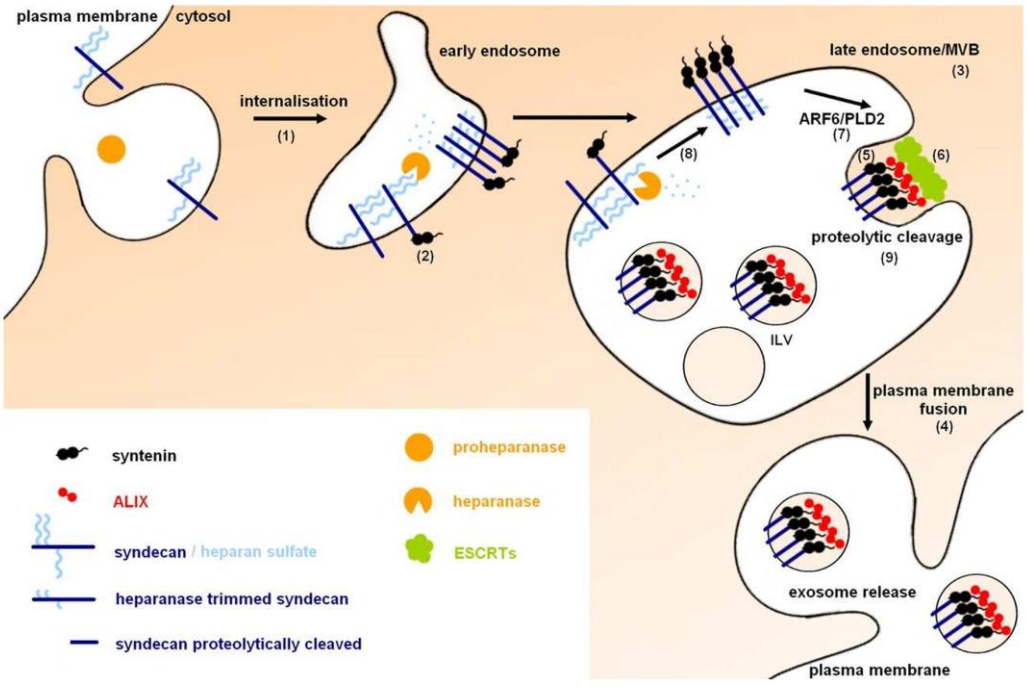

Figure 5: **Role of Alix in Exosome biogenesis.**

Adapted from (Friand, David, & Zimmermann, 2015)

Syndecan–syntenin–ALIX regulates the formation of ILVs. Heparan sulfate chains are susceptible to cleavage by heparanase, which in turn promotes the clustering of Syndecans. This clustering is followed by interactions with Syntenin, ALIX, and ESCRTs, leading to the subsequent formation of ILVs.

ESCRT complex	Function	Yeast protein	Human protein	ESCRT activity	Biological role
0	Clustering of Ub cargo	VPS27	HRS(HGS)	Interaction with Pi3P,ESCRT-I and Clathrin	MVB biogenesis
		Hse1	STAM1/2	Binds ubiquitiylated cargo	MVB biogenesis
I	Membrane budding	Vps23	TSG101	Binds Ub,ESCRT-0, Bro1 and viral proteins	MVB biogenesis, Viral budding and replication, Cytokinesis
II	Membrane budding	Vps36	VPS36	Binds PI containing membranes, Ub and ESCRT-I	MVB biogenesis
III		Vps20	CHMP6	Binds ESCRT-II and Doa4,acts as nucleator of Snf7 polymer	MVB biogenesis
III		Snf7	CHMP4	Main driver of membrane scission, binds Bro1	MVB biogenesis, Viral budding and replication, Cytokinesis
III		Vps24	CHMP3	Caps Anf7 polymer, recruits Vps2	MVB biogenesis, Viral budding, Cytokinesis
III		Vps2	CHMP2	Recruits Vps4, initiates ESCRT disassembly	MVB biogenesis, Viral budding, Cytokinesis
III related	ESCRT disassembly	Did2	CHMP1	Recruits Vps4	MVB biogenesis, Cytokinesis
III related		Vps60	CHMP5	Binds Vta1	MVB biogenesis
ESCRT associated		Vps4	VPS4	AAA ATPase disassembles ESCRT-III, active function in MVB membrane scission	MVB biogenesis, Viral budding and replication, Cytokinesis
ESCRT associated		Vta1	VTA1 (LIP5)	Binds Vps4 to promote ESCRT-III recycling	MVB biogenesis, Viral budding

Table 1: **ESCRTs subunits and associated proteins.**

Adapted from (Diaz, Zhang, Ollwerther, Wang, & Ahlquist, 2015).

1.5 Cargo sorting to exosomes

Various mechanisms are used for sorting different classes of molecules in endosomes, such as proteins, nucleic acids, and lipids (Table 2) (Bobrie, Colombo, Raposo, & Théry, 2011). These sorting processes are crucial as exosomal content profiles dynamically change in response to the cell state, determining their functional properties (Jia et al., 2021). Thus, exosome sorting is highly selective and tightly regulated.

Exosome composition		
Category	**Examples**	**Role**
Proteins		
Tetraspanins	CD9, CD63, CD37, CD81, CD82, CD53	Exosome biogenesis, exosome cargo selection, targeting and uptake
ESCRT machinery/MVB biogenesis	Alix, TSG-101	Exosome biogenesis
Heat Shock Proteins (Hsp)	Hsp90, Hsc70, Hsp60, Hsp20, Hsp27	Exosomes release, signalling
Membrane transport and fusion	GTPases, Annexins, Flotillin, Rab GTPases, dynamin, syntaxin	Exosome secretion and uptake
Major Histocompatibility Complex (MHC) molecules	MHC Class I, MHC Class II	Antigen presentation to generate immunological response
Cytoskeletal proteins	Actin, Cofilin, Tubulin	Exosome biogenesis and secretion
Adhesion	Integrin-α,-β, P-selectin	Exosome targeting and uptake
Glycoproteins	β-galactosidase, O-linked glycans, N-linked glycans	Exosomes targeting and uptake
Growth factors and cytokine	TNF-α, TGF-β, TNF-related apoptosis inducing ligand (TRAIL)	Exosome targeting and uptake, signalling
Other signalling receptors	Fas ligand (FasL), TNF receptor, Transferrin receptor (TfR)	Exosome targeting and signalling including apoptosis induction and iron transport
Category	**Role**	
Lipids		
Cholesterol	Exosome secretion	
Ceramides	Cargo sorting and exosome secretion	
Sphingomyelin	Exosome rigidity and signalling	
Phosphatidylserine	Exosome formation, signalling and uptake	
Phosphatidylcholine	Exosome formation and structure	
Phosphatidylethanolamine	Exosome formation and structure	
Phosphatidylinositol	Exosome formation and structure	
Gangliosides	Exosome rigidity	

Table 2: **Exosome composition and their main role**s.
Adapted from (Gurung, Perocheau, Touramanidou, & Baruteau, 2021).

1.5.1 Lipids

Among the phospholipids found in mammalian cells, phosphatidylcholine (PC) is the most abundant (45-55%); phosphatidylethanolamine (PE) is another significant phospholipid, comprising most of the remaining half of the phospholipids. The other lipids are cholesterol, phosphatidylinositol (PI), phosphatidylserine (PS), sphingomyelin (SM), phosphatidic acid (PA), and glycosphingolipids. (Vance, 2015).

PC, for instance, is characterized by its cylindrical shape and ability to form a bilayer structure that appears as a planar surface. In contrast, PE, cholesterol, and other negatively charged lipids like PS, PA, PG, and PI possess inverted cone-shaped molecular structures, contributing to negative membrane curvature and facilitating the hemifusion process (Fuller & Rand, 2001; Meher & Chakraborty, 2019). On the other hand, Lysolipids like lysophosphatidylcholine and lysophosphoglycan have a large headgroup and conical shape which leads to positive membrane curvature (Figure 6)(Sardar, Dewangan, Panda, Bhowmick, & Tarafdar, 2022; Tarafdar, Chakraborty, Bruno, & Lentz, 2015).

The phospholipids distribution varies across different organelles and membranes, tuned to fulfil their particular biological role. For instance, in the plasma membrane, PE and PS are predominantly enriched in the inner layer, while they are depleted from the outer leaflet by phospholipid flippases. On the other hand, PC and SM are more abundant in the outer layer. Interestingly, exosomal membranes show a reverse lipid distribution. In general, it seems that exosomes are more enriched in cone-shaped lipids like negatively charged lipids PE, PS, PA, and ceramides, especially in their outer leaflet. (Booth et al., 2006; Pegtel & Gould, 2019). These differences in lipid distributions may provide some clues about the vesicle biogenesis pathway, as the lipid composition of vesicles resembles that of specific organelles, such as the plasma membrane or endosomes.

It is therefore important to understand the lipid composition of exosome membranes for comprehending their role in intercellular communication. Exosomal membranes are characterized by higher levels of SM, cholesterol, and ceramide, which not only influence the structure and secretion of exosomes but also play a role in cargo sorting (Skotland et al., 2019; Skryabin et al., 2020).

Interestingly, exosomes have a similar lipid composition to the lipid rafts. In comparison with other EVs, exosomes possess a higher lipid order and are more stable against detergents (Skotland et al., 2019). Membrane fluidity of exosomes is decreased due to this lipid composition. Exosomes have a rigid membrane structure, allowing them to efficiently transport cargo and provide communication between cells while maintaining stability in extracellular environments. Aside from their role in intercellular communication, exosomes seem to be stable enough to survive in body fluids.

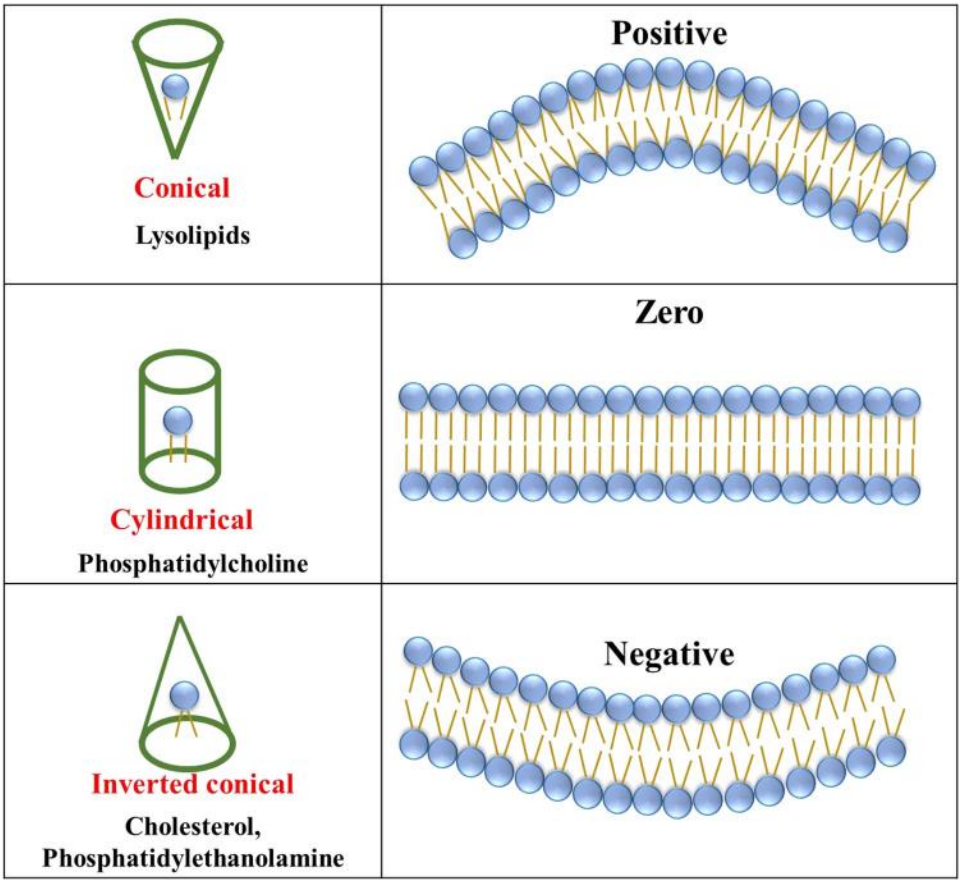

Figure 6: **Shape of lipids and their effect on positive or negative membrane curvature.**
Adapted from (Sardar et al., 2022)

1.5.2 Proteins

Exosomal membrane cargoes are transported either from the Golgi apparatus to endosomes or internalized from the plasma membrane during ILVs formation in the endosome pathway. Some transmembrane proteins like the tetraspanin family (CD9, CD63, and CD81) and integrins as well as cytosolic proteins like ESCRT proteins TSG101 and Alix, heat shock proteins (Hsp), actin and flotillins, are incorporated in exosomes (Zhang, Liu, Liu, & Tang, 2019). Protein sorting at endosomes can be selectively regulated by a variety of pathways. These proteins originate from the plasma membrane, endosomal pathway, and cytosol rather than the nucleus, mitochondria, and endoplasmic reticulum proteins (Figure 7).

Exosomes contain the highest concentration of CD81, despite the fact that it is primarily located in the plasma membrane, whereas CD63 is mainly found in the endosomes (Hemler, 2003). Tetraspanins can promote the assembly of protein complexes with other membrane proteins, like major histocompatibility complex (MHC) class II proteins (Escola et al., 1998; Raposo et al., 1996), intercellular adhesion molecule-1 (ICAM-1) (Segura et al., 2005), syndecans (Baietti et al., 2012), integrins (Rieu, Géminard, Rabesandratana, Sainte-Marie, & Vidal, 2000).

As above described, both ESCRT-dependent and ESCRT-independent machinery plays a key role not only in ILVs biogenesis but also in protein sorting within exosomes. Certain proteins can be sorted into exosomes via monoubiquitination (contrasting from polyubiquitination targeting cargo for proteasomal degradation). The ubiquitin-interacting-motif (UIM) domain of the ESCRT 0 protein Vps27/Hrs can bind to ubiquitinated cargo and concentrate them in clathrin-rich domains of the endosomes to bud away from limiting membrane and form ILVs (Hurley & Emr, 2006; Polo et al., 2002). Before encapsulation within an ILV, ubiquitin needs to be removed from the proteins by deubiquitinating enzymes like ubiquitin thioesterase Doa4, which can be recruited into endosomes with the assistance of Alix/Bro1 (Luhtala & Odorizzi, 2004).

Sorting of other cargo occurs independently of the ESCRT machinery. Some proteins, such as HIF1α, have a KFERQ motif that directly binds to LAMP2A with the help of Alix, Syntenin-1, Rab31, and ceramides in an ESCRT-independent manner (Dores, Grimsey, Mendez, & Trejo, 2016; Ferreira et al., 2022).

Exosomes are also rich in molecular chaperones known as heat shock proteins (HSPs), which have the capability to bind to misfolded proteins (Mathew, Bell, & Johnstone, 1995) (Alderson, Kim, & Markley, 2016). Several HSPs have been observed within exosomes, including the Hsp70 family, Hsp40/DnaJ proteins, Hsp90, Hsp20, and Hsp27 (J. Li et al., 2016; Reddy, Madala, Trinath, & Reddy, 2018; Takeuchi et al., 2015; Théry et al., 2001; Wubbolts et al., 2003).

Syntenin is an exosomal scaffolding factor that plays a crucial role in the assembly of exosomal proteins through its multiple protein-binding motifs. It binds to phosphatidylinositol-4,5-bisphosphate (PIP2) present in the inner leaflet of the membrane (Latysheva et al., 2006). Syntenin also interacts with CD63 and plays an essential role in the exosome sorting of syndecan (Friand et al., 2015) and interacts with Alix.

As mentioned before, Alix not only binds to syntenin but also interacts with TSG101 and CHMP4 of ESCRTs proteins. Therefore, ESCRT proteins are clearly present in exosomes. TSG101 has increasingly been used to identify exosomes (Henne, Buchkovich, & Emr, 2011; Radulovic & Stenmark, 2018).

Generally, the protein sorting into the EVs is a complex process that depends on various factors, like cell type, the EVs origin, and finally the specific intracellular communication that allows EVs attachment to the receiving cells and trigger signaling events.

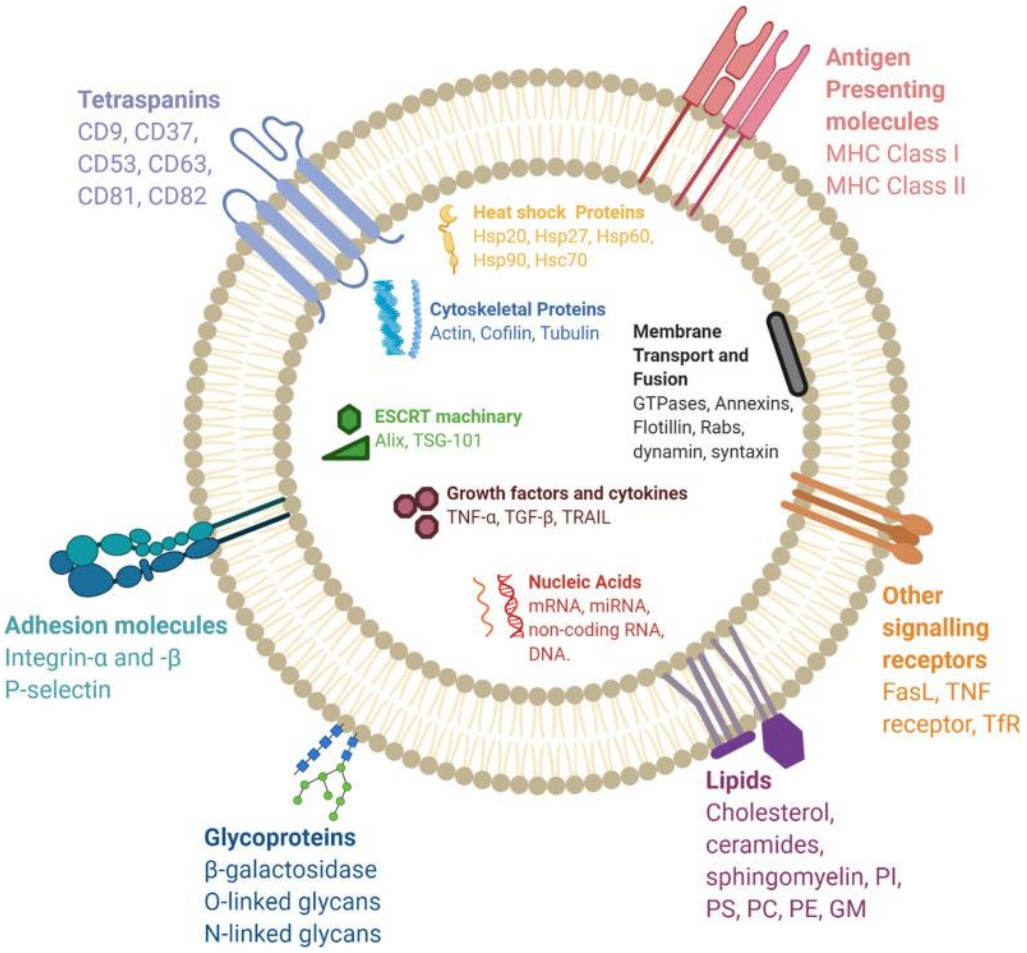

Figure 7: **Exosome composition.**
Adapted from Adapted from (Gurung et al., 2021)

1.5.3 Nucleic acids

In 2007, for the first time, Valadi and collaborators discovered the presence of messenger RNAs (mRNAs) and microRNAs (miRNAs) in exosomes (Valadi et al., 2007). Their study attracted considerable attention as they demonstrated that these RNAs could be protected in extracellular environments and could regulate translation and gene expression in the recipient cell (Montecalvo et al., 2012). Since then, many investigations show the presence of other exosomal RNA species, like long non-coding RNA (lncRNA), transfer RNA (tRNA), small nuclear RNA (snRNA), and small nucleolar RNA (Ge et al., 2020; Zhang et al., 2019).

microRNAs can be directed to the exosomes by different mechanisms that are dependent on the cell type (Guduric-Fuchs et al., 2012). RNA-binding proteins (RBPs) like hnRNPA2B1, hnRNPK, YBX1, major vault protein (MVP), and MEX3C participate in the exosome sorting of miRNAs (Eden et al., 2016; Groot & Lee, 2020; A. L. Wozniak et al., 2020). In colon carcinoma cells, MVP is participated in targeting miR-193a to exosomes (Teng et al., 2017). Most of the RBPs are located in the nucleus, and we still do not know how they can translocate into the cytoplasm and involve in miRNA sorting.

Some lipids also appear to be involved in the export of miRNA into exosomes, like ceramides. Kosaka et al., showed that overexpression of sphingomyelinase 2 (nSMase2) which breaks sphingolipid into ceramides, increases the miRNA sorting. Conversely, blocking the expression of nSMase2 by GW4869 or decreasing its expression by siRNA could reduce the amount of sorted microRNA (Kosaka et al., 2010). Alix might be involved in the export of microRNA in exosomes, as the absence of Alix in hepatocyte exosomes results in a drastic decrease in exported miRNA (Iavello et al., 2016).

There is a conflict of opinion regarding the sorting of DNA molecules by exosomes. Jeppesen et al., demonstrated an exosome-independent mechanism for the extracellular secretion of DNA and histones (Jeppesen et al., 2019). Takahashi et al., and Torralba et al., reported the sorting of guide DNA (gDNA) as well as some nuclear proteins into exosomes (Takahashi et al., 2017; Torralba et al., 2018).

1.6 Maturation and fate of MVBs

MVBs are heterogeneous due to the diverse cargo sorting of ILVs and the different mechanisms involved in ILVs generation. Several subpopulations of MVBs could coexist within a single cell, resulting in a heterogeneous exosome population. MVBs have two distinct fates: degradative MVBs (dMVBs) can undergo degradation after fusion with lysosomes, while secretory MVBs (sMVBs) can fuse with the plasma membrane for exosome release.

ILVs can also fuse back with the limiting membrane of MVBs in an Alix dependent-manner, allowing for the recycling of some proteins (Le Blanc et al., 2005; van der Goot & Gruenberg, 2006).

The regulation of the balance between the degradative and secretory functions of MVBs remains largely unclear, but it undoubtedly influences cellular processes and functions. The pH within MVBs is a crucial factor in determining whether MVBs will undergo degradation or secretion. Reduction in the levels of Sirtuin 1 (SIRT1) inhibits the expression of endosomal proton pump V-ATPase, which is responsible for acidification of the lysosomes and protein degradation, impairing lysosomal activity and leading to increased secretion of exosomes in breast cancer cells (Latifkar et al., 2019).

Some insights into the mechanisms which choose MVBs' fate have been recently established. It has been shown that the first level of regulation of this balance is influenced by the sorting machinery at MVBs (Willms et al., 2016). For instance, MHCII exhibits two regulatory mechanisms for sorting into the MVBs of DCs, each leading to a different fate. In the first mechanism, MHCII triggers the sorting of ILVs within MVBs for lysosomal degradation, which is dependent on ubiquitination and involves ESCRT machinery. While in the second mechanism, MHC II sorts into ILVs together with CD9, which subsequently triggers the secretion of exosomes through ESCRT-independent machinery (ubiquitin-independent) (Buschow et al., 2009).

Autophagy proteins have an important role in MVBs' fate. One unique process in MVBs maturation is the fusion of autophagosomes with MVBs to form amphisomes (Zhao, Codogno, & Zhang, 2021). These amphisomes play a crucial role in either participating in the degradation process within MVBs or being secreted into the cellular microenvironment. This delicate equilibrium between MVBs and autophagy is a pivotal mechanism that helps maintain cellular homeostasis during pathological processes, as depicted in Figure 8. It has been observed that the induction of autophagy or the increased expression of LC3 in K562 cells facilitated the fusion of MVB with autophagic vacuoles while suppressing the release of exosomes (Berg, Fengsrud, Strømhaug, Berg, & Seglen, 1998).

Moreover, it has been shown that depletion of PIKfyve (phosphoinositide kinase, FYVE-type zinc finger containing) in PC3 cells increased the secretion of exosomes containing CD63 and induced secretory autophagy, this suggests that these pathways are tightly connected (Hessvik et al., 2016).. Ubiquitination of TSG101 promotes the fusion of amphisomes with lysosomes (Majumder & Chakrabarti, 2015). In general, these represent a dynamic equilibrium between the autophagic pathway and the EV release pathway, where perturbations in one pathway have the potential to influence the other (Peng, Yang, Ma, Li, & Li, 2020).

On the other hand, the Atg5, an autophagosome protein, regulates the pH of the late endosomes and guides MVBs to the plasma membrane for exosome secretion and it is is dissociated from its effect in autophagy (Guo et al., 2017; Guo, Sadoul, & Gibbings, 2018).

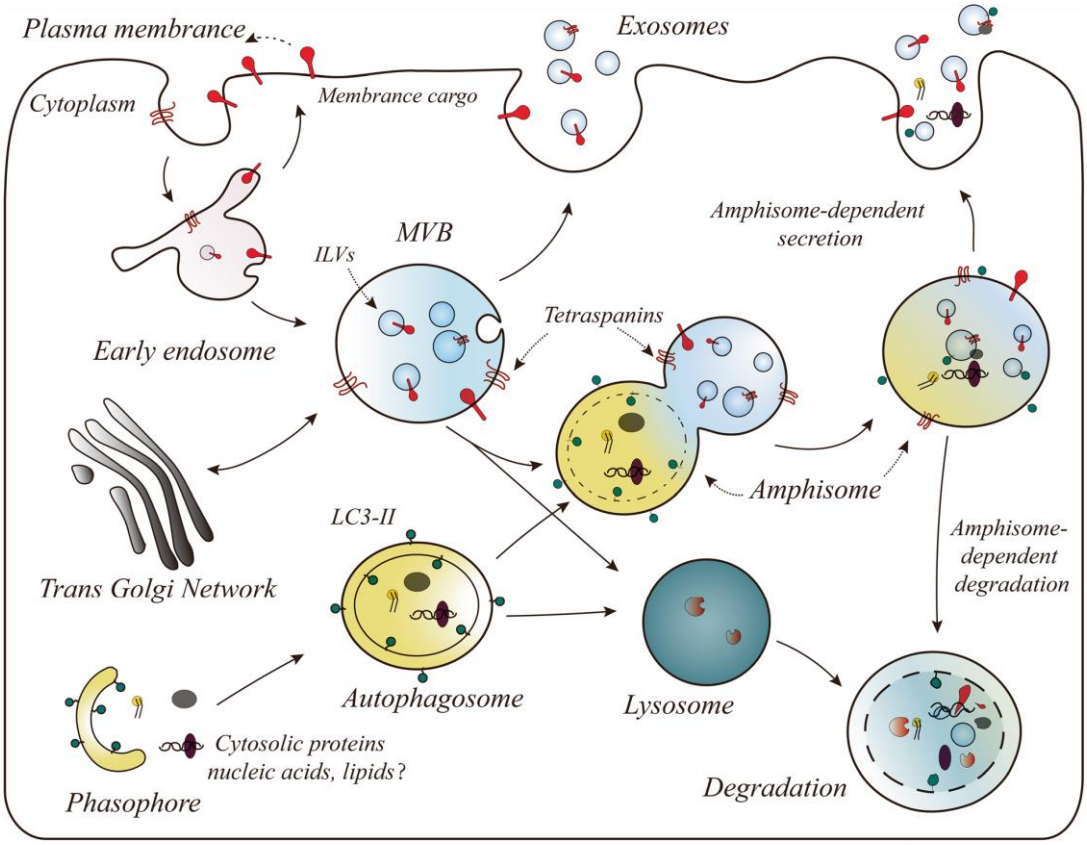

Figure 8: **MVB morphogenesis**.
Adapted from (Peng et al., 2020)
Exosome release, lysosome degradation and secretion or degradation of cargo through an amphisome-dependent mechanism.

Rab GTPase, a group of small GTPases can regulate MVB's fate as well (Bucci, Thomsen, Nicoziani, McCarthy, & van Deurs, 2000). There is a wide variety of Rab proteins that affect MVB trafficking to cell membranes. For instance, Rab7, a GTPase promotes MVB degradation, leading to a decrease in exosome secretion. However, Baietti et al., showed that the knock-down of Rab7 reduced Syntenin-Syndecan-Alix-dependent exosome secretion in MCF7 cells,

(Baietti et al., 2012). Inactive Rab7 promotes the release of Rab11a-positive exosomes while inhibiting the release of total exosomes in HCT116 cells (Fan et al., 2020). On the other hand, Rab31 can recruit GTPase-activating protein TBC1D2B to inactive Rab7, subsequently inhibiting MVB degradation, and facilitating fusing with the plasma membrane to increase exosome secretion (Wei et al., 2021). Rab27a enables the movement of exocytic vesicles to the plasma membrane through direct binding to the SM protein (sec1/munc18) (Ostrowski et al., 2010).

Notably, additional analysis had shown the participation of other GTPases, such as Rab2b, Rab5a, Rab9a, Rab35, Rab11, and RAL-1 in MVB biogenesis and trafficking to the plasma membrane to secrets exosomes (Hsu et al., 2010; Im et al., 2019; Johnson et al., 2016; L. Yang et al., 2019). A few key players like actin filaments and microtubules control this vesicular traffic system. Small GTPases activate some motor proteins like kinesin and dynein, which operate along microtubules and facilitate MVBs transport (Hessvik & Llorente, 2018; Martín-Cófreces, Baixauli, & Sánchez-Madrid, 2014; Messenger, Woo, Sun, & Martin, 2018). Additionally, proteins such as Alix and Clathrin play a crucial role in guiding MVBs towards the plasma membrane, likely by interacting with actin networks that are closely associated with the membrane (Cabezas, Bache, Brech, & Stenmark, 2005; Calabia-Linares et al., 2011).

1.7 Fusion of MVBs with the plasma membrane and exosomes release

The fusion of MVBs with the plasma membrane is regulated by SNARE proteins, including synaptobrevin, YKT6 (Gross, Chaudhary, Bartscherer, & Boutros, 2012; Ruiz-Martinez et al., 2016), and Vamp7 (Rao, Huynh, Proux-Gillardeaux, Galli, & Andrews, 2004). These SNARE proteins are comprised of four transmembrane domains and a hydrophilic amino acids-rich domain. The SNARE proteins assemble into a complex that helps the fusion process by bringing the two membranes together. The SNARE complex is composed of a v-SNARE (v for vesicular) such as VAMPs, located on the MVB, and a t-SNARE (t for target) such as Syntaxin, located on the plasma membrane (Bonifacino & Glick, 2004; Jahn & Scheller, 2006; Koike & Jahn, 2019).

In a model of Alzheimer's disease in neurons, VAMP8, a late endosomal v-SNARE, was found to play a role in the fusion of tau-carrying vesicles with the cell membrane (Pilliod et al., 2020). Furthermore, the t-SNARE protein Syntaxin 4 facilitates the fusion of HCV virus-carrying MVBs with the membrane of infected cells, leading to the exosomal release of the virus (Ren et al., 2017). Moreover, down-regulation of t-SNARE, Syntaxin 6 expression in prostate cancer cells significantly reduces exosome production (Peak et al., 2020).

The SNARE complex further requires the involvement of various proteins, including tethering factors (Bröcker, Engelbrecht-Vandré, & Ungermann, 2010) and Rab GTPases. These proteins are essential for the proper assembly and activity of the SNARE complex. It appears that the silencing of Rab27a has a significant impact on MVBs behavior, as it interferes with proper docking with the plasma membrane and promotes fusion with each other, leading to an increase in their size (Ostrowski et al., 2010; Pegtel & Gould, 2019; Stenmark, 2009) (Figure 9).

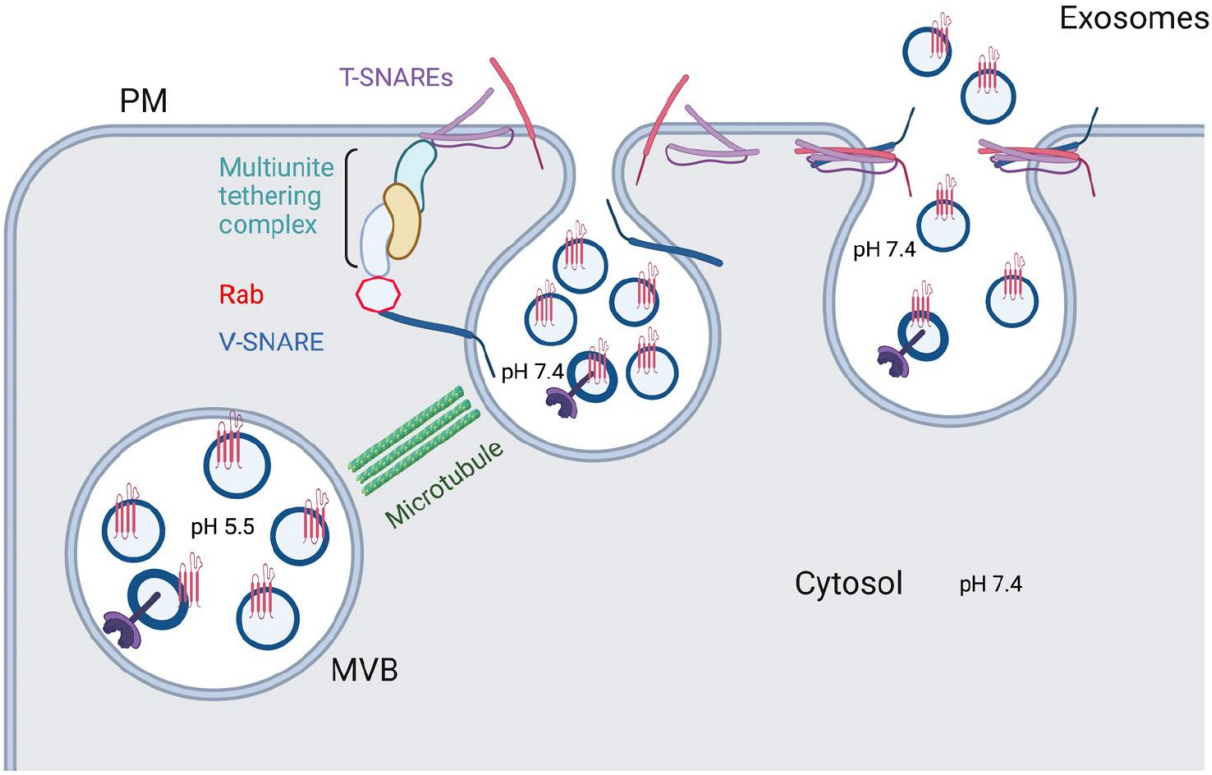

Figure 9: **Exosome secretion.**

Adapted from (Krylova & Feng, 2023)

SNARE complexes, combine with Rab GTPase, microtubules, and tethering factors, drive MVBs fusion with plasma membranes and exosome secretion.

1.8 Exosomes recognition by receiving cells

Exosomes have garnered increasing attention due to their capability to selectively enter cells and induce phenotypic changes in recipient cells through the transfer of molecular contents. There is evidence suggesting that extracellular vesicles originating from different sources have the propensity to interact with particular cells types (Hazan-Halevy et al., 2015; Jurgielewicz, Yao, & Stice, 2020; Rana, Yue, Stadel, & Zöller, 2012). In a study conducted in our lab in 2014, immunofluorescence assays were used to follow exosomes. The results revealed that GFP-CD63 labeled exosomes derived from neuroblastoma cells were capable of binding to the surface of hippocampal neurons, while they are mainly endocytosed by glial cells. On the other hand, GFP-TTC-exosomes derived from neurons subjected to synaptic stimulation displayed specific binding and internalization only by neurons. This suggests that exosomes released by different cell types within the nervous system have different and specific preferences for binding and internalization by receiving cells (Chivet et al., 2014).

Another research revealed that CCL2, a cytokine presents in the tumor microenvironment that promotes tumor growth and progression, can be incorporated onto the surface of cancer exosomes. This incorporation facilitates their selective uptake by cells expressing receptors for these cytokines, leading to immune system alterations within the pre-metastatic niche. Consequently, this process contributes to an elevated metastatic burden (Lima et al., 2021).

Some exosomes can also be taken up by their cell of origin and trigger autocrine responses. For example, researchers used hollow gold nanoparticles containing exosomes derived from human placental mesenchymal stem cells (MSCs). They showed that exosomes are preferentially taken up by, and induce cell death of the cell of origin (Sancho-Albero et al., 2019).

Exosomes exhibit preferential interactions with specific cell types, a phenomenon observed in various conditions, including cancer and pathophysiology. In a study conducted by Emam et al., it was demonstrated that exosomes derived from murine C26 colorectal cancer cells were taken up more efficiently by C26 cells compared to exosomes derived from murine melanoma cells (B16BL6) (Emam et al., 2019). Similarly, in the context of traumatic brain injury, Chen et al., demonstrated that intracerebroventricular microinjection of exosomes derived from human adipose mesenchymal stem cells (hADSC-exo) primarily entered microglia/macrophages. This resulted in the suppression of microglia/macrophage activation, inhibition of inflammation, and improvement in functional recovery (Chen et al., 2020).

The mechanisms allowing the preferential interaction of exosomes to specific cell types are not well understood. However, their surface components like proteins and lipids probably play an important role in mediating this process.

1.8.1 Proteins

It has been reported that proteins present on the surfaces of both exosomes and target cells facilitate the recognition, binding, and subsequently internalization. This internalization can be fully inhibited by pretreatment of the exosomes with Proteinase K (PK) (Escrevente, Keller, Altevogt, & Costa, 2011; Smyth, Redzic, Graner, & Anchordoquy, 2014).

1.8.1.1 Tetraspanins

As above mentioned, different members of tetraspanins are highly enriched on the surface of exosomes such as CD63, CD9, and CD81 (van Niel et al., 2011). In the study conducted by Théry et al, they use RUSH system to track the intracellular trafficking of EV markers CD9 and CD63, from the endoplasmic reticulum to their respective intracellular destinations, namely, the plasma membrane and late endosomes. The immunoprecipitation of CD63 and CD9 EVs derived from Hela cells suggests the presence of different EV populations secreted by these cells: one containing both CD63 and CD9, another with CD63 only (exosomes) and one with CD9 only (ectosoms) (Mathieu et al., 2021).

There is some evidence suggesting that CD9 plays a crucial role in the docking and uptake of exosomes by recipient cells. Human perivascular stem cell exosomes facilitate the migration, proliferation, and osteogenic differentiation of bone marrow mesenchymal stem cells. All these effects are relying on the interaction of tetraspanins (CD9/CD81) on the exosomal surface with their binding partners, such as immunoglobulin superfamily member 8 and prostaglandin F2 receptor inhibitor (PTGFRN) showing an important role in EV bioactivity (J. Xu et al., 2019).

Similarly, tetraspanins on recipient cells are also involved in the uptake process of exosomes. It has been shown that the knockdown of CD81 on the cell surface of MSCs, effectively blocks the cellular attachment of exosomes through the colocalization of integrin (CD29) with CD81, thereby inhibiting the radiation-induced uptake of exosomes (Hazawa et al., 2014).

Other tetraspanins also play an important role in exosomal binding and attachment, like CD63 and CD151. Studies have revealed that wild-type exosomes can significantly enhance the uptake of fluorescence-labeled siRNA in autologous brain endothelial cells. Conversely, when cells are treated with the tetraspanin CD63 antibody, which blocks exosome delivery, the fluorescence intensity in receiving cells decreases (T. Yang et al., 2017).

1.8.1.2 Integrins

Integrins have a significant influence on the binding and uptake of exosomes by target cells. Integrins are transmembrane receptors consisting of two subunits (α and β) that play essential

roles in cell adhesion and cell signaling. Integrins are found on almost all cells' surfaces and can facilitate binding to components of the extracellular matrix (ECM), leading to the recruitment of intracellular signaling molecules that regulate cell spreading, migration, ECM organization, and endocytosis (Kadry & Calderwood, 2020; Nolte, Nolte-'t Hoen, & Margadant, 2021).

Engineering exosomes enriched with integrins can be used to increase or inhibit their binding to specific cell types, thereby altering exosomes' pharmacokinetics and increasing their accumulation in different organs like the brain, lungs, or liver (Hoshino et al., 2015). For instance, Tspan 8 and integrin α4-containing exosomes have shown a preferential uptake by pancreatic cells (Rana et al., 2012).

Inhibiting integrin αVβ3 on the surface of leukemia-derived exosomes using antibodies could significantly reduce their interaction and association with human choroid plexus papilloma cells (Erb et al., 2020). Likewise, pre-treatment of exosomes derived from human primary astrocytes with an RGD peptide known to block the interaction of integrins with their ligands, significantly diminished exosome uptake by neurons (You et al., 2020).

Integrin LFA-1 interactions with ICAM-1 have been associated with the uptake of macrophage-derived exosomes by brain microvascular endothelial cells that form the blood-brain barrier (Yuan et al., 2017). According to a recent study, fibronectin, a major component of hepatocyte exosomes, has been shown to mediate the attachment of exosomes to integrin receptors on target cells. Promoting exosomal uptake via endocytic mechanisms (X. Li, Chen, Kemper, & Brigstock, 2021). According to these findings, integrins play an important role in exosome binding and internalization, and they can be used to manipulate exosome-cell interactions.

1.8.1.3 Proteoglycans

Proteoglycans (PGs) are complex macromolecules consisting of a core protein covalently decorated with linear glycosaminoglycan chains (GAGs). These GAG chains comprise alternating glucuronic acid and N-acetylglucosamine or N-acetylgalactosamine residues, which make two types of PGs: heparan sulfate PGs (HSPGs) and chondroitin sulfate PGs (CSPGs), respectively.

PGs play a key role in cancer cell invasion, metastasis, and reprogramming (Masola, Zaza, Gambaro, Franchi, & Onisto, 2020). HSPGs have been proposed to function as internalizing receptors for different macromolecular cargoes, including viruses and exosomes (Christianson & Belting, 2014). This internalization is dependent on HSPG synthesis and HS-sulfation in receiving cells. Recent studies have also shown that syntenin regulates the uptake of exosomes and the efficiency of viral transduction by modulating the expression levels of CD63 and syndecans, transmembrane proteoglycans (Kashyap et al., 2021).

There is some evidence indicating that HSPG present on endothelial cells acts as a receptor for exosomes released from neural stem cells thereby shuttling proteins across the blood-brain barrier. As a result, targeting nanomedicines toward HSPGs could enhance drug delivery to the brain (Joshi & Zuhorn, 2021).

1.8.1.4 Lectins

Numerous types of lectins recognize and bind to carbohydrate moieties present on the surface of cells or molecules. Several biological processes can be affected by this interaction, including cell-cell recognition, immune system response, and recognition of pathogens (Johannes, Wunder, & Shafaq-Zadah, 2016; P. S. Sung & Hsieh, 2021; W. D. Xu, Huang, & Huang, 2021).

Lectins have been found to be enriched in EVs and these lectins on the surface of EVs can facilitate attachment to recipient cells, thereby enhancing EV uptake efficiency (Barrès et al., 2010; Hao et al., 2007; Yuan et al., 2017). For instance, exosomes derived from MSCs can be taken up by Hela cells. This uptake involves the recognition of surface-bound sialic acid-binding immunoglobulin (Ig)-like lectins (siglecs), as blocking siglecs with antibodies results in decreased uptake of MSC exosomes (Shimoda, Tahara, Sawada, Sasaki, & Akiyoshi, 2017).

Exosomes released from dengue virus-activated platelets can bind to CLEC5A, a C-type lectin on neutrophils, leading to their activation and formation of neutrophil extracellular traps (P. S. Sung, Huang, & Hsieh, 2019).

However, lectins can also interfere with EV functionality. For example, Bonjoch et al., in 2017 demonstrated that REG3, a soluble lectin, interacts with the glycoproteins present on the surface of macrophages-derived exosomes, thereby interfering with their internalization (Bonjoch, Gironella, Iovanna, & Closa, 2017).

Overall, lectins mediate many aspects of the interaction between EVs and recipient cells, such as uptake efficiency and intracellular signaling.

1.8.2 Lipids

As I mentioned above, lipid-driven mechanisms have a main role in ESCRT-independent ILV formation, membrane budding, vesicle formation, and protein sorting (Gao et al., 2021). Currently, several studies have shown the involvement of lipids, as well as proteins in the exosomes internalization by receiving cells (O'Dea et al., 2020).

The lipid composition of exosomes, particularly the percentage of PC, PE, and Cholesterol has been identified as important in the uptake of exosomes by liver cells. For example, higher PC concentrations in exosomes result in increased uptake by macrophages (Kumar et al., 2021). In

another investigation, PC enriched-exosomes showed enhanced efficiency in delivering small molecular drugs to cancer cells, thereby inhibiting tumor cell growth (Zhan et al., 2021).

Moreover, some studies have examined the role of PS on EV-cell interaction. In one experiment, liposomes with varying lipid compositions were used to measure the hepatitis A virus infectivity associated with exosomes. The presence of PS in liposomes was found to block the infectivity of exosomes, suggesting a suppressive effect of PS on cellular uptake (Costafreda, Abbasi, Lu, & Kaplan, 2020).

According to these studies, modifying the lipid composition of exosomes could serve as a strategy to target specific cell types.

1.9 The biological action of exosomes on target cells

Even if the exact mechanisms underlying exosome targeting are poorly understood, it is now widely accepted that once attached to the target cell, exosomes convey messages either directly or through the transfer of their cargo to the receiving cells. The following mechanisms can be employed to achieve this: 1) Direct interaction with extracellular receptors and activation of downstream signaling pathways. 2) Fusion with the plasma membrane or 3) Internalization through endocytosis or micropinocytosis (Butreddy, Kommineni, & Dudhipala, 2021; Hamzah, Alghazali, Biris, & Griffin, 2021; van Niel, D'Angelo, & Raposo, 2018).

1.9.1 Cell signaling from the cell surface

In this pathway, the intraluminal cargo is not necessarily essential for communication. While, the interaction between surface molecules on exosomes such as tetraspanins, immunoglobulins, and proteoglycans with the surface receptors of recipient cells can trigger a downstream signaling cascade (Gurung et al., 2021).

For example, certain exosomes contain membrane-associated molecules, such as MHC class I and II, which can interact with T lymphocytes, leading to an immune response (Tkach et al., 2017). In addition, exosomes released from dendritic cells can enhance caspase activation and induce apoptosis by interacting with ligands expressed on the surfaces of tumor cells, such as tumor necrosis factor (TNF), Fas ligand (FasL), and TNF-related apoptosis-inducing ligand (TRAIL), which then interact with TNF receptors (Munich, Sobo-Vujanovic, Buchser, Beer-Stolz, & Vujanovic, 2012). Another example involves fibronectin present on exosomes that can bind to the integrins in fibroblast cells. This binding leading to the activation of downstream signaling pathways involving focal adhesion kinase (FAK) and Src family kinases (SFKs), which are associated with invasion and migration (Chanda et al., 2019).

1.9.2 Fusion with the plasma membrane

Exosomes can also directly fuse with the cell membrane and subsequently release their content into the cytosol of receiving cells (Montecalvo et al., 2012; Parolini et al., 2009). The first step of this pathway involves bringing the two membranes within a distance of less than 10 nm, with the help of some cell-adhesion machinery and specialized proteins such as fusogens, ligand-receptors, or glycoproteins, in order to provide the necessary energy (Petrany & Millay, 2019; Whitlock & Chernomordik, 2021).

There is some evidence supporting the direct fusion delivery method. Fluorescent lipid dequenching, using a probe like R18, has been utilized to study this process. R18 is incorporated into the exosome bilayer at self-quenching concentrations, and its fluorescence is de-quenched upon fusion with unlabeled recipient membranes, allowing monitoring of membrane fusion event. They have demonstrated the significance of cholesterol in the cellular membranes of receiving cells for exosomal membrane fusion. Depleting cholesterol from the acceptor cells effectively prevented the fusion processes (Montecalvo et al., 2012). This process has been observed in dendritic cells as well as tumor cells. Moreover, it has been suggested that the low pH of the tumor microenvironment could contribute to increased cell membrane rigidity, increased sphingomyelin, and enhanced exosome fusion (Parolini et al., 2009).

1.9.3 Internalization

Although fusion between EVs and the plasma membrane of recipient cells could be considered the most efficient method for cargo delivery into the cell, endocytosis seems to be the primary pathway for exosome cargo delivery into recipient cells (Mulcahy, Pink, & Carter, 2014).

Next paragraphs describe possible EV uptake mechanisms, which are represented in Figure 10.

1.9.3.1 Phagocytosis

Phagocytosis is the cellular process of engulfing large particles (>0.5μm), like dead cells or bacteria through the invagination of the plasma membrane. This internalization requires receptor-mediated recognition. These foreign particles are then engulfed within vacuoles called phagosomes, which subsequently mature and fuse with the EEs and LEs and finally lysosomes to form a phagolysosome (Dixon, Mekhail, & Fairn, 2021; Nguyen & Yates, 2021) (Levin, Grinstein, & Canton, 2016).

Phagolysosomes are specialized compartments containing a variety of enzymes, such as Phosphatidylinositol-3-kinase (PI3K) and phospholipase C, which play a crucial role in breaking down the phagocytosed particles (Gillooly, Simonsen, & Stenmark, 2001). Research

has demonstrated the significance of PI3K in the internalization of leukemia-derived exosomes by macrophages. Blocking PI3K using antibodies, significantly reduced the ability of macrophages to phagocytose leukemia exosomes (Feng et al., 2010). Additionally, it is known that EVs released by malignant cells bear PS on their outer surface. This PS can bind to surface receptors on recipient cells and trigger phagocytosis (Donoso-Quezada, Ayala-Mar, & González-Valdez, 2021).

The activity of the actin cytoskeleton is essential for the regulation of phagocytosis since actin filaments coat and surround the phagosome. Thus, disruption of actin prevents the formation of these structures (Ju, Guo, Edman, & Hamm-Alvarez, 2020).

This pathway is predominantly used by immune cells like monocytes, macrophages, and dendritic cells. However, under specific circumstances, it can be utilized by other cells like fibroblasts, endothelial cells, and epithelial cells (El-Sayed & Harashima, 2013).

1.9.3.2 Macropinocytosis

Unlike other endocytic pathways, macropinocytosis does not originate from receptor binding or cell surface contact, like phagocytosis (Kerr & Teasdale, 2009). Macropinocytosis is a pathway of endocytosis, which allows the nonspecific internalization of large amounts of fluid and solutes into circular cups. These cups are formed through actin polymerization at the plasma membrane, called membrane ruffles. The regulation of Rho-family GTPase promotes this actin polymerization (Lim & Gleeson, 2011; Lim, Gosavi, Mintern, Ross, & Gleeson, 2015). Ruffles can entrap droplets of the medium into large vesicles called macropinosomes (>250 nm diameter). PI3K has been demonstrated to participate in the formation of macropinosomes, which are eventually transferred and digested in the endo/lysosomal system. (Buckley & King, 2017; Stow, Hung, & Wall, 2020; J. T. Wang, Teasdale, & Liebl, 2014).

Micropinocytosis has been shown to be important in cellular processes, like antigen presentation, pathogen invasion, migration, signaling, and protein recycling (Lin, Mintern, & Gleeson, 2020).

A growing number of researchers indicate that macropinocytosis plays an important role in the uptake of exosomes. pharmacological inhibitors targeting PI3K, like wortmannin, have been used to investigate this process, and it has been demonstrated that trophoblast-derived exosome internalization by placental cells is reduced (H. Li et al., 2020). Moreover, using DMA, which disrupts microtubule polymerization, significantly decreases the uptake of macrophage-derived exosomes into vascular smooth muscle cells (Z. Wang et al., 2019).

1.9.3.3 Clathrin-mediated endocytosis

Clathrin-mediated endocytosis is a receptor-mediated pathway that occurs in both cancer and healthy cells in order to maintain membrane homeostasis, facilitate nutrient uptakes (e.g., iron or cholesterol), and regulate cell-to-cell communications (Tarasenko & Meinecke, 2021). Clathrin is composed of three clathrin heavy chains (B190 kDa) and three clathrin light chains (B25 kDa) which assemble into a triskelia scaffold, forming clathrin-coated vesicles (Kaksonen & Roux, 2018). The interaction between clathrin molecules and the extracellular cargo is triggered by the recruitment of adaptor proteins (Luo et al., 2019). This interaction initiates a cascade of protein-lipid interactions, including phosphatidylinositol 4,5-bisphosphate (PI(4,5)P2), resulting in a conformational change in adaptor protein 2, which in turn leads to the formation of clathrin-coated vesicle (Behzadi et al., 2017; Kadlecova et al., 2017; Kaksonen & Roux, 2018). This process is rapid, with the formation of pits that undergo invagination, finally forming clathrin-coated vesicles within 30–120 sec (Ju et al., 2020). Clathrin-coated vesicles occupy 0.5–2% of the cell surface and have an average diameter of ~100 nm s (Joseph & Liu, 2020; Kaksonen & Roux, 2018; Merrifield, Perrais, & Zenisek, 2005).

The internalization of exosomes by cardiomyocytes (Eguchi et al., 2019) and immune cells (Morishita et al., 2021) was diminished by using Chlorpromazine, which inhibits the assembly of clathrin-coated vesicles. Another cell-permeable clathrin inhibitor known as PitStop2(PS2), which selectively binds to clathrin and blocks clathrin-mediated endocytosis, also reduced exosome uptake (von Kleist et al., 2011). Finally, it has been demonstrated that altering the expression of the clathrin-heavy chain using siRNA effectively inhibited exosome uptake by macrophages.

Dynamin, a large mechanical GTPase, forms a collar-like structure around the neck of invaginations to pinch off vesicles from the plasma membrane through GTP hydrolysis (Cocucci, Gaudin, & Kirchhausen, 2014; Ehrlich et al., 2004). Dynasore, which interferes with the GTPase activity of dynamin and quickly blocks the formation of coated vesicles (Macia et al., 2006), was found to inhibit exosome uptake by Hek293T (Joshi, de Beer, Giepmans, & Zuhorn, 2020), hepatocytes, and myeloma cells (X. Li et al., 2021; Tu et al., 2021). However, it is important to note that dynamin also participates in clathrin-independent endocytosis (Henley, Krueger, Oswald, & McNiven, 1998).

All these evidences suggest that clathrin-mediated endocytosis can serve exosome uptake.

1.9.3.4 Caveolae-mediated endocytosis

Caveolae-mediated endocytosis was discovered ~60 years ago as another potential endocytic pathway (Yamada, 1955). Caveolins are integral membrane proteins, which form omega-

shaped plasma membrane invaginations, creating small flasks with a diameter of 50–100 nm, called caveolae. Caveolae are abundant on the plasma membranes of most eukaryotic cells, although they are not present in every cell.

Among caveolin proteins, caveolin-1 is the most common structural protein, which belongs to the caveolin protein family. Caveolin-1 is embedded within the inner leaflet of the membrane bilayer. According to biochemical studies, caveolae are detergent-resistant and enriched in highly hydrophobic membrane lipids such as cholesterol and sphingolipids (Estadella et al., 2020; Mazumdar, Chitkara, & Mittal, 2021; Shin, Soung, Schwartz, & Kim, 2021).

It has been demonstrated that caveolae-mediated endocytosis plays an important role in many crucial biological processes, such as inducing cell signaling, and regulation of lipids, membrane proteins, and fatty acids in both cancerous and healthy cells (Donahue, Acar, & Wilhelm, 2019; Foroozandeh & Aziz, 2018).

Knockdown of caveolin using shRNA reduces the internalization of tumor-derived exosomes in myeloma cells (Tu et al., 2021), and genistein, a tyrosin-kinase inhibitor known to block caveolae-mediated endocytosis, reduced uptake of endothelial progenitor cell-derived exosomes (J. Wang, Li, Cheng, & Liu, 2020).

1.9.3.5 Lipid-raft mediated endocytosis

A variety of cellular processes are mediated by lipid rafts, including cell adhesion, membrane trafficking, and signal transduction (Helms & Zurzolo, 2004; Lajoie & Nabi, 2007). In particular, lipid rafts appear to be critical for lipid and protein sorting during endocytic and secretory processes (Gagescu et al., 2000). Several functions of lipid raft endocytosis have been described, including pathogen entry (Pelkmans, Kartenbeck, & Helenius, 2001), recycling of extracellular ligands (Benlimame, Le, & Nabi, 1998), and endocytosis of glycosylphosphatidylinositol(GPI)-anchored proteins (El-Sayed & Harashima, 2013; Nichols et al., 2001). Lipid rafts are enriched in cholesterol, sphingolipids, and GPI-anchored proteins (Mulcahy et al., 2014). Metabolic perturbation of these lipids affects exosome uptake.

For instance, the use of Methyl-β-cyclodextrin to disrupt intracellular cholesterol transport results in reduced exosome uptake by breast cancer cells (Koumangoye, Sakwe, Goodwin, Patel, & Ochieng, 2011). Pretreatment of dendritic cells with sphingolipid synthesis inhibitor impairs exosome uptake (Izquierdo-Useros et al., 2009). Therefore, lipid raft-mediated endocytosis represents one of the pathways involved in exosomal uptake.

All These different pathways of exosome entry can co-exist within a single cell. For example, exosome uptake by ovarian tumors and melanoma cells was demonstrated to simultaneously

occur through cholesterol-associated lipid rafts, clathrin-mediated endocytosis, phagocytosis, as well as micropinocytosis (Emam et al., 2018; Plebanek et al., 2015).

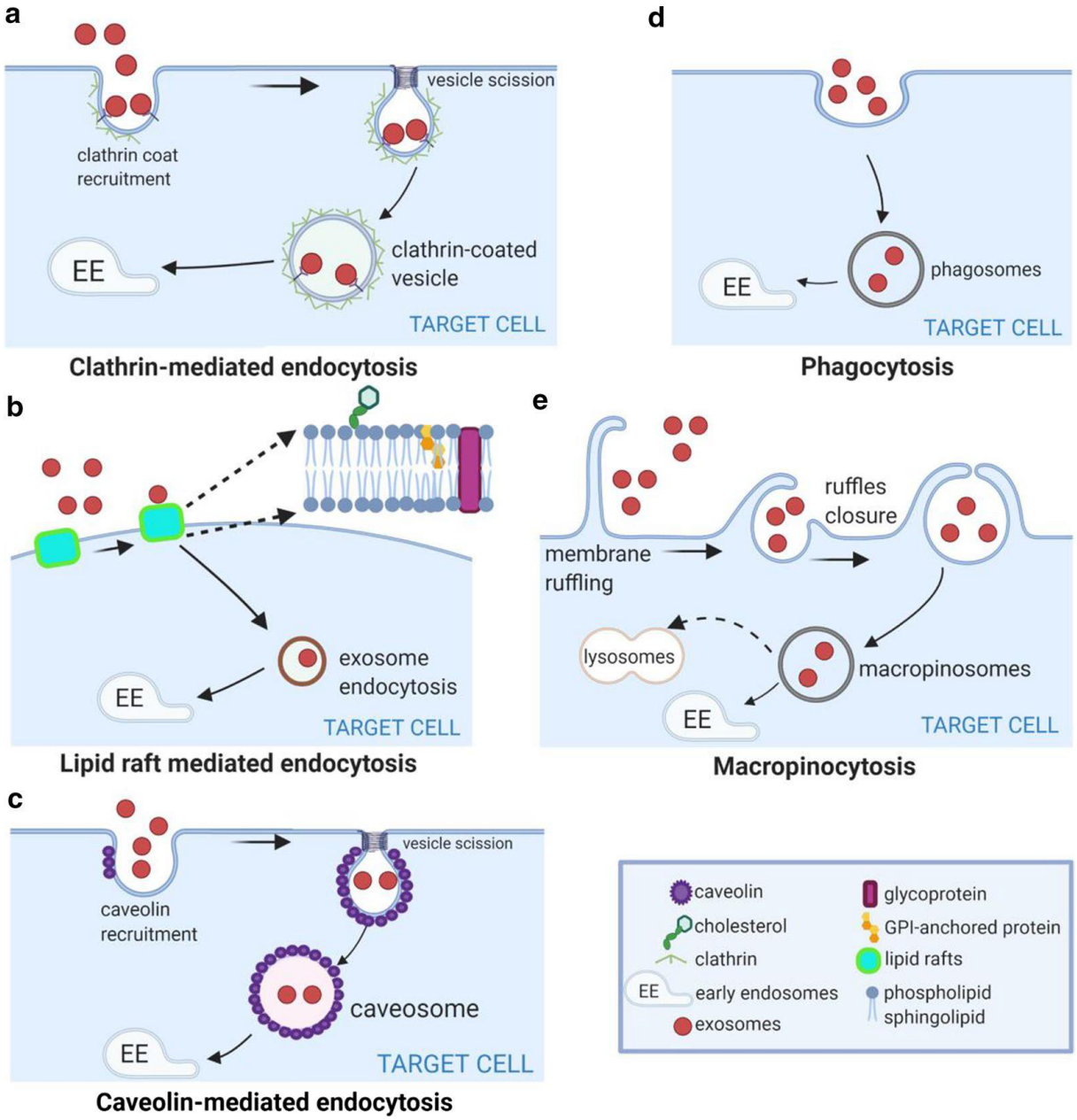

Figure 10: **Exosome internalization through endocytosis**.

Adapted from (Gurung et al., 2021)

Different endocytic pathways:

a. Clathrin-mediated endocytosis.
b. Lipid-raft mediated endocytosis.
c. Caveolin-mediated endocytosis.
d. Phagocytosis.
e. Macropinocytosis.

1.10 The fate of internalized exosomes (Endosomal escape)

As we know, EVs are heterogonous and use different mechanisms of internalization that may influence the fate of their content. Understanding the functional implications of cargo transferred by EVs needs a comprehensive knowledge of the final step after internalization (Corbeil et al., 2020; Mathieu, Martin-Jaular, Lavieu, & Théry, 2019).

Following endocytosis, all materials are internalized and directed to the early endocytic pathway (van Niel et al., 2018). once in endosomes, lysosomes have been suggested as a potential termination point of EVs, as in the case of exosomes from DU145 prostate cancer cells, which were cleared within lysosomes of Hela cells (Heusermann et al., 2016; Roberts-Dalton et al., 2017). To maintain the functional effects of EVs content, it is necessary for the cargo to escape from endosomal-lysosomal confinement. This escape may happen within EEs, LEs, or in the lysosome. It may occur by fusion between EVs and endosomal membrane (Le Blanc et al., 2005) endosomal rupture, or endosomal permeabilization (Joshi et al., 2020; Varkouhi, Scholte, Storm, & Haisma, 2011).

Li H. et al., demonstrated that trophoblast-derived exosomes containing miRNA517a could deliver and reach RNA-induced silencing complex (RISC) proteins, and colocalized with P-bodies—a key site for cytoplasmic RNA regulation. The data suggest endocytic escape of exosomal miRNA (H. Li et al., 2020). Yao Z, et al., have demonstrated that exosomes can interact with LEs/MVBs and release their contents at this level by using a dequenching R18 probe (Yao et al., 2018). Moreover, this process could be facilitated by LBPA, also known as BMP, an anionic lipid that is present in the endosomal membrane that is involved in ILV formation. LBPA is closely related to virus endosome penetration and is regulated through interaction with the protein Alix (Matsuo et al., 2004).

Joshi et al., used GFP-CD63-containing exosomes incubated with Hek cells expressing a cytosolic anti-GFP nanobody fused to mCherry (anti-GFP fluobody). Once exosomes fused with the endosomal membrane, the GFP inside the exosomes became exposed to the anti-GFP fluobody in the cytosol of receiving cell. They also showed colocalization between the exosomes and fluobody within LEs and lysosome compartments using correlative light and electron microscopy (CLEM). Eventually, they have been revealed that acidic pH and cholesterol accumulation within the late endosome facilitated such fusion (Bonsergent & Lavieu, 2019; Joshi et al., 2020).

1.10.1 Back-fusion of ILVs to the endosome limiting membrane: a pathway for EVs entry

CD63 has been shown to recycle within the endocytic pathway of endothelial cells (Kobayashi et al., 2000) or MHC II is exported from the late endosome to the plasma membrane (Murk, Stoorvogel, Kleijmeer, & Geuze, 2002). Immunogold electron microscopy has detected Mannose-6-phosphate receptors, which are known to cycle between the Golgi and endosomes rather than lysosomes, suggesting potential escape from ILVs through back-fusion (Geuze, Slot, Strous, Hasilik, & von Figura, 1985). In general, the delivery process of intraluminal proteins to other cell destinations needs their transportation to the endosome limiting membrane through membrane fusion of ILVs with the limiting membrane of the endosome (van der Goot & Gruenberg, 2006). Thus, it has been speculated that the commitment to ILVs is not a terminal event and that the back-fusion of ILVs to the limiting membrane of endosomes might represent a return pathway.

A recent study in 2021 used an elegant chemically controlled system to demonstrate that back fusion indeed exists. Here, the authors used cells expressing in the cytosol two inactive parts of a protease capable of cleaving a protein made of CD63 fused to a GFP with a nuclear localization signal (NLS). Both parts of the protease can be brought together using a "dimerizer", an analog of rapamycin. Upon addition of dimerizer, cleavage of available GFP-CD63 (i.e. GFP exposed in the cytosol unlike the GFP of ILVs) would liberate NLS-GFP which accumulates in the nucleus. This allowed them to show that back-fusion is part of the normal MVB life cycle. Furthermore, they also showed that ILVs inert to back-fusion comprise a significant fraction of exosomes destined for secretion. Perrin et al., also reported that lysosomal pH, cholesterol, and LBPA all have an impact on back-fusion, and all these factors are intimately interconnected. LBPA possesses fusogenic characteristics, which can be affected by changes in pH(Kobayashi et al., 2002). Elevated endosomal pH could disrupt LBPA and its fusogenic properties (Figure 11)(Perrin et al., 2021).

Currently one of the main challenges in using EVs is that there is still limited knowledge underlying the mechanisms of EVs cargo release into the cytoplasm. The mechanism of back-fusion is distinct from intracellular fusion mediated by SNARE complexes. In back-fusion, the luminal face of the MVB membrane undergoes fusion with the ILVs contained within it, while on the other side, the cytoplasmic face of MVBs regulates fusion with the plasma membrane. In fact, the molecular mechanisms allowing back-fusion remain unknown.

Many researchers in the past suggested that LBPA in the late endosomal membrane and Alix play an important role in the back-fusion process. Additionally, the cytosolic protein Alix interacts with LBPA, which is predominantly found on ILVs and lysosomal membranes, while

very minimally present on MVB-limiting membranes, thereby promoting ILV back-fusion (Möbius et al., 2003). Hence, trapping LBPA in the endosomal lumen potentially reduces the recruitment of Alix and subsequently inhibits back-fusion (Gruenberg, 2020; Showalter et al., 2020).

These findings raise interesting questions as to how cytosolic Alix interacts with LBPA, given its limited presence on MVB limiting membrane? Do the back-fusion processes facilitate LBPA accessibility to cytosolic Alix, eventually contributing to the formation of new ILVs?

Thus far, we clearly know that the lipid environment plays a crucial role in back-fusion and endosomal sorting, however many aspects of these processes remain unknown.

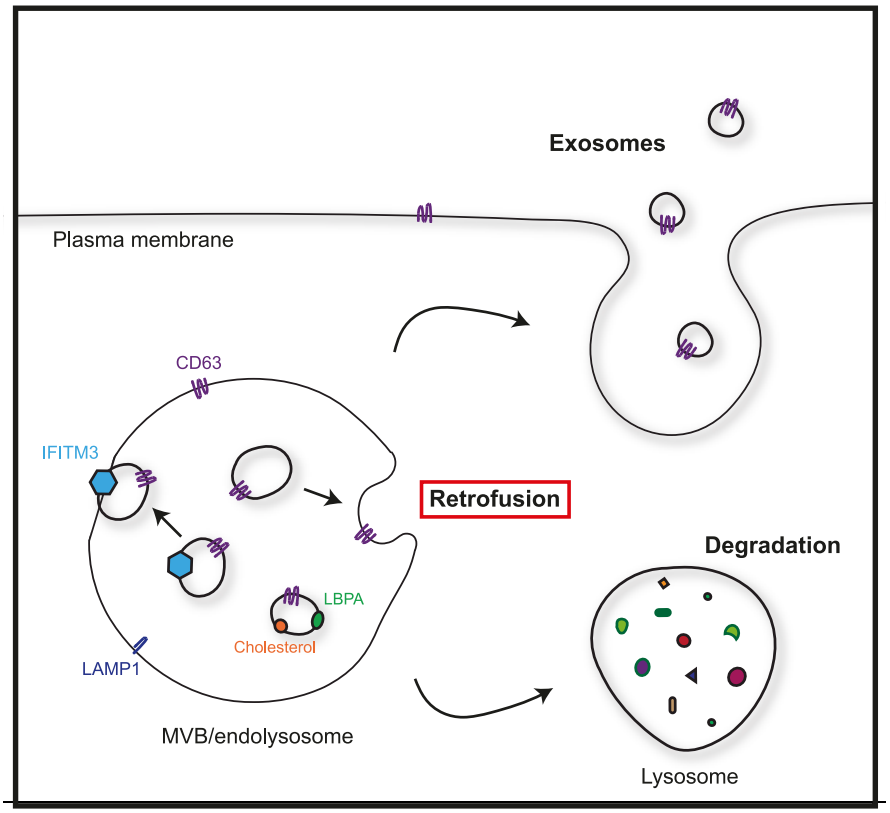

Figure 11: **Alternative fates for ILVs.**

Adapted from (Perrin et al., 2021)

Retrofusion, a process influenced by the lipid environment of the endocytic pathway, was prevented upon cholesterol or LBPA accumulation. interferon-induced transmembrane proteins 3 (IFITM3), promote accumulation of cholesterol in MVBs and block retrofusion.

1.11 Virus fusion

Enveloped viruses acquire a lipid bilayer envelope derived from host cell membranes during their assembly and budding process. This envelope encapsulates the viral particle or virion, protecting the nucleocapsid that contains the viral genetic information (Más & Melero, 2013; Weissenhorn, Hinz, & Gaudin, 2007).

The entry of enveloped viruses into a new host cell involves several steps. First, glycoproteins present on the virus surface mediate the interaction between the virus and the host cell during the infection process (Cossart & Helenius, 2014; Grove & Marsh, 2011; Mercer, Schelhaas, & Helenius, 2010). Then the viruses can enter host cells through endocytic processes. The major pathway is clathrin-mediated endocytosis, which is used by semliki forest virus (SFV) (Helenius, Kartenbeck, Simons, & Fries, 1980) and vesicular stomatitis virus (VSV) (Matlin, Reggio, Helenius, & Simons, 1982). Once inside the cell, most enveloped viruses navigate through canonical endocytic pathways involving early endosomes, late endosomes, or endolysosomes. Depending on the environmental cues, they can fuse with the membranes of the respective compartments (Amara & Mercer, 2015; Mercer & Helenius, 2012). Membrane fusion is a critical process for enveloped viruses to deliver the nucleocapsid, including the viral genome and proteins, into the host cell cytoplasm, thereby initiating a new infection cycle. The fusion protein present in enveloped viruses facilitates membrane fusion (Más & Melero, 2013; Weissenhorn et al., 2007). It has been demonstrated that enveloped viruses entering cells through endosomes require an acidic pH to initiate the fusion process. The pH level within the endosome plays a key role in determining the virus's ability to fuse and enter the host cell, eventually leading to infection (Cox et al., 2015; Miyauchi, Kim, Latinovic, Morozov, & Melikyan, 2009). The pH dependence of fusion may vary among enveloped viruses, and this variability could be associated with the specific site of fusion within the endosome (Kielian, Marsh, & Helenius, 1986; J. White, Matlin, & Helenius, 1981).

Indeed, different enveloped viruses have variations in their pH requirements for membrane fusion. For example, viruses like SFV and VSV require a slightly acidic environment (~pH 6) to fuse with the early endosomal membrane. In contrast, viruses such as influenza, lymphocytic choriomeningitis virus (LCMV), and Uukuniemi virus (UUKV) require a more acidic environment (~pH 5) found in late endosomes to fuse with host cell membranes (Johannsdottir, Mancini, Kartenbeck, Amato, & Helenius, 2009; Kielian et al., 1986) (Figure 12).

In the case of enveloped viruses mentioned above, the acidic pH alone is sufficient to induce conformational changes in viral glycoproteins and activate the fusion process. However, for other viruses like retroviruses and coronaviruses, low pH may not be enough for membrane fusion and protease activity may also be required (Kielian & Helenius, 1984; Kleinfelter et al.,

2015; Matos et al., 2013; Nieva, Bron, Corver, & Wilschut, 1994; Zaitseva, Yang, Melikov, Pourmal, & Chernomordik, 2010).

This fusion event does not occur simultaneously with the release of the capsid into the cytoplasm. It has been observed that microtubule depolymerization does not affect virus fusion, while it does reduce the viral RNA release into the cytoplasm. This suggests that RNA release and fusion happen sequentially. Specifically, the fusion takes place during the transport of viral particles between early and late endosomes. As a result, the nucleocapsid is released into the ILV lumen within MVBs, where it remains hidden (Le Blanc et al., 2005). Subsequently, ILVs containing the capsid can utilize the back-fusion pathway to release the viral capsid from the ILVs lumen into the cytoplasm (Luyet, Falguières, Pons, Pattnaik, & Gruenberg, 2008)(Figure 13).

Inhibition of viral capsids release into the cytoplasm has been observed when anti-LBPA antibodies or Alix downregulation using siRNA were used (Abrami, Lindsay, Parton, Leppla, & van der Goot, 2004; Le Blanc et al., 2005). Bissig et al., have provided important insights into the role of the protein Alix, and its interacting phospholipid LBPA in the process of RNA release. They demonstrated that LBPA, which exhibits fusogenic properties at the acidic pH of late endosomes (Gruenberg, 2020), recruits Alix onto late endosomes through the calcium-bound Bro-1 domain. This triggers conformation changes and dimerization of Alix, which are crucial for the delivery of viral nucleocapsids to the cytosol (Bissig et al., 2013).

Further key regulator involved in this process is phosphatidylinositol-3- phosphate (PTGFRN) signaling mediated by its binding protein Sorting nexin 16 (Snx16), which supports the invagination of membranes. Inhibition of PI3 kinase disrupts protein sorting into MVBs and reduces ILV formation. In the absence of ILVs, viral fusion happens at the limiting membrane of empty MVBs, facilitating the concurrent delivery of RNA (Le Blanc et al., 2005).

On the other hand, their investigation revealed that TSG101, through specific interactions with Alix, mediates receptor sorting into MVBs. Although this interaction is not necessary for viral fusion with ILVs, it is crucial for the release of the nucleocapsid from within MVBs to the cytoplasm, thus controlling the back-fusion process. Both TSG101 and Alix proteins appear to have distinct but coordinated roles in controlling this process (Bissig & Gruenberg, 2014; Falguières et al., 2008; Luyet et al., 2008).

Gräße et al., revealed that the transport of endocytosed viral particles to MVBs was prevented in HPV 16 cells depleted of CD63 or syntenin-1. They also highlighted the essential role of Alix, which acts as a partner for syntenin-1, in HPV infection. Thus, they suggested that the interaction between CD63, syntenin-1, and Alix is important for HPV capsid disassembly and, eventually, viral infection. (Gräßel et al., 2016).

Once the appropriate lipid composition, regulatory factors, and pH conditions are suitable, ILVs undergo back-fusion with the limiting membrane, leading to the release of viral contents (Kobayashi et al., 1998; Saeed, Kolokoltsov, & Davey, 2006).

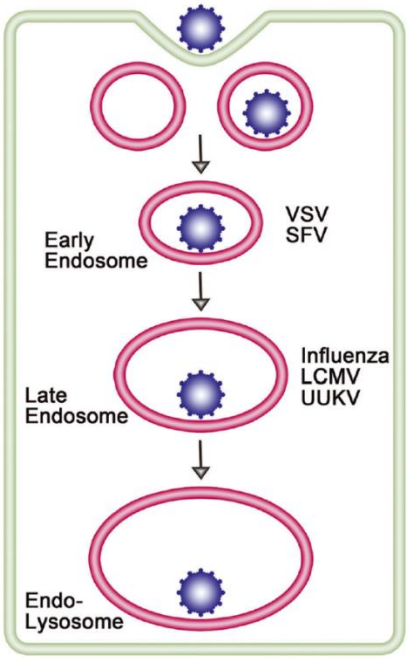

Figure 12: **Enveloped virus fusion**.

Adapted from (J. M. White & Whittaker, 2016).

Enveloped virus entry through different endosomal compartments.

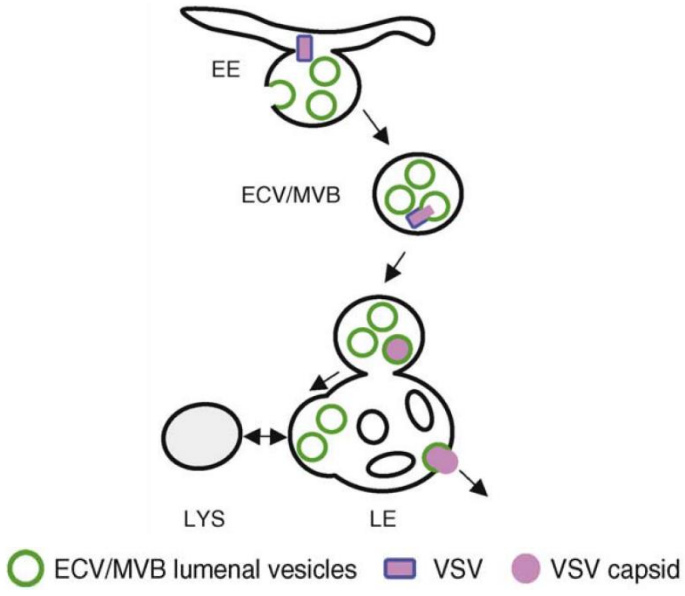

Figure 13: **Pathway followed by VSV capsids**.

Adapted from (Gruenberg, 2009).

Endocytosed VSV particles enter early endosomes (pH 6.2) which then mature into MVBs (pH 5.0). VSV envelope fuses with ILV membranes, leading to the release of the viral capsid into the ILV lumen, where it remains hidden. Eventually capsid delivery to the cytoplasm through back-fusion of late endosomes with the limiting membrane.

1.12 The protein Alix

Alix, also known as ALG-2 interacting protein X, or PDCD6IP (programmed cell death 6 interacting protein), and apoptosis interacting protein 1 (AIP1), is a highly conserved cytosolic protein present in various eukaryotic cells. It exhibits a broad expression across different organisms, ranging from yeast to zebrafish, highlighting its significance in cell biology research. Initially identified for its calcium-dependent nature and association with the apoptosis-linked gene 2 (ALG-2), Alix has been implicated in numerous cellular pathways, including endosomal sorting and trafficking, viral budding, cytokinesis, and apoptosis, among others (Missotten, Nichols, Rieger, & Sadoul, 1999; Vito, Pellegrini, Guiet, & D'Adamio, 1999) (Figure 14).

Comprised of 868 amino acids (96 kDa), Alix consists of three distinct protein domains. The N-terminal Bro1 domain spans 358 amino acids and adopts a helical triangle-shaped fold known as an 'α-helical hairpin.' Positioned between amino acids 362 and 702, the central domain forms a V-shaped structure comprising eleven α-helices that create two arms. Lastly, the C-terminal proline-rich domain (PRD) is a flexible region consisting of 166 amino acids (Bissig & Gruenberg, 2014). An illustration in Figure 15 showcases Alix's interactions with several binding partners.

The Bro1 domain exhibits a high affinity for calcium, primarily mediated by its Asp97 and Asp178 amino acid residues. Additionally, the Lys104 and Phe105 residues within this domain facilitate binding to LBPA. Moreover, Alix interacts with the ESCRT-III protein CHMP4 through its Bro1 domain. Another interaction involves Alix binding to the SH2 domain of Src, leading to Alix phosphorylation. This phosphorylation event enhances Alix's interaction with different partners (Bissig et al., 2013; Dejournett et al., 2007; Matsuo et al., 2004; M. H. H. Schmidt, Dikic, & Bögler, 2005; Zhou et al., 2009). The Bro1 domain of Alix binds to Gag NC of HIV. It has been shown that RNA bridges interaction between NC and Bro1. This nucleoprotein complex recruits CHMP4 during virus budding process (Sette, Dussupt, & Bouamr, 2012).

Following the Bro1 domain, Alix contains coiled-coils regions that contribute to the formation of the V-domain. Through the V-domain, Alix is capable of forming dimers by folding together in a head-to-tail arrangement (Pires et al., 2009; Strack, Calistri, Craig, Popova, & Göttlinger, 2003). This V-shaped domain of Alix plays a crucial role in recognizing and interacting with the YPXL motif present in the p6 Gag protein of HIV-1 and the p9 Gag protein of EIAV, thereby facilitating virus budding from the plasma membrane (Strack et al., 2003). Additionally, the V-domain interacts with other proteins, such as the YPX3L motif in protease-activated receptor 1 (PAR1) (Dores et al., 2012), syntenin (Baietti et al., 2012), and ubiquitin

(Dowlatshahi et al., 2012). Furthermore, a study using truncated forms of Bro1 and V domains suggests that Alix interacts with components involved in actin polymerization through these two domains (Pan et al., 2006).

The C-terminal PRD domain of Alix, rich in proline and tyrosine residues, interacts with centrosomal protein 55 (CEP55), which recruits CHMP4B and Cbl-interacting protein of 85 kDa (CIN85), as well as endophilin (Chatellard-Causse et al., 2002). Other interactors of the PRD domain include the ESCRT-I protein TSG-101 and ALG-2 (Strack et al., 2003). Studies have revealed that the interaction between the SH3 domain of c-Src and the PRD region of Alix increases exosome secretion by activating ESCRT-mediated ILV formation (Hikita et al., 2019).

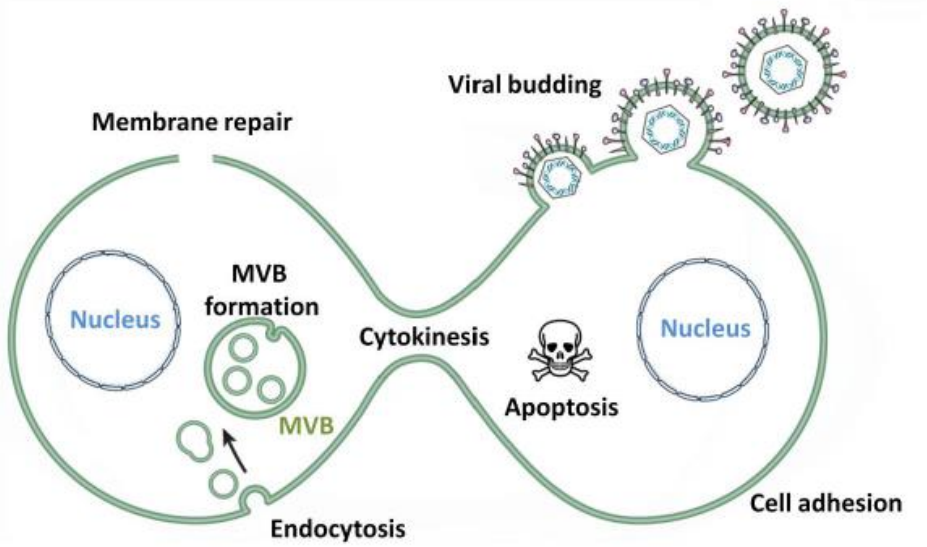

Figure 14: **Cellular processes involving Alix**.

Adapted from (Raiborg & Stenmark, 2009).
The diagram provides an overview of the cellular processes in which Alix is involved.

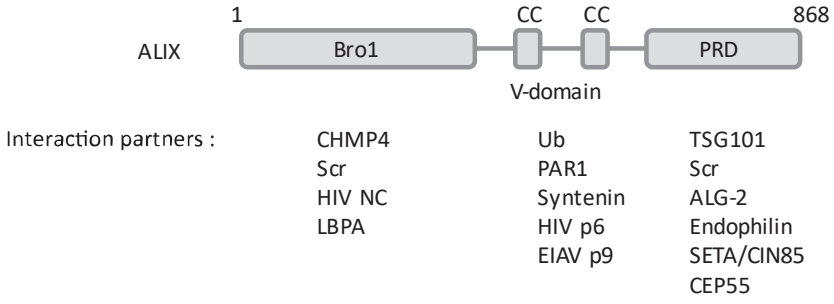

Figure 15: **Schematic representation of the Alix domain and its interactors.**

Adapted from (Bissig & Gruenberg, 2014).
Alix is composed of three domains. (Bro1, V and proline-rich domains, PRD) and the interacting proteins.

1.12.1 The numerous biological functions of Alix

1.12.1.1 Membrane repair

It is widely accepted that calcium is an important signaling molecule in the repair of damaged membranes. When the plasma membrane is damaged, calcium influx occurs at the site of injury, initiating a series of signaling events aimed at facilitating repair (Andrews, Almeida, & Corrotte, 2014). First, ALG-2, a ubiquitous calcium-binding protein, plays a key role. Upon binding calcium, ALG-2 undergoes a conformational change, enabling its interaction with Alix. This interaction serves to recruit downstream components, including late-acting CHMP4B, CHMP3, and CHMP2A subunits, along with the AAA+ ATPase VPS4B, to the site of damage. These recruited components collectively facilitate the excision of the damaged membrane. Studies have demonstrated that the depletion of these proteins leads to impaired membrane repair, albeit to varying extents (Jimenez et al., 2014; Scheffer et al., 2014; Shukla, Larsen, Ou, Rose, & Hurley, 2022). While the precise mechanism of calcium-mediated membrane repair involving Alix remains elusive, it is evident that Alix plays a critical role in this process.

1.12.1.2 Viral budding

Viruses have evolved strategies to exploit the cellular machinery of the host cells in order to replicate their genetic material, synthesize viral proteins, and ultimately exit the host cell. One example is observed in retroviruses, such as HIV-1 and EIAV, which utilize the ESCRT machinery to facilitate their release from host cells (Sundquist & Kräusslich, 2012). Enveloped viruses have specific protein sequences that directly bind to Alix. For example, in EIAV or murine leukemia virus, the p9 Gag protein contains a YPDL sequence motif that interacts with Alix. Studies have shown that silencing Alix expression by RNAi strongly inhibits virions production and virus budding in EIAV and murine leukemia viruses, respectively (Martin-Serrano, Yarovoy, Perez-Caballero, & Bieniasz, 2003; Strack et al., 2003).

In the case of HIV, The PTAP motif of p6Gag interacts with the TSG101 subunit of the ESCRT-I complex, while the YPXnL motif interacts with Alix (Garrus et al., 2001; Strack et al., 2003). These interactions subsequently recruit downstream components of the ESCRT-III complex and VPS4, facilitating the completion of the viral budding process (Figure 16).

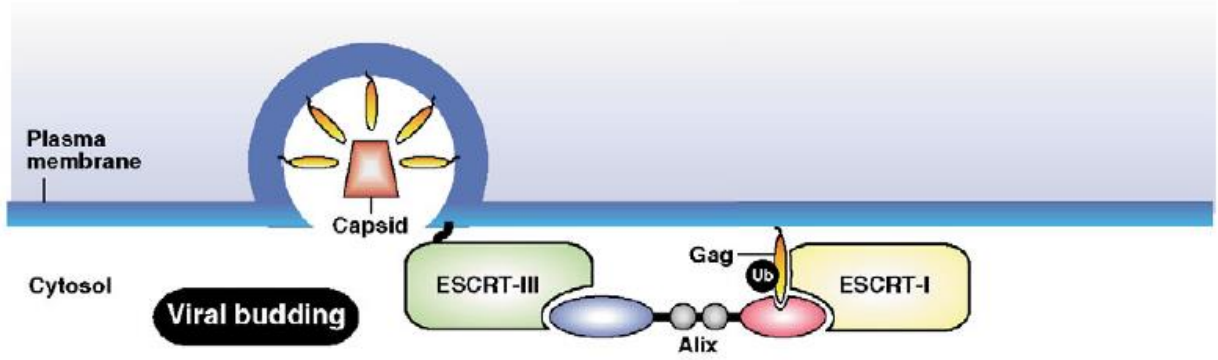

Figure 16: **Role of Alix in viral budding.**
Adapted from (Odorizzi, 2006).
Recruiting Alix to the plasma membrane during viral budding. depicted as a key mediator for ESCRT-I and ESCRT-III,

1.12.1.3 Cell adhesion

Cell adhesion is a fundamental process that involves the attachment and interaction of cells with adjacent cells and the extracellular matrix, and it is closely linked to cell signaling and migration (Hynes, 2002).

The molecular mechanisms underlying focal adhesion, a key aspect of cell adhesion, have been investigated extensively, shedding light on its intricate work. Focal adhesion acts as the connection points between cells and the extracellular matrix, involving different components like actin, integrins, and focal adhesion kinases such as FAK and PYK2 (M. A. Wozniak, Modzelewska, Kwong, & Keely, 2004). Notably, there is evidence that suggests Alix in the regulation of cell adhesion. A study by Schmidt et al., discovered that Alix interacts with CIN85 and localizes to focal adhesion sites, where it associates with FAK and PYK2, thereby preventing their activation. The phosphorylation of Alix by Src has been shown to disrupt its interaction with CIN85, leading to the loss of its inhibitory effect on focal adhesions and resulting in enhanced cell adhesion. These findings highlight the regulatory role of Alix in modulating cell adhesion (Odorizzi, 2006; M. H. H. Schmidt, Chen, Randazzo, & Bogler, 2003; M. H. H. Schmidt et al., 2005).

Furthermore, Alix has been found to directly interact with components of the actin cytoskeleton (Pan et al., 2006) further supporting its involvement in the regulation of cell adhesion.

1.12.1.4 Cell death

Apoptosis is a genetically regulated process of programmed cell death, which is mediated by caspases, a family of cysteine proteases. There are two main pathways that can initiate apoptosis: The intrinsic pathway and the extrinsic pathway.

The intrinsic pathway involves signals originating within mitochondria, known as the mitochondrial pathway. The main initiator of this pathway is the release of Cytochrome-C, which activates caspase 9. The extrinsic pathway is initiated by interactions mediated by transmembrane death receptors. The best ligands include FasL/FasR, and TNF-α/TNFR1 bind to death receptors leading to the activation of caspase 8 (Elmore, 2007).

Alix initially identified as a molecule that interacts with ALG-2, a calcium-binding protein involved in programmed cell death, has been implicated in apoptosis. In adult rats, Alix expression is upregulated in striatal neurons degenerating in a model of Huntington's disease and hippocampal neurons in a model of epilepsy (Blum et al., 2004; Hemming, Fraboulet, Blot, & Sadoul, 2004). Moreover, upregulation of Alix induces cell death in cerebellar granule neurons, while a truncated form of Alix or the C-terminal half of Alix (Alix-CT) blocks its interaction with ALG-2/ESCRT and promotes neuronal survival. The binding of Alix to ALG-2 needs a 12 amino acid segment in the C-terminal PRD domain. Overexpression of AlixΔALG-2, lacking the ALG-2 binding site, reduces apoptosis in chick embryos, emphasizing the essential role of the interaction between Alix, ALG-2, and ESCRTs complexes in cell death (Trioulier et al., 2004).

The interaction of Alix and ALG-2 is essential for the recruitment and activation of pro-caspase-8 on endosomes containing TNF-R1. Moreover, the expression of a mutant form of Alix (AlixΔALG-2) significantly prevents cell death without affecting TNFR1 endocytosis (Mahul-Mellier et al., 2008).

According to these findings, Alix appears to play a crucial role in the process of apoptosis, which is heavily reliant on its interaction with other proteins.

1.12.1.5 Cytokinesis

Cytokinesis is the last step of mitotic cell division, which involves the division of the cell's cytoplasm into two daughter cells. In the final stage of cytokinesis, a delicate membrane tubule needs to be resolved from the inside, to enable the separation of the two daughter cells (D'Avino, Giansanti, & Petronczki, 2015). This crucial step is mediated by various proteins such as CEP55 that localizes to a central position within the midbody. During the scission stage of cytokinesis, both Alix and TSG-101 have been shown to interact with CEP55 through the GPP motif in their PRD domain (Morita et al., 2007). This interaction is responsible for the recruiting CHMP4, a

component of the ESCRTIII complex, which assembles and polymerizes to form filaments that help in cytokinesis (Carlton, Agromayor, & Martin-Serrano, 2008; Guizetti et al., 2011). Eventually, the disassembly of CHMP4 is carried out by Vps4, facilitating the scission process (Elia, Sougrat, Spurlin, Hurley, & Lippincott-Schwartz, 2011). These findings demonstrate the important role played by Alix and TSG-101 in cytokinesis.

1.12.1.6 Endocytosis

Alix appears to play a negative regulatory role in the endocytosis of growth factor receptors on plasma membranes, specifically prior to ESCRT-mediated endosome protein sorting. Upon binding to ligands, the epidermal growth factor receptor (EGFR) becomes activated, leading to its internalization through endocytosis. This process is facilitated by the ubiquitylation of the receptor's cytosolic domain, which recruits Cbl. Cbl, in turn, recruits and phosphorylates CIN85/SETA along with endophilin, forming a complex that promotes receptor internalization (Soubeyran, Kowanetz, Szymkiewicz, Langdon, & Dikic, 2002).

However, Alix competes with Cbl to interact with SETA. The PRD domain of Alix binds to the SH3 domain of SETA, preventing the formation of the endocytic complex. The results of Schmidt, et al., in Hela cells, showed that overexpressed Alix completely sequestered the SETA-endophilin complex, preventing its binding to Cbl. Interestingly, this resulted in a reduction in the endocytosis of EGFR (M. H. H. Schmidt et al., 2004). Src, a protein kinase, regulates the inhibitory effect of Alix by binding its SH2 and SH3 domains to the Bro1 and PRD domains of Alix, respectively. This leads to the phosphorylation of Alix, blocking its ability to interact with SETA and causing its relocation to the cytosol (M. H. H. Schmidt et al., 2005) (Figure 17).

These results conflict with another experiment conducted by Mercier et al., in 2016, which used mouse embryonic fibroblast (MEF) cells. Their study showed that using a high concentration of EGF (which triggers clathrin-independent endocytosis, CIE, of the EGFR) resulted in delayed degradation in Alix ko cells. In contrast, no effect of the absence of Alix was detected on clathrin-mediated endocytosis of the EGFR induced by a low concentration of EGF (Mercier et al., 2016). It is important to note that the previous studies were conducted in Hela cells using low concentrations of EGF. Thus, the discrepancies between both studies may simply arise from these differences in cell type and EGF concentration. Alix was also demonstrated to be necessary for clathrin-independent endocytosis. In the Alix KO MEFs, the internalization of cholera toxin chain B and the β chain of interleukin-2 receptor both of which depend on CIE, were significantly impaired. Notably, the uptake of transferrin receptors through clathrin-mediated endocytosis remains unaffected. It has been shown that the interaction between Alix

and CIN85, as well as endophilin, is indispensable for cargo internalization via CIE and the regulation of cell migration (Mercier et al., 2016).

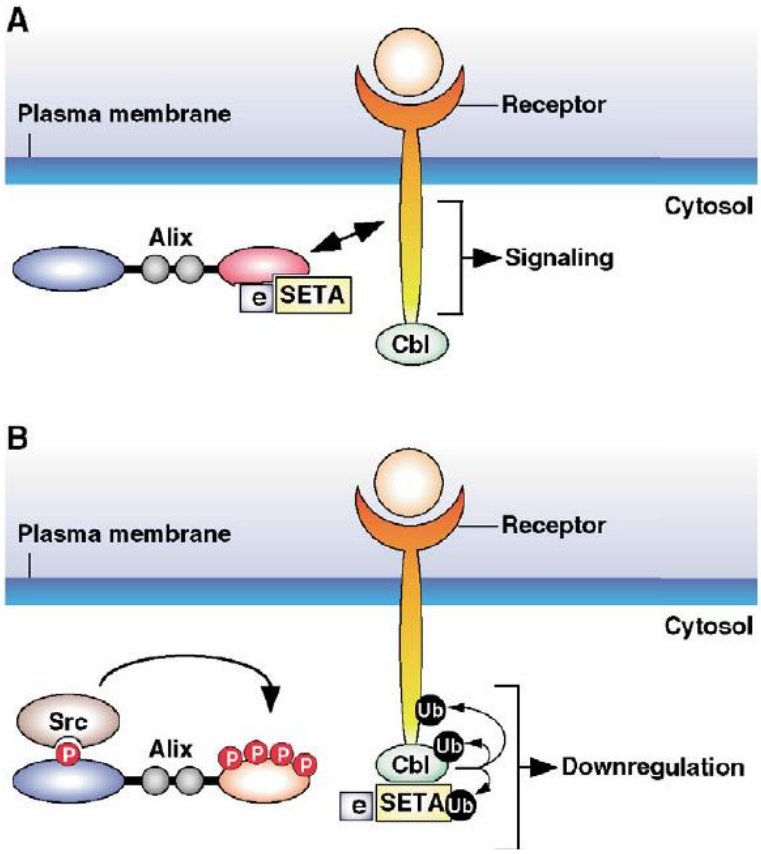

Figure 17: **Role of Alix in EGFR endocytosis.**

Adapted from (Odorizzi, 2006).

A. In the non-phosphorylated form, Alix inhibits the interaction between the endophilin-SETA complexes with Cbl, thereby preventing the endocytosis of EGFR.

B. Upon Alix phosphorylation by Src, Alix undergoes a conformational change that prevents its interaction with the endophilin-SETA complex. This enables CbI to bind to the endophilin-SETA complex, mediating the ubiquitylation and promoting receptor endocytosis.

1.13 Aim of the Thesis

Extracellular vesicles (EVs) are recognized to play an important role in physiological and pathological intercellular communication processes. EVs carry lipids, proteins, and microRNAs which can be shuttled between cells, thereby allowing intercellular communications. The transfer of biologically active EVs cargoes into receiving cells begins with endocytosis of the EVs which are thought to fuse with the endosomal membrane. This is analogous to the content delivery of some enveloped viruses, which requires their fusion with the endosomal membrane in a way dependent on acidic pH and the protein Alix.

Many years ago, Rémy Sadoul's laboratory conducted the first study of EVs derived from neurons and showed the interaction and internalization of EVs derived from neurons or neuroblastomas by other neurons. Although unpublished, their data suggests that Alix is not indispensable for EV formation and secretion. However, they showed that the absence of Alix protein greatly affects the delivery of EVs contents to the cytosolic compartment of receiving cells, a function related to its ability to regulate enveloped viral infection and the back fusion process in the endosome.

The aim of my thesis is to characterize the molecular mechanisms driving the fusion of EVs with target membranes of cells or liposomes. For this, we used luciferase complementation assay to follow the fusion of EVs to membranes of receiving cells and fluorescence membrane-mixing assay to quantify EV membrane fusion to liposomes. We also intend to test if alike viruses, Alix is required for the fusion of EVs with endosomal membranes.

Finally, we examined how Alix is associated with EVs, as the protein had been reported to be both cytosolic and extracellular suggesting that it can cross membranes.

Chapter 2 MATERIAL & METHODS

2.1 Plasmids

To generate HiBitCD63-myc, HiBit-Linker primers were inserted into hCD63-Myc pcDNA3.1 using the BamH1 site. The Hsp70 cDNA was obtained from mouse brain cDNA by RT-PCR. For amplification, a forward primer incorporating the HiBit sequence and a reverse primer containing the myc sequence was used. The resulting HiBitHsp70-myc cDNA was inserted into the expression vector LgBit (pCMV-LgBiT vector, Promega). To facilitate this insertion, the LgBit sequence within the vector was excised using restriction enzymes Nhe1 and Xba1. The HiBitHsp70-myc cDNA was then integrated into the vector at the excision site, replacing the removed LgBit sequence.

To facilitate the production of proteins fused with HiBit and myc tags, the LgBit sequence in the LgBit expression vector was replaced by a HiBit-myc sequence with a Nhe1 restriction site positioned between the HiBit and the myc region, using inverse PCR. This vector is named pHiBit-myc.

HiBit-Alix-myc was obtained by inserting the mAlix sequence amplified from pFlag-Alix into the pHiBiT-myc vector using the Nhe1 site. Rab5-LgBit and Rab7-LgBit were obtained by amplifying and inserting Rab5 or Rab7 cDNA at the N-terminus of LgBit within the pCMV-LgBit vector using the Nhe1 site. To obtain CD63-pHluorin, the Super Ecliptic pHluorin cDNA was amplified via PCR from pSPORT6 CD63-pHluorin (gift from Van Niel G., Paris France). This PCR-amplified pHluorin cDNA was then inserted at the C-terminus of CD63-myc into the EcoR1 restriction site of pcDNA3 CD63-myc.

To express and purify the truncated mAlix cDNA (1-714nt, Alix ΔPRD) in bacteria, the cDNA was inserted into the pETm11 vector, which includes an N-terminal histidine tag.

All plasmids were then transformed into Top10 chemically competent *E.coli* with DNA purified using NucleoBond Xtra Midi endotoxin-free kit (Macherey-Nalgene). All sequences were verified by sequencing. pGFP-CD63, were from our lab (Chatellard-Causse et al., 2002; Chivet et al., 2014).

Plasmids	Primer	Sequence
HiBitCD63-myc	Forward	5'- TACCGAGCTCGGATCCATGGTGAGCGGCTGGCGGCTGTTCAAGAAGATTAGCGGGAGTTCTGGCGGCTCGAGCGGTGGATCCATGGCGGTGG-3'
	Reverse	5'- CCACCGCCATGGATCCACCGCTCGAGCCGCCAGAACTCCCGCTAATCTTCTTGAACAGCCGCCAGCCGCTCACCATGGATCCGAGCTCGGTA-3'
HiBitHsp70-myc	Forward	5'- TCACTATAGGGCTAGATGGTGAGCGGCTGGCGGCTGTTCAAGAAGATTAGCGGGAGTTCTGGCGGCTCGAGCGGTGGATCCGCCAAGAACACGGCGATC-3'
	Reverse	5'- CCTAGGTGTTTCTAGCTACAGATCTTCTTCAGAAATAAGTTTTTGTTCATCCACCTCCTCGATGGTGGGTCCT-3'
HiBitAlix-myc	Forward	5'- CGGTGGATCCGCTAGCATGGCGTCGTTCATCTGG-3'
	Reverse	5'- GTTTTTGTTCGCTAGCCTGCTGTGGATAGTAGGACTG-3'
Rab7LgBit	Forward	5'- TCACTATAGGGCTAGCATGGACTACAAGGACGACGACGACAAGGGATCCATGACCTCTAGGAAGAAAGTG-3'
	Reverse	5'- CATGGTGAGCGCTAGCATTGATCCACCGCTCGAGCCGCCAGAACTCCCGGATCCGCAACTGCAGCTTTCCGCTG-3'
Rab5LgBit	Forward	5'- TCACTATAGGGCTAGCATGGACTACAAGGACGACGACGACAAGGGATCCATGGCTAGTCGAGGCGCAACAAGACC-3'
	Reverse	5'- CATGGTGAGCGCTAGCATTGATCCACCGCTCGAGCCGCCAGAACTCCCGGATCCGTTACTACAACACTGATTCCTGGTTGG-3'
CD63Phluorin	Forward	5'- AGATCTGTTGGAAGTTATGGGAAGTAAAGGAGAAGAACT-3'
	Reverse	5'- GATATCTGCAGACTATTTGTATAGTTCATCCATGCCATGT-3'

Table 3: **Primers used to generate plasmids.**

2.2 Antibodies

Antibodies	Supplier	Species (type)	Dilution	Usage
Anti-Myc	Santa Cruz Biotechnology	Rabbit (polyclonal)	1/1000	WB/IF
Anti-Alix	Sadoul Lab	Rabbit (polyclonal)	1/2000	WB
Anti-Alix	1A12	Mouse (monoclonal)	1/500	WB/IP
Anti- CD9	Invitrogen	Mouse (monoclonal)	1/1000	WB
Anti-actin	Sigma	Mouse (monoclonal)	1/10000	WB
Anti-syntenin	Abcam	Rabbit (polyclonal)	1/1000	WB
Anti-Flotillin-1	BD Transduction	Mouse (monoclonal)	1/1000	WB
Anti-LgBit	Promega	Mouse (monoclonal)	1/500	IF
Anti-Rabbit IgG HRP	Jackson Immunoresearch	Goat (polyclonal)	1/10 000	WB
Anti-Mouse IgG HRP	Jackson Immunoresearch	Goat (polyclonal)	1/10 000	WB
Anti-Rabbit IgG Alexa Fluor 488	Molecular probe	Goat (polyclonal)	1/1000	IF
Anti-Rabbit IgG Alexa Fluor 594	Molecular probe	Goat (polyclonal)	1/1000	IF
Anti-Mouse IgG Alexa Fluor 488	Molecular probe	Goat (polyclonal)	1/1000	IF
Anti-Mouse IgG Alexa Fluor 594	Molecular probe	Goat (polyclonal)	1/1000	IF

Table 4: **Antibodies used in this study.**

2.3 Cell culture

2.3.1 Adherent Cells

Human embryonic kidney 293 (Hek293) cells represent a specific immortalized cell line derived from human embryonic kidney cells obtained from a female fetus in 1973 (Kavsan, Iershov, & Balynska, 2011).

Hek293 cells were cultured in Dulbecco's Modified Eagle's Medium (DMEM, GIBCO) supplemented with 10% heat-inactivated fetal bovine serum (FBS, GIBCO). The cells were incubated in a controlled environment at 37°C with 5% CO_2. Upon reaching 70% confluence, the cells were rinsed twice with phosphate-buffered saline (PBS). subsequently, 0,05% Trypsin-EDTA solution was added for 5 minutes at 37°C. The cells were seeded at 1×10^4 cells/cm^2 for maintenance or at 4.3×10^4 cells/cm^2 for EV secretion.

2.3.2 Suspension cells

Cellules FreeStyle™ 293F (ThermoFisher Scientific) were maintained in FreeStyle™ 293 Expression Medium (GIBCO). The cells were incubated at 37°C with 8% CO_2 and shaking at 125 rpm. Cells were diluted at the time their density reached 3×10^6 cells/ml. For routine maintenance, the cells were seeded at 0.5×10^6 cells/ml twice per week.

2.3.3 Generation of Stable Cell Lines constitutively expressing LgBit

For the generation of stable LgBit Hek cell lines, Hek293 cells were seeded (4×10^4 /cm^2). 24 hours later cells were transfected using a calcium phosphate precipitation procedure with a plasmid encoding LgBit containing a hygromycin resistance gene. One day after transfection, cells were treated with 200µg/µl of Hygromycin B to select for the transfected cells.

2.4 Transfection method

2.4.1 Adherent cells

Cells were seeded (4×10^4 cells/cm^2) either on poly-ornithine coated plates or on glass coverslips 24 hours before transfection. For the calcium phosphate precipitation, DNA (5µg, 7µg, and 15µg for 10 cm^2, 24 cm^2, and 57 cm^2 dishes respectively) was diluted in 0.26 M of $CaCl_2$. The DNA-$CaCl_2$ solution was gently mixed with an equal volume of sterile 2X HeBS (HEPES buffered saline) solution (Sigma) and left to precipitate for 20 min at room temperature.

Subsequently, the mixture was added to the culture medium of cells. After 6h of incubation, the medium was carefully replaced by pre-warmed culture medium or exo-free medium (medium previously prepared by ultracentrifugation for 18 h, at 140 000 g using a 45Ti rotor of the culture medium (DMEM, 10% FBS)) for donor cells. Before adding the new medium, the cells were washed 2 times with PBS in order to remove any remaining transfection reagents.

2.4.2 Suspension cells

To transiently transfect 293F cells, cells were seeded (1×10^6 /ml) and transfected using a polyethyleneimine (PEI) reagent. DNA (10 µg /ml) was diluted in Opti-MEM. PEI was then added to the DNA at a 3:1 ratio(w/w). The mixture was gently mixed and incubated for 20 min at RT. The DNA-PEI complex was then applied dropwise to the culture medium on the cells.

2.5 Immunofluorescence

The cells were fixed for 20 min in 4% paraformaldehyde (PFA) in PBS. After three washes with PBS, cells were permeabilized and saturated non-specific sites in a solution containing 0.3% Triton X-100 and 5% Goat Pre-Immune serum in PBS for 20min. Coverslips were then incubated with primary antibodies in the same buffer for 1h. Following three washes with PBS, coverslips were incubated with secondary antibodies conjugated to Alexa Fluor 488, or Alexa Fluor 594 for 1h and subsequently were rinsed 3 times with PBS. Nuclei were labeled with 2µM Hoechst 33258 (Sigma) for 5 min. The coverslips were then mounted with Mowiol (Calbiochem) onto microscope slides. Images were generated using confocal microscopy (Olympus). All steps were performed at room temperature.

2.6 EVs purification

Supernatant from Hek293 or 293F cells were first cleared of debris and dead cells by two successive centrifugation steps at 2 000 x g for 10 min and at 20 000 x g for 30 min. The resulting supernatant was filtered through a 0.22 µm filter Millex GV PVDF (Millipore) in order to eliminate microvesicles. Following filtration, the supernatant was ultracentrifuged for 90 min at 100 000 x g (speed 29 000 rpm, SW41Ti or SW32.1Ti rotors, Beckman Coulter). The pellet was washed once with PBS to eliminate any contaminating proteins. EVs were resuspended in Opti-MEM (Gibco) for incubation with receiving cells or in PBS for other experimental purposes. EVs were purified freshly on the same day as the experiments to ensure the quality and integrity of the sample.

2.7 Nanoparticle Tracking Analysis

Nanoparticle tracking analysis (NTA) is a method that can be used for visualizing and analysing particles in liquid samples. This technique is useful for determining the size distribution profile of the small particle (ranging between 10 and 1000 nanometres (nm) in diameter) moving under Brownian motion. The NTA software uses the Stokes-Einstein equation to calculate the hydrodynamic diameters of these particles (Filipe, Hawe, & Jiskoot, 2010).

For NTA analysis, the purified EVs were diluted in filtered PBS and this solution was continuously injected with a syringe pump into the NanoSight NS300 (Malvern Instrument Limited, United Kingdom). The pump speed was set to 20, vesicles were visualized using a 488nm laser, and their Brownian motion was captured by video recording. The camera level was set at 15 and the detection threshold was set at 7. For each sample, three separate 60-second videos were captured, processed, and analyzed using the NTA software v3.2. The software could determine the size and the number of particles present in the solution. For each sample, 5 000 tracks were analyzed.

2.8 Western blot

Cells were re-suspended in a lysis buffer (20 mM Tris PH 7.5, 150 mM NaCl, 1 mM $MgCl_2$, 1% Triton X-100) for 20min on ice. The cell lysates were cleared of cellular debris by centrifugation at 16 000 x g for 5 min. The protein concentration of cell lysate was obtained using the Pierce BCA Protein Assay kit (Thermo Scientific, Illinois, USA). For each sample, either 10 µg of cell lysate or 2×10^9 particles of vesicles were mixed with 4X Laemmli buffer and boiled for 5min. For detecting CD9, non-reduced conditions were used, in which the loading buffer did not contain β-mercaptoethanol. The proteins were separated by SDS-polyacrylamide gels (10 or 12%) at 130V and then transferred to a nitrocellulose membrane (Millipore) for 1h at 100 V using a liquid transfer device in a buffer containing 3g/L Tris, 14.4g/L Glycine, 0.4g/L SDS, and 10% isopropanol. Membranes were blocked in TBS (Tris-buffered saline) containing 0.05% Tween 20, and 5% milk and incubated overnight at 4°C with the primary antibody (diluted in 5% milk TBS-T). Following incubation with secondary HRP-conjugated antibodies (horseradish peroxidase-coupled secondary antibody) for 1 h at room temperature. Immunoreactive bands were revealed using a solution containing 100mM Tris pH 8.5, 1.25mM Luminol, 2mM acid coumaric, and 0.009% of H_2O_2. Protein bands were quantified using the Image J plot profile tool for further analysis.

2.9 Luciferase assay

To monitor the EV fusion with endosomal compartment of receiving cells we choose to use Luciferase complementation assay optimized for accurate measurement of protein interactions in cells. NanoBiT is a split reporter consisting of two subunits, high-affinity NanoBiT (HiBit) with 11 amino acids and large (LgBit) 17kD of nanoluciferase. The individual subunits do not possess luciferase activity, but when HiBit and LgBit associate, the complex regains its NanoLuc enzymatic activity and can convert substrate (fumirazine) to the luminescence product (Furimamide) (Figure 18).

We fused the HiBit peptide to the N-terminal part of EVs protein, which are on the luminal side of EVs. HiBit-fused protein EVs were then incubated onto cells expressing LgBit and luminescence monitored. The increase in luminescence reflects interaction of HiBit/ LgBit, which, in theory, can only occur after fusion of EVs to membranes of LgBit expressing cells (Figure 21A, Result). The luciferase substrate, fumirazine is cell permeable so that can be used to monitor luminescence for up to 2 hours without affecting cell viability (Nano-Glo Live Cell Assay System, Promega).

Receiving Hek 293 cells were seeded (4×10^4 /cm^2) in 20cm^2 dishes and transfected 24h later with plasmids encoding LgBit protein. 6 h post-transfection, the receiving cells were trypsinized and seeded at 1×10^4 cell/well into poly-ornithine coated white flat bottom 96-well plates (ThermoScientific). The cells were cultured overnight for proper attachment. On a subsequent day, fresh EVs purified from cells expressing a HiBit-fused protein were incubated with the receiving cells at 2×10^9 particles/well at 37°C for the specified time period.

After incubation, the culture medium of the receiving cells was replaced with Opti-MEM containing 0.1 μM DrkBiT and incubated with NanoLuc substrate (Nano-Glo Live Cell Assay System; Promega) according to the manufacturer's instructions for 30min at 37°C. The luminescence signal was measured using a plate reader (BMG labtech/clariostar).

Finally, 0.5% Ttiron X-100 was added to ensure complete cell lysis. The luminescence signal was measured after 15 min. The ratio of luminescence signal from cells incubated with EVs to control cells incubated in Opti-MEM without EVs was calculated for each experiment. Three wells were quantified in each experimental group.

In some experiments, luciferase activity was continuously measured during the EVs incubation period. In these cases, the luciferase substrate was added together with EVs. Continuous monitoring of the luminescence was performed from the initial time point (T0) up to 2 hours.

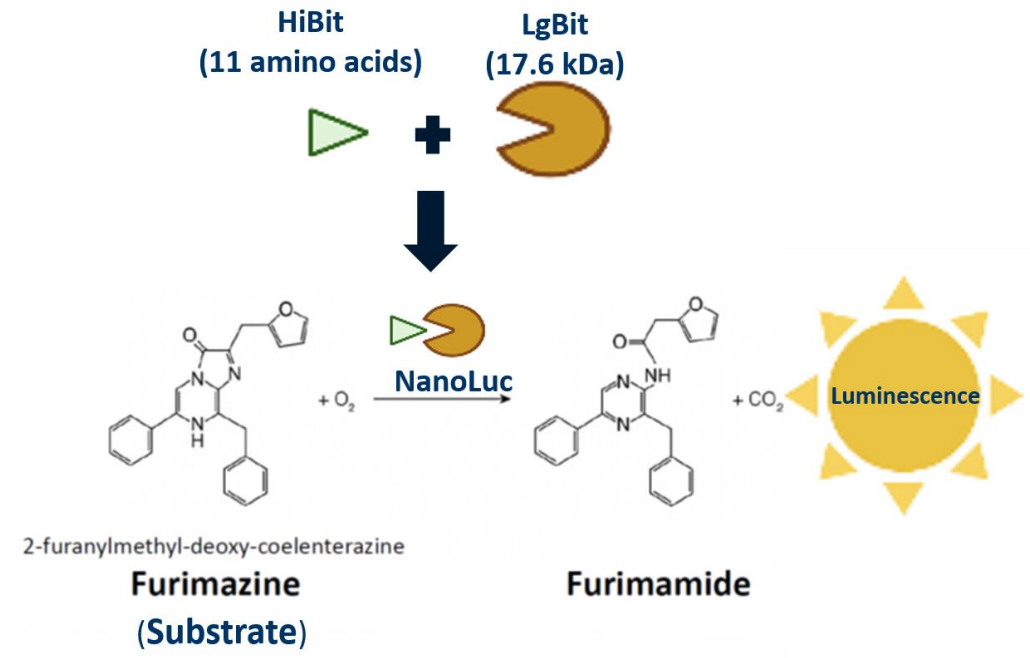

Figure 18: **HiBit/LgBit nanoluc luciferase strategy**.
The system comprises two subunits: the high-affinity NanoBiT (HiBit) with 11 amino acids and the large (LgBit) subunit, a 17kD nanoluciferase fragment. When combined, they regain NanoLuc enzymatic activity, facilitating the conversion of the substrate (fumirazine) into the luminescence product (Furimamide).

2.10 Detergent-free cell fractionation

To recover the cytosol from cells expressing LgBit. Cells were washed two times with PBS, incubated with detergent-free buffer (20 mM Tris PH 7.5, 150 mM NaCl, 1 mM $MgCl_2$), and gently detached from the plate using a scrapper. Cells were mechanically disrupted by sonication (pulse control mode 0.5 Cycle, 100% Amplitude for 10 seconds) (Hielscher Ultrasonics GmbH, UP50H, Germany) for four cycles while incubating on ice between each cycle. This lysate was then centrifuged for 10min, at 1500g to remove intact cells and large debris. The supernatant was then ultracentrifuged at 100 000 g for 1h to recover the cytosolic fraction.

2.11 Preparation of Liposomes

Liposomes were prepared with the lipid composition of SphingoMyelin: PhosphatidylSerine: Cholesterol 5:2.5:2.5 for mimicking the membrane composition of endosomes. A desired molar ratio of lipid solutions was diluted in chloroform in a glass vial. The organic phase was evaporated under vacuum pumping overnight, forming a lipid film. This lipid film was then hydrated with an appropriate volume of PBS buffer solution. To ensure a uniform distribution

of liposome size, the lipid mixture was gently extruded 15 times through polycarbonate membrane filters with a pore size of 100nm (Avanti Polar lipids). The size and concentration of liposomes were checked using NTA.

2.12 Protein purification

To express and purify the Alix ΔPRD protein, a 1L culture of *Escherichia coli* BL21(DE3) bacteria transformed with the pET11- Alix ΔPRD plasmid was grown at a temperature of 37°C. Expression of the fusion protein HIS-Alix ΔPRD was induced by adding 0.1mM isopropyl-β-D-galactopyranoside (IPTG) when the optical density at 600 nm reached 0.6. The induction was continued for 4 hours at 37˚C. Cells were harvested by centrifugation for 15 min at 6500rpm using the JLA8.1000 rotor (Beckman). The cell pellet was resuspended in 25ml of buffer A (50mM Tris-HCl pH7.5; 100mM NaCl; 2mM βmercaptoethanol). Cells were lysed by sonication and the lysate was centrifuged for 20min at 20,000rpm using the JA25.50 rotor (Beckman). The supernatant was loaded onto a nickel column previously equilibrated in buffer A. The column was then washed with buffer A containing 10 mM imidazole to remove nonspecific proteins. Finally, protein elution was achieved using buffer A supplemented with 250mM imidazole, and the elution was monitored using a Bradford solution (Bio-rad). The eluted protein was concentrated using 30kDa concentrating tubes (Amicon). The concentrated protein was then loaded onto a Superdex S200 Increase gel filtration column (GE HEalthcare) previously equilibrated with HBS buffer (20mM Hepes pH 7.5; 150mM NaCl). Finally, fractions corresponding to the monomeric form of Alix ΔPRD were collected.

2.13 Alix ΔPRD interaction with EVs

A total of 3×10^9 Particles of EVs were incubated with 60µl of Alix ΔPRD at a concentration of 42 µM for 15 min at pH 7. To adjust the pH, a volume fraction of MES (24% v/v of 20mM) was added to the mixture, reaching a final pH of 5.5, and incubated for 1h at room temperature.

The incorporation of Alix ΔPRD protein into EVs was checked on sucrose gradient analysis. Proteo-EVs were diluted in 80% sucrose (w/v), 40mM MES at pH7 or pH5.5 solutions to achieve a final 60% sucrose concentration. These diluted proteo-EVs were carefully placed at the bottom of 14 × 89 mm centrifugation tubes in polyallomer or ultraclear™ and overlaid with 10 ml continuous gradient of 8% - 55% sucrose solution in 40 mM MES at pH7 or pH5.5 solutions. The gradients were then ultracentrifuged at 130 000 x g overnight at 4°C (Optima XPN-80 ultracentrifuge and SW 41rotor - Beckman Coulter). Fractions of 1 ml were collected from the top of the gradient, then washed with 9 ml of PBS, and EVs were pelleted by

centrifugation at 130 000 x g for 90min. Each pellet was resuspended in 30 µl Laemmli buffer and analyzed on western blot.

2.14 Alix ΔPRD interaction with liposomes

A total of 1.5×10^{11} particles of liposomes were incubated with 10µl of Alix ΔPRD at a concentration of 42 µM for 15 min at pH 7, a volume fraction of MES (24% v/v of 20mM) was added to the mixture, reaching a final pH of 5.5 and incubated 1h at room temperature.

The binding of Alix ΔPRD protein to liposomes was monitored using a discontinuous sucrose gradient flotation assay. After incubation, the liposome preparation was diluted in 80% sucrose solutions (w/v) in 40mM MES pH 5.5 or 40mM Tris pH 7 to achieve a final concentration of 60% sucrose. The diluted sample was layered at the bottom of 11 × 34 mm centrifugation tube (Beckman Coulter). Subsequently, this layer was overlaid with 3 additional layers of 0.4 ml each of sucrose solutions with concentrations of 40%, 30%, and 10%. Centrifugation was performed in TLS 55 rotor at 130 000 x g for overnight at 4°C (Optima XPN-80 ultracentrifuge, Beckman Coulter). Each fraction was recovered from the gradient and analyzed on SDS-PAGE using Coomassie blue labelling.

2.15 Cryo-EM

Isolated EVs (7.2×10^{10} particle/ml) were dissolved in either 20mM Tris pH 7 or 20mM MES pH 5.5 and incubated for 1h at room temperature. Some samples were treated with or without Proteinase K. Then EVs were pelleted by centrifugation for 35min at 100 000 g to obtain a more concentrated EV solution for Cryo-EM. The pellet was resuspended in 50µL of either 20mM Tris pH 7 or 20mM MES pH 5.5, depending on the experimental condition.

For Cryo-EM imaging, 3.5µL of samples were then loaded onto holey carbon grids (Quantifoil, Cu, 1.2/1.3) and plunged frozen in liquid ethane using a Vitrobot Mark IV (Thermo Fisher Scientific) (7 s blot time, blot force 0). The frozen grids were transferred to a Glacios electron microscope (Thermo Fischer Scientific) at an accelerating voltage of 200 kV. Images were taken using a Falcon2 camera with EPU. The images were recorded for a total exposure time of 1.5 s and a total dose of 40 electrons/Angstroms. The magnification was set to 121 000x (unbinned pixel size of 1.2 Angstroms/pixel).

2.16 Membrane mixing assay

The membrane mixing experiments were based on the FRET technique. EVs were labeled during the isolation process. For that, cell culture media were collected and cleared of debris through two successive centrifugation steps: 2 000 x g for 10 min and 20 000 x g for 30 min).

The supernatant was incubated with a mixture of 0.01% v/v of two dyes, 2.5mM DiI (Merck, CAT: 42364) and DiD (Thermo Fisher, D7757) in DMSO at a ratio of 1:1. This incubation took place at 37°C for 30min. The labeled EVs were then purified by filtration and ultracentrifugation, as previously described. To enhance the efficiency of labelling, the EVs were subjected to a second staining step using the same labelling protocol on the EVs pellet. Restained EVs were loaded onto a PD10 column (Sephadex^{TM} G-25M) to remove any unbound dyes.

Afterward, 0.2×10^{9} particles of labeled EVs were diluted in PBS and incubated with $0.6x10^{11}$ non-labeled liposomes at a ratio of 1:300 (fluorescence EVs to non-labeled liposomes). Additionally, 10µl of Alix ΔPRD protein (20µM) was added to the mixture. The fluorescence intensity of the donor dye (DiI) was measured every 120 secs, with an excitation wavelength of 530 nm and emission wavelengths of 570 nm. In the beginning, the fluorescence emission from the DiI was transferred to and absorbed by the DiD which served as the baseline. Subsequently, 24% v/v of 20mM MES solution was added to achieve a pH of 5.5 and the fluorescence intensity was measured. All experiments were performed using a plate reader (BMG labtech/clariostar).

2.17 CRISPR/Cas9 genome editing

To generate the Hek293 alix KO cell line, a pair of plasmids are used, each encoding the mutant Cas9 nuclease, which cuts only one strand of DNA, and a guide RNA (gRNA) (double nickase plasmid, Santa Cruz Biotechnology). One plasmid in the pair contains a puromycin resistance gene, while the other plasmid in the pair contains a GFP marker for visual confirmation of successful transfection. The sequences of the gRNA are designed by Santa Cruz to target exon 1 of the human *alix* gene and Biotechnology. The sequence of forward gRNA was 5'- CCAGTACTGCCGCGCGGCGG-3', and for reverse gRNA was 5'- CGCCGCTTGGGTAAGTCTGC-3'.

Hek293 cells at a low passage number were transfected with the pair of plasmids using calcium phosphate and cultured for 72h. Transfected cells were selected with 2µg/ml puromycin for one week. The surviving cells were trypsinized and then seeded at a density of 300 cells into a 100 mm dish. Single cells could grow to form a clone (~50-100 cells) after a few days. Single-cell clones were expanded, and 30 clones were analyzed by immunoblot using rabbit anti-Alix

polyclonal antibody. This analysis revealed that only 8 clones show a detectable level of Alix protein. Genomic DNA (gDNA) was then extracted from each negative clone, and each gDNA was amplified by PCR using *alix* gene-specific primers (5'- ATGGCGACATTCATCTCGGT-3' and 5'- TCCGCCCAGGTTACAGGATT-3'). The PCR products were ligated into the pGEM-T vector using a TA cloning kit (Promega) and were transformed into E. coli. Subsequently, 10 or more clones from each ligation were sequenced in their entirety. The Hek293 Alix KO cell line selected carried deletions between the two target sites in coding exon 1 on both of its *alix* alleles rendering both functionally null.

2.18 Fluorescence assay

For the fluorescence assay, vesicles were purified from Hek293 cells transfected with CD63pHluorin. A total of 0.2×10^9 particles were loaded onto black flat bottom 96-well plates. The plates were then transferred to a plate reader (BMG labtech/clariostar), and fluorescence emission was measured using a 500–600-nm band-pass filter. The fluorescence intensity was recorded every 30 secs for 70 min. Subsequently, 24% v/v of 20mM MES solution was added to achieve a pH of 5.5 and the fluorescence intensity was measured.

2.19 EVs protein digestion by Proteinase K

Purified EVs were incubated for 15min at room temperature with either 40mM Tris pH 7 or 40mM MES pH 5.5 buffer. EVs were incubated with or without 0.1% Triton X-100 and 50 µg/ml proteinase K (Euromedex, EU0090-B) for 30min at 37°C. To neutralize the activity of proteinase, the samples were placed on ice and 10 mM phenylmethylsulfonyl fluoride (PMSF) was added for 15min. Then samples were boiled immediately with the loading buffer.

2.20 Immuno-precipitation

Purified EVs were incubated for 1h at room temperature in Tris pH 7 or MES pH 5.5 buffer. Samples were precleared with 50 µL protein G sepharose. Then they were incubated with 1.2 µg of control mouse IgG or 1.2 µg of mouse Alix antibodies overnight at 4°C with agitation. Following antibody binding, 50 µL protein G sepharose beads were added and incubated for 1h at 4 °C with agitation. The samples were centrifuged at 12 000g for 30 seconds at 4°C, and the sepharose beads were washed three times with 500 µl of cell lysis buffer. Beads were resuspended in 20µl of 1X SDS sample buffer and heated at 95°C for 5 min, followed by 1 min

of microcentrifugation. The supernatant was loaded on SDS-PAGE gel and analyzed by western blot.

2.21 Statistical analysis

For statistical analysis, Prism 8 (Graphpad version 8.0.2 (263), January 30, 2019) was used. The results are presented as means ± Standard Deviation (SD). Statistical significance between groups was determined using either a Student's t-test or its non-parametric correspondent the Mann-Whitney U test depending on the data distribution. The value “n” shows the number of independent biological replicates. The graphs with error bars indicate SD (±) except for Figure 26A, Figure 27D, and Figure 28B, where box plots were used to show the distribution of the median (whiskers = min and max values).

The significance level “p” is represented as usual:

- for $p < 0.05$ *,
- for $p < 0.01$ **,
- For $p < 0.001$ ***.

Chapter 3 RESULTS

3.1 HiBitCD63: an EV-encapsulated cargo

To enable the luminescence assay for EVs cargo delivery, our initial approach involved tagging the cargo of EVs with HiBit. For this purpose, we specifically selected CD63, a tetraspanin protein known as a marker for EVs and found in their membrane. In our methodology, we fused HiBit at the N-terminal end and introduced a Myc tag at the C-terminal end of the CD63 protein (Figure 19A).

CD63 is known to be concentrated inside late endosomes. To investigate the subcellular localization of HiBitCD63 in Hek cells overexpressing it, we co-expressed HiBitCD63 along with proteins known to be specific markers for early (GFP-Rab5) and late (GFP-Rab7) endosomes. By conducting immunostaining using anti-myc antibodies, we observed that HiBitCD63 colocalizes with both endosomal proteins even if there seemed to be a higher degree of colocalization with the late endosomal protein Rab7 (Figure 19B). Thus, overexpressed HiBitCD63 colocalizes with both early and late endosomes.

We next checked the presence of this HiBitCD63 in the EVs. For this purpose, we purified EVs by ultracentrifugation of cell culture supernatants from Hek cells overexpressing HiBitCD63 or CD63. As expected, both proteins were detected in both the lysates and 100 000g vesicle pellet of HiBitCD63 and CD63 expressing cells but not in untransfected cells (control). Alix was also detected in lysates and EVs. Alix and HiBitCD63 were enriched in EVs (Figure 19C).

We used a nanoparticle tracking analysis (NTA) device (Nano Sight, Malvern) to measure the number and the size of the vesicles that were purified from Hek cells transfected or not with CD63. As seen in Figure 19D, where the black line in each graph represents the mean values obtained from 3 independent measurements (Red color) of the same EV sample, the majority of vesicles had a diameter of approximately 90-130 nm across all three groups. Only a small fraction of vesicles exceeded a diameter of 300 nm. In this, as well as in further experiments, we noticed that untransfected cells secreted less EVs than CD63 transfected cells, suggesting that CD63 overexpression favors exosome secretion (see also bellow the comparison with Hsp70 expressing cells).

We then investigated if HiBit fused to the N-terminal part of CD63 sits as expected inside EVs. For this, we fractionated the cytosol from membrane fractions of LgBit-expressing cells. We then incubated the cytosolic fraction containing LgBit with EVs containing HiBitCD63 and measured luminescence by adding the Nano-Glo reagent. The luminescence was compared between intact EVs and EVs solubilized with 0.5% Triton X-100. The graph shows that the luminescence measured from intact EVs is less than 2% of that detected in the presence of Triton (Figure 19E) revealing that the vast majority of HiBit is present inside EVs.

A

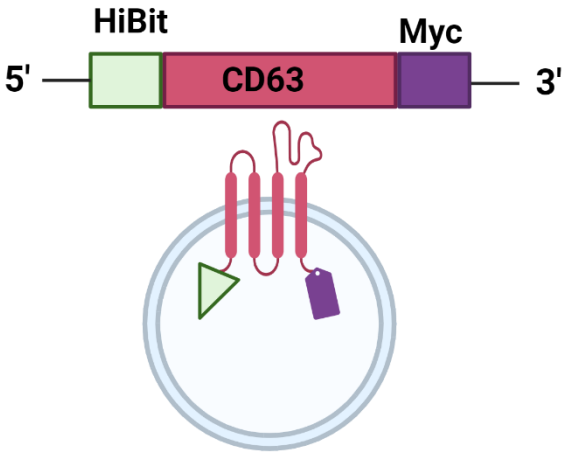
HiBit
Myc
5'
CD63
3'

B

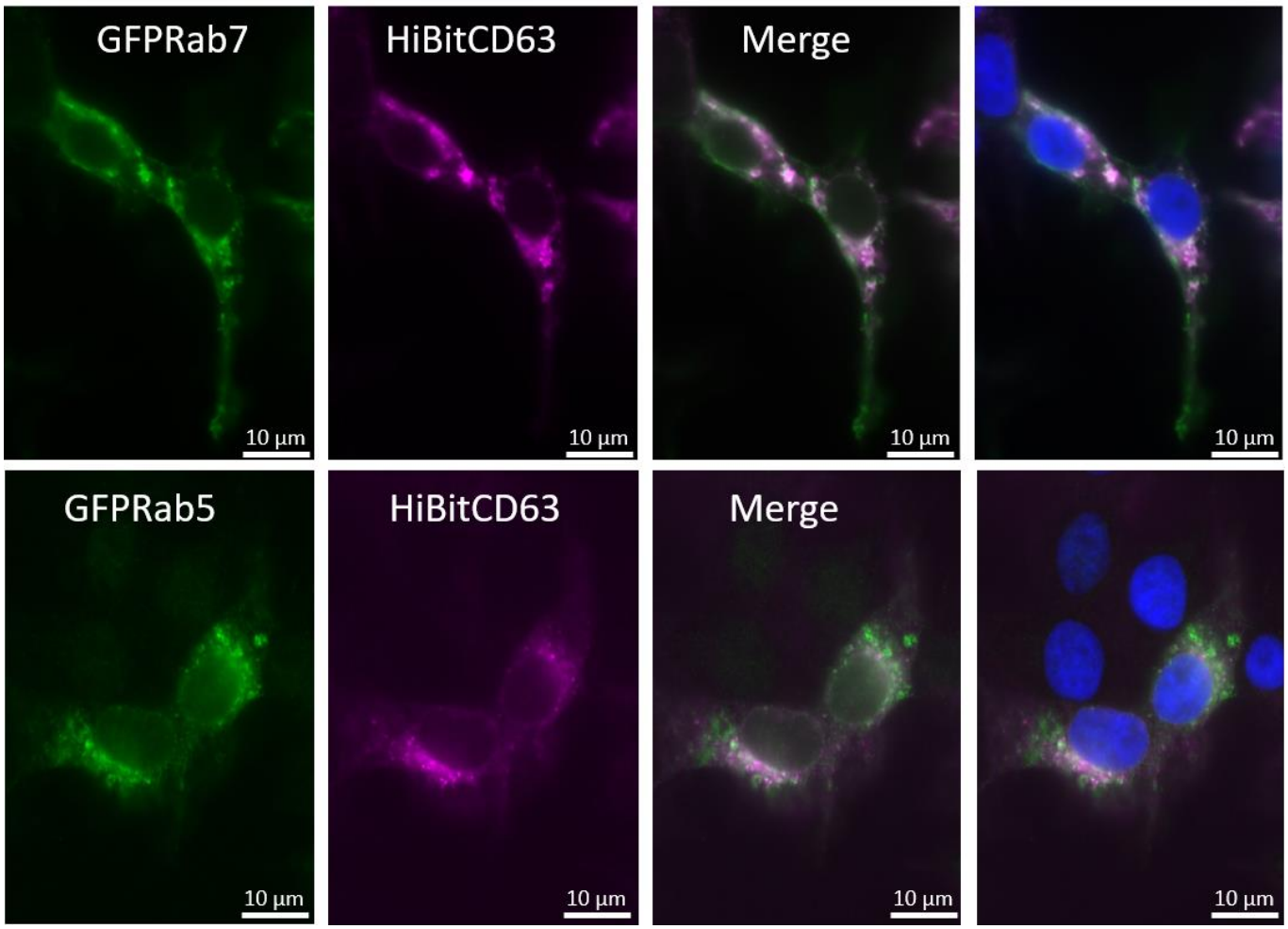
GFPRab7
HiBitCD63
Merge
GFPRab5
HiBitCD63
Merge
10 µm

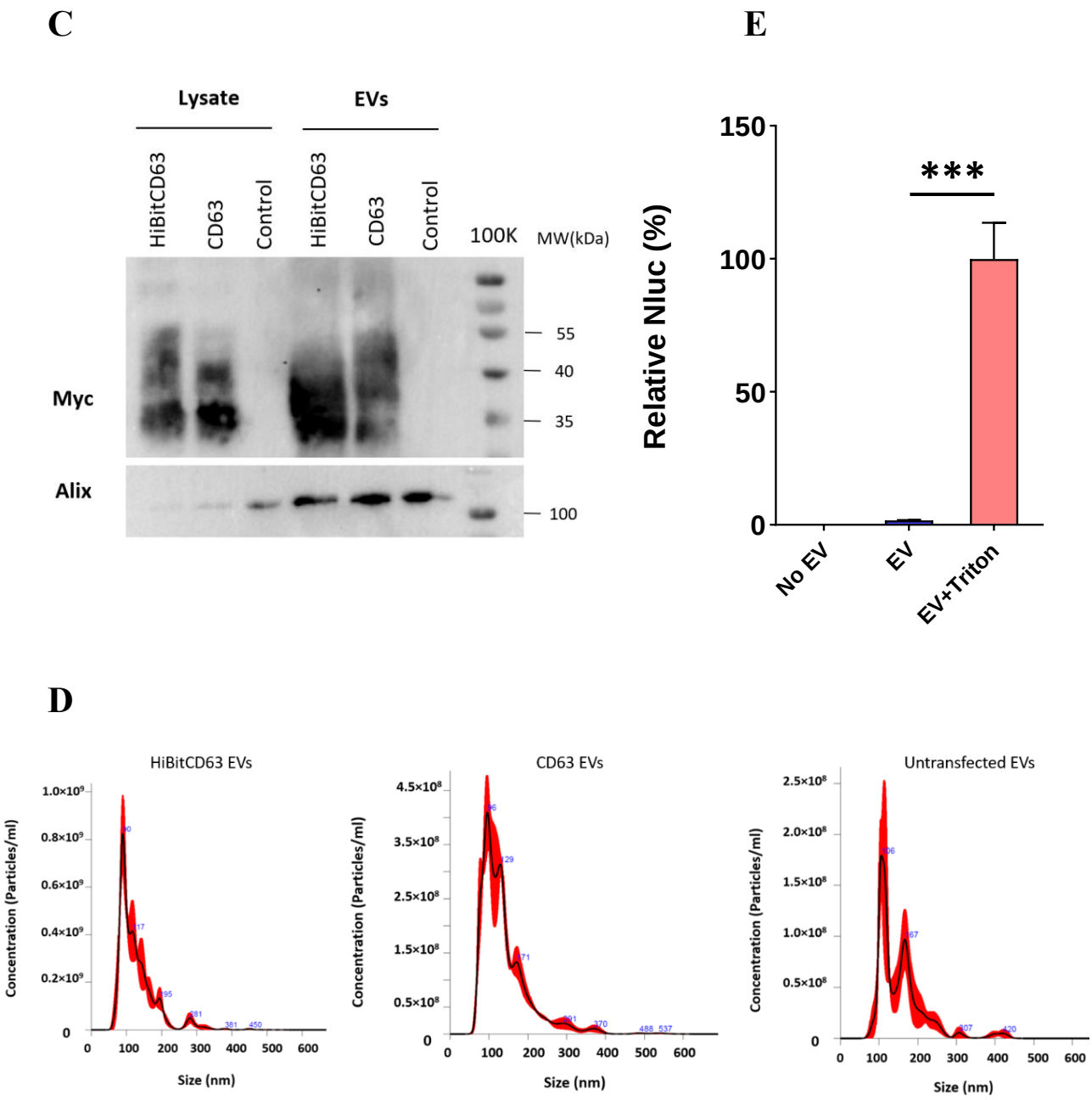

Figure 19: **Monitoring the expression of HiBitCD63:**

(A) Schematic representation of HiBit-tagged CD63 and the protein orientation in the EVs membrane.

(B) Confocal fluorescence images of HiBitCD63 co-expressing Hek cells with GFPRab5 and GFPRAb7, cells were labeled with anti-myc antibody (Scale bars, 10µm).

(C) Western blot showing the expression of HiBitCD63 and CD63 in both the lysate and EVs from Hek cells using anti-myc antibody and normalized by the intensity of the Alix band using anti-Alix monoclonal antibody.

(D) NTA analysis of EVs obtained from Hek 48h condition medium, the black line represents mean values obtained from 3 independent measurements (Red color).

(E) Quantification of HiBitCD63 within EVs, HiBitCD63 EVs from Hek cells were incubated with cytosol of Hek cells expressing LgBit, treated or not with detergent. Triton solubilized EVs were set to 100%. (Representative experiment, mean±SD is represented, n=3 wells).

3.2 EVs uptake detection

Before attempting to detect the interaction between HiBitCD63 of EVs with LgBit expressed in cells we first verified that EVs carrying CD63 could bind to and be endocytosed by Hek cells. Here, we used GFP-CD63, which had already been used in the lab to label EVs (Chivet et al., 2014). EVs were isolated from cells expressing GFP-CD63 and measured the number and the size of the vesicles via NTA. The majority of vesicles had a diameter of approximately 82 nm. And a small population of 130 nm (Figure 20A). GFP-CD63 EVs were incubated for 6h on Hek cells. Cells were washed 2 times with PBS and then observed by confocal fluorescent microscopy. As seen in Figure 20B fluorescence could be detected in discrete intracellular spots, which could represent EVs accumulated inside endosomes. However, it is remarkable that only a few fluorescent EV-containing cells could be seen. Intriguingly, very little fluorescence could be detected on the cell surface or the substrate.

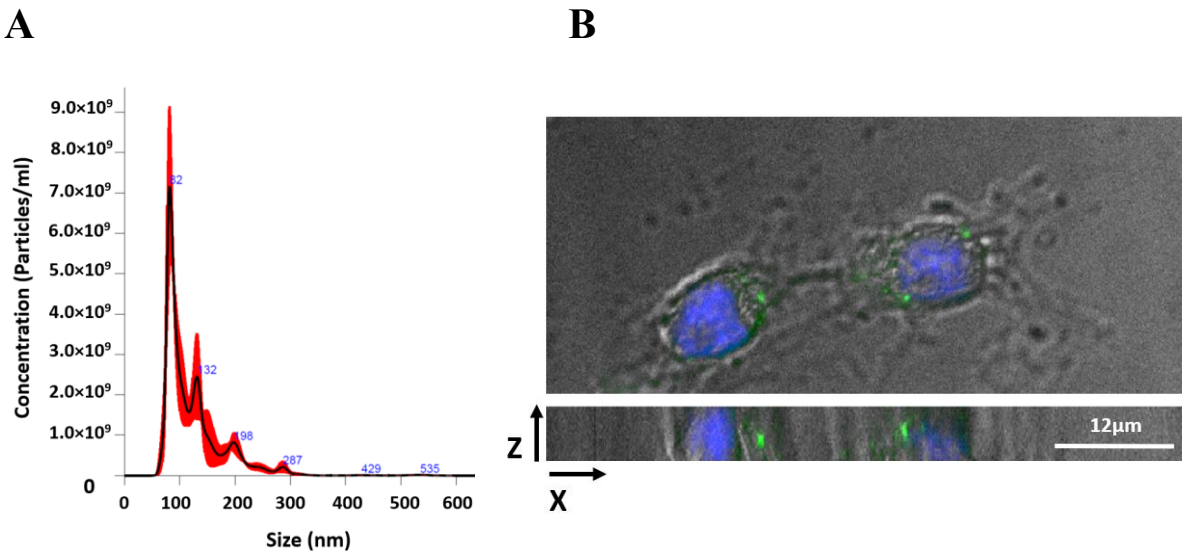

Figure 20: **Monitoring EVs uptake.**

(A) NTA analysis of GFP-CD63-containing EVs obtained from Hek 48h condition medium, the black line represents mean values obtained from independent measurements (Red colour)

(B) Confocal fluorescence images of GFP-CD63 EVs uptake using fluorescence confocal microscopy, Hek target cells were incubated with GFP-CD63 EVs for 6h. Green= EVs, Blue= Nucleus. A vertical section clearly shows the intracellular localization of EVs (Scale bar, 12µm).

3.3 Luminescence enhancement over Time: Incubation of receiving cells with EVs

The next step was to incubate LgBit-expressing cells with EVs derived from HiBit-expressing cells and monitor luminescence based on the complementation of HiBit and LgBit. In theory, the luminescence should be detected when HiBit inside the EVs is delivered to the cytosol of LgBit expressing receiving cells (Figure 21A).

Purified EVs were incubated with receiving cells during 2h, 4h, and 6h. Following incubation, cells were washed 2 times with PBS, and then luminescence was measured by adding Nano-Glo reagent, a cell-permeable nanoluciferase substrate. The luminescence strongly increased with time in LgBit-expressing cells incubated with EVs containing HiBitCD63 (Figure 21B). This increase suggested that HiBit from HiBitCD63 contained in EVs comes in contact with LgBit in the cytosol of the recipient cells possibly reflecting EVs fusion. In the next step, we solubilized the cells with 0.5% detergent (Triton X-100) in order to reach the highest level of interaction between HiBitCD63 and cytosolic LgBit. As we can see in Figure 21C, after adding detergent the luminescence increased by almost 3 times. This increase in luminescence may reflect the solubilization of EVs bound to the substrate, to the cell surface, or inside endosomes, bringing in contact the EV HiBitCD63 with the cell solubilized LgBit. Noteworthy is that the 3 times increase in luminescence is underestimated as Triton interferes with luminescence, as seen in control where LgBit expressing cells had not been incubated with EVs. Indeed, the background level of luminescence due to LgBit is reduced 4.6 times by the presence of Triton.

We had trouble reproducing these encouraging results. Indeed, in some cases, only a minimal increase in luminescence could be seen in LgBit cells expressing incubated up to 6h with HiBitCD63 EVs. However, adding 0.5% Triton X-100 increased the luminescence by 4 times, demonstrating the presence of HiBitCD63 EV on, or inside cells (Figure 21D). This suggested that in these cases, HiBitCD63 EVs had bound to, or were endocytosed by receiving cells, but that fusion of the EVs with membranes of receiving cells had not occurred. similar results were obtained using N2A, Hela and MCF7 cells as receiving cells.

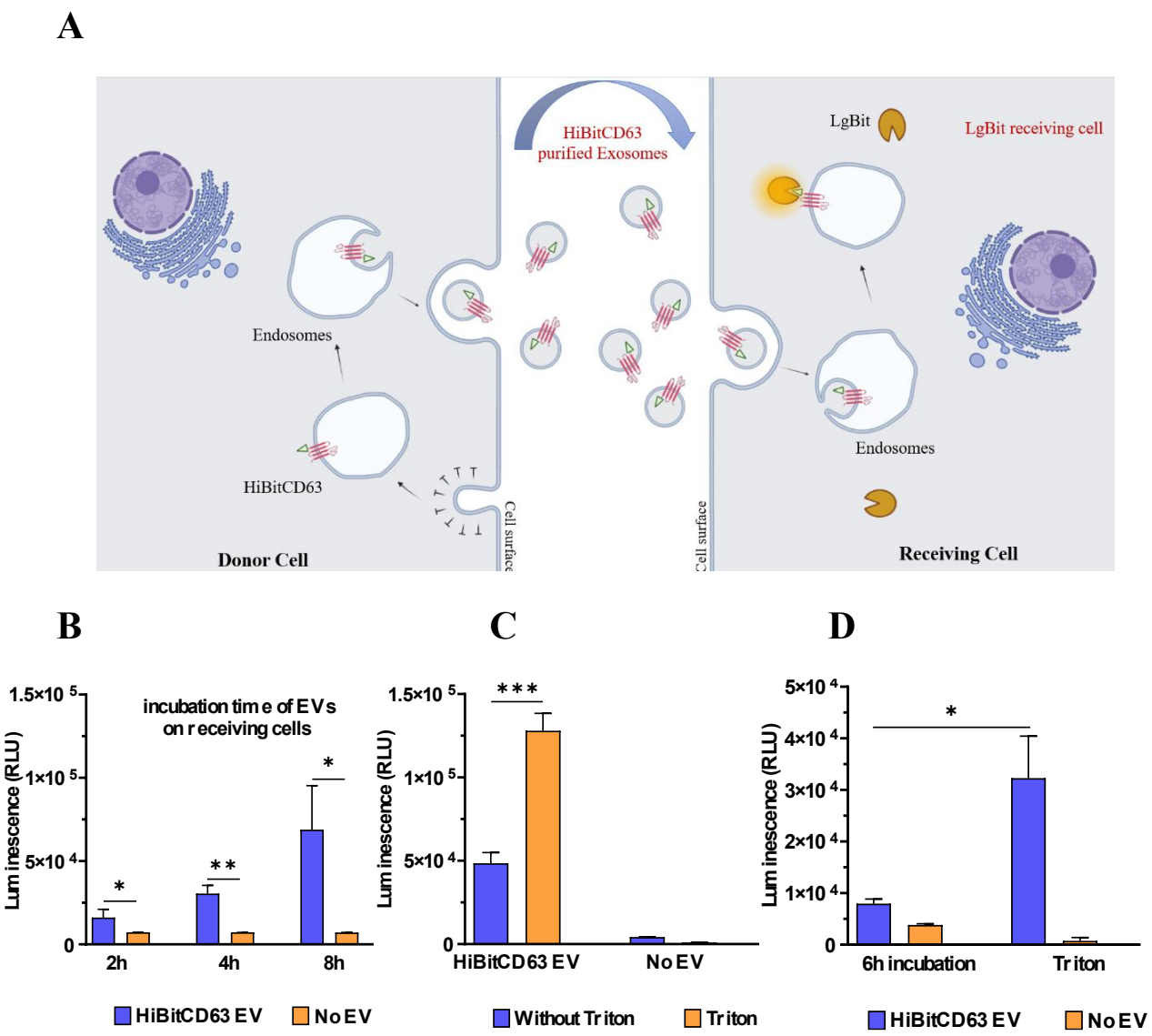

Figure 21: **Summary of the luminescence assay.**

(A) Schematic representation of the luminescence assay. An EV containing a HiBitCD63 is internalized by LgBit-expressing receiving cells, followed by the cytoplasmic release of the cargo. The complementation of HiBit with LgBit results in the generation of luminescence.

(B) Luminescence activity measurement after incubation of HiBitCD63 EVs on LgBit-expressing cells, (Representative experiment, mean ±SD is represented, n=3 wells).

(C) Luminescence activity measurement after 6h incubation of HiBitCD63 EVs on LgBit-expressing cells, treated or not with detergent, (Representative experiment, mean ±SD is represented, n=3 wells).

(D) Luminescence activity measurement after 6h incubation of HiBitCD63 EVs on LgBit-expressing cells, treated or not with detergent, (Representative experiment, mean ±SD is represented, n=3 wells).

3.4 Background reduction with LgBit stable cell line as receiving cell

We noticed that cells expressing LgBit transiently, produce luminescence even without HiBit (Figure 21B), possibly because of the very high levels of LgBit expression obtained by transient transfection. Thus, we decided to reduce this background by generating stable Hek cell lines (Hek-LgBit), expressing cytosolic LgBit. As seen in Figure 22A, immunostaining with anti LgBit antibody, revealed that in transient transfection, LgBit is expressed in the cytosol, although high expression was also observed in the nucleus. Moreover, it was noted that only 30% of the cells exhibited LgBit, whereas, in the cell line, LgBit was detected in almost every cell as expected, with cytosolic expression. However, the level of luminescence obtained by transient transfection was obviously much higher than that seen in the cell line (Figure 22A). When purified EVs containing HiBitCD63 were incubated on Hek-LgBit receiving cell line for 4h, luminescence gradually increased during 2h compared to cells incubated with no EVs. A maximum ratio of approximately two-fold was sometimes seen at 2h (Figure 22B).

In all experiments shown thus far, the Nano-Glo reagent, which is cell permeable, was added after the cells had been incubated with EVs. Measurements were done once the incubation medium had been changed for the Opti-MEM (Minimal Essential Medium), an improved cell culture medium without serum, containing Nano-Glo reagent. We then tested an alternative protocol, in which the Nano-Glo reagent was added simultaneously with EVs in order to continuously monitor luminescence from T0 on. The luminescence increased with time after 1h when it reached 2 fold which was measured without EVs. The luminescence decreased thereafter, possibly indicating a potential degradation of the luciferase substrate or its product during incubation in the medium (Figure 22C). However, what we consider here is the amount of increase in the level of luminescence during EVs incubation compared to the control. Due to the enhanced reproducibility of this paradigm, we continued our experiments using this protocol.

As previous studies suggested that EVs-content delivery, occurs at the endosomal level (Joshi et al., 2020). We intended to concentrate LgBit at endosomes. To achieve this, we expressed in the receiving cells LgBit fused with proteins, which are specific for early (Rab5LgBit) and late (Rab7LgBit) endosomes. The luminescence signal was measured after the addition of EVs containing HiBitCD63 together with the Nano-Glo reagent and continuously followed for 2h. The luminescence ratio between cells incubated with EVs and those incubated without EVs increased over time reaching 2- and 3-fold for Rab5LgBit and Rab7LgBit respectively (Figure 23). This increase suggested that HiBit from HiBitCD63 contained EVs encounters LgBit which is expressed on the cytosolic face of the endosomal membrane in the recipient cells. This

observation could reflect EV fusion with the endosome compartment, especially at the late endosomal level.

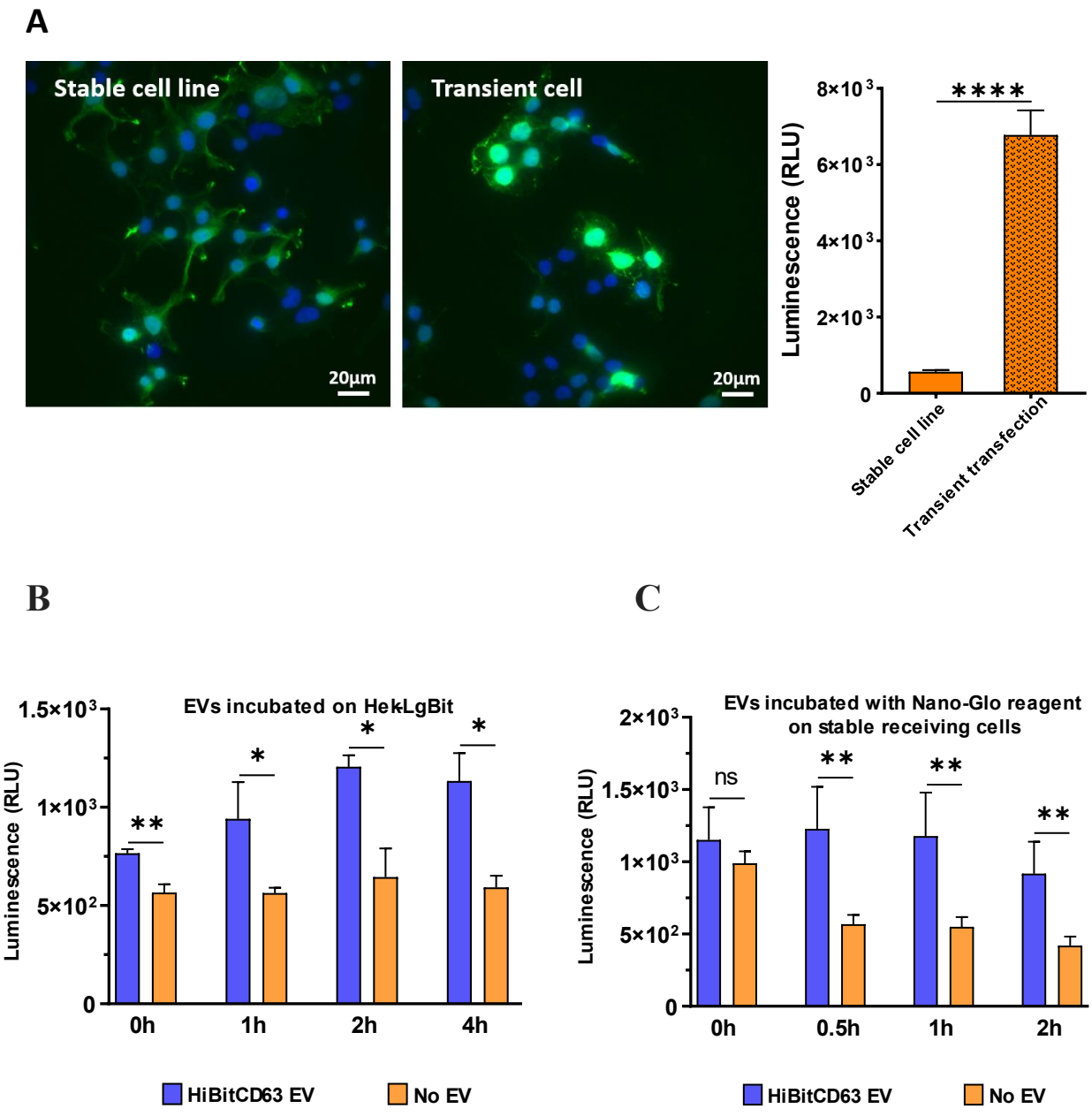

Figure 22: **LgBit stable cell line as receiving cell.**

(A) Fluorescence images of LgBit expression in stable Hek cell line and transiently transfected Hek cells using anti-LgBit antibody (Scale bar, 20µm). Luminescence activity is measured in both groups (Representative experiment, mean ±SD is represented, n=6 wells).

(B) Luminescence activity measurement after incubation of HiBitCD63 EVs on the stable LgBit cell line (Representative experiment, mean ±SD is represented, n=3 wells).

(C) Luminescence activity measurement during incubation of HiBitCD63 EVs on the stable LgBit cell line together with Nano-Glo substrate (Representative experiment, mean ±SD is represented, n=3 wells).

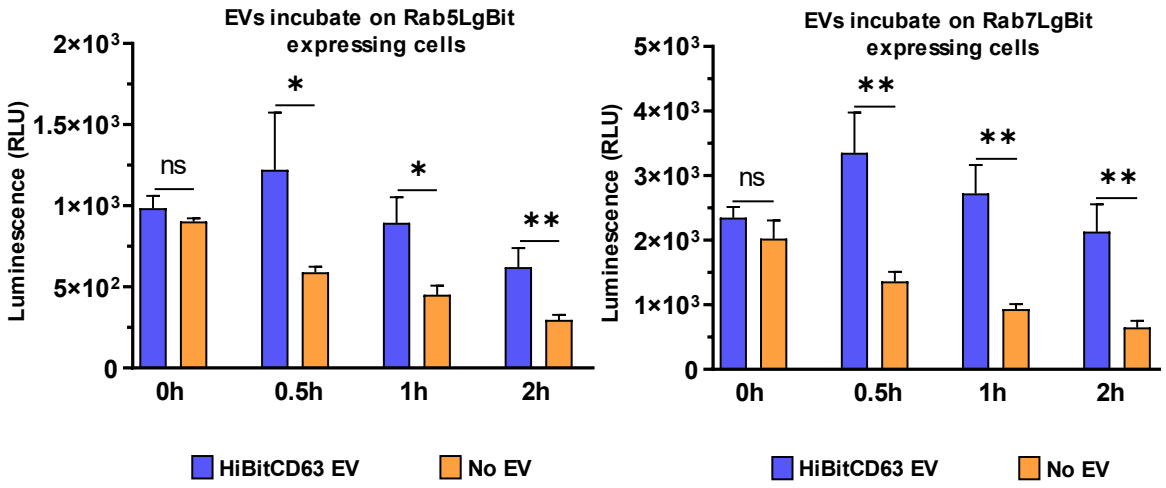

Figure 23: **Localization of LgBit in endosomes of receiving cell**.

Luminescence activity measurement during incubation of HiBitCD63 EVs on the Rab5LgBit- or Rab7LgBit-expressing cells together with Nano-Glo substrate (Representative experiment, mean ±SD is represented, n=3 wells).

3.5 Potential leaking of soluble LgBit from recipient cells into the medium

As described above, a small fraction of EVs containing HiBitCD63 has HiBit outside of the lumen that is therefore accessible to LgBit. We reasoned that cells might release LgBit into the supernatant during incubation with the EVs. This soluble LgBit could interact with HiBit on the surface of EVs thereby making a functional Nanoluc. To test this, we incubated EVs with a supernatant of cells expressing LgBit. The cells had been treated as cells incubated with EVs for 4 hours before the supernatant was harvested and centrifuged to remove cell debris. The result shows that the luminescence was 3.5 times higher than that measured in supernatants incubated with no EVs (Figure 24). Triton X-100 solubilization, making HiBit accessible to the soluble LgBit of the cell supernatant increased the level of luminescence by a factor of 23.5 fold. Therefore, this simple experiment reveals that LgBit is released by cells during the time of incubation with EVs. Consequently, this interaction between soluble LgBit and non-encapsulated HiBit-tag is bound to produce a nonspecific luminescence signal.

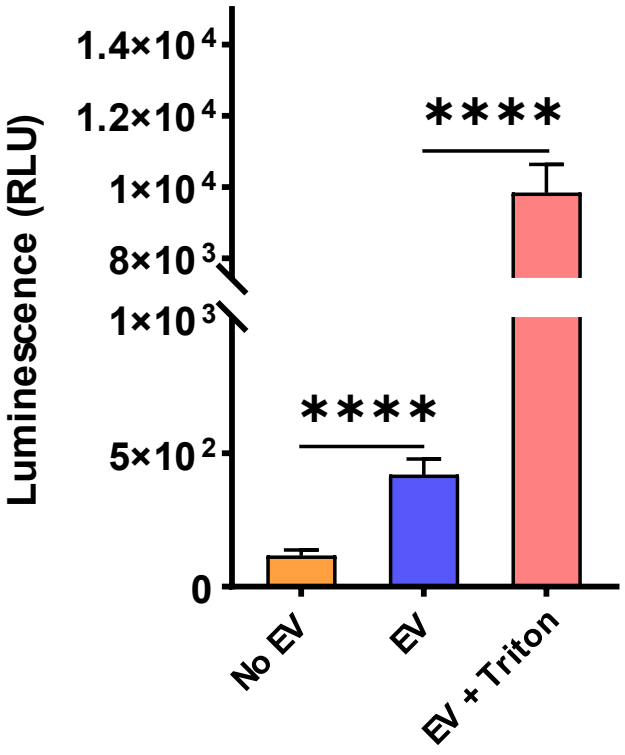

Figure 24: **Monitoring the presence of LgBit in the medium.**

Luminescence activity measurement of HiBitCD63 EVs on LgBit-expressing Hek cells medium, the detergent treatment was set to 100%, (Representative experiment, mean±SD is represented, n=3 wells)

3.6 Use of DrkBit for background reduction

In 2021, Somyia et al. used a similar approach as ours to monitor the fusion of EVs to cells and were faced with similar artifacts. To block the nonspecific complementation of HiBit and LgBit, they developed a soluble, membrane-impermeable peptide analog of HiBit (DrkBit), which binds to and inhibit LgBit thereby effectively competing with the non-encapsulated HiBit-tag and blocks the extracellular LgBit (Somiya & Kuroda, 2021). Inspired by their work, we used this peptide to avoid nonspecific signals due to extra-EVs HiBit.

We repeated our experiments with EVs. Nano-Glo reagent was added together with EVs on receiving cells expressing cytosolic LgBit (Hek-LgBit cell line), Rab5LgBit (transient transfection), or Rab7LgBit (transient transfection). Luminescence was measured continuously from T0 up to 2h in the presence of DrkBit peptide. As described above, the luminescence gradually increased in the absence of DrkBit. The increase was totally blocked in the presence of DrkBit (Figure 25A, B), suggesting that the increase in luminescence detected in the absence of DrkBit, is due to non-capsulated HiBit binding to LgBit which is secreted by receiving cells during incubation with EV (Figure 23). To ensure the reliability of our results, it is thus indispensable to use the DrkBit peptide during incubation and luminescence measurement.

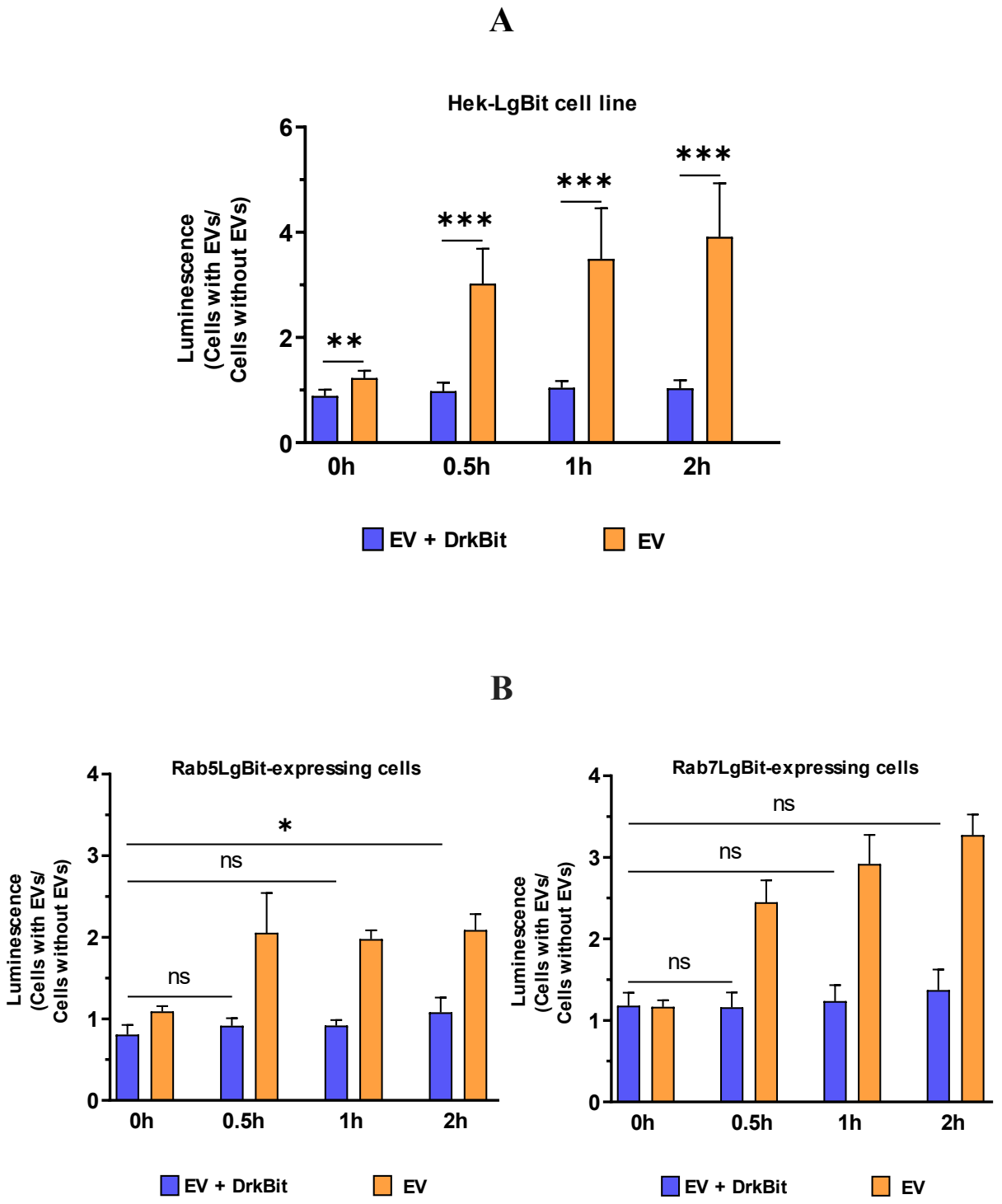

Figure 25: **Effect of DrkBit peptide**.

(A) Luminescence activity measurement during incubation of HiBitCD63 EVs on the stable LgBit cell line together with Nano-Glo substrate, in the presence and absence of DrkBit (Representative experiment, mean ±SD is represented, n=3 wells).

(B) Luminescence activity measurement during incubation of HiBitCD63 EVs on the Rab5LgBit- or Rab7LgBit-expressing cells together with Nano-Glo substrate, in the presence and absence of DrkBit (Representative experiment, mean ±SD is represented, n=3 wells).

3.7 Luminescence enhancement via EVs incubation with receiving cells in the presence of Fusogenic protein

It has recently been reported that the inherent capacities for the uptake of EVs by receiving cells are significantly limited (Bonsergent et al., 2021; Joshi et al., 2020). In the studies conducted by Somiya et al, it was demonstrated that the cargo delivery efficiency of EVs was below the basal level in luminescence assay (Somiya & Kuroda, 2021). Therefore, they proposed modification of EVs in order to become potent delivery vectors. As we were concerned about the fusion step, we tested the fusion of EVs bearing wild type VSV-G, the glycoprotein G of the Vesicular Stomatitis Virus (VSV), which allows membrane fusion of the virus with endosomal compartments. Here, we prepared EVs cells expressing both VSV-G^+ and HiBitCD63 and measured the number and the size of the vesicles via NTA. The main population of vesicles had a diameter of approximately 110 nm and only a small fraction of vesicles was larger than 200nm. It is worth noting that vesicles containing VSV-G tended to be slightly larger in size compared to those without. However, the number of vesicles secreted from cells was comparable between the two groups. (Figure 26A). EVs were incubated for various time duration (2h,4h,6h,8h, and overnight). Following incubation, cells were washed 2 times with PBS, and then luminescence was measured by adding substrate. As seen in Figure 26B, the luminescence progressively increased over the course of the incubation period. This increase was two-fold more compared to the absence of VSV-G. No significate increase was observed even after overnight incubation without VSV-G. Thus, the fusion efficiency of EVs membrane within receiving cells is limited, and fusogenic protein seems to be required for facilitating this process.

As mentioned above, the endosomal protein Alix was found to be necessary for VSV RNA release (Le Blanc et al., 2005). And miRNA downloading of EVs (unpublished paper from the lab). To investigate the involvement of the protein Alix in the fusion process between HiBitCD63-containing EVs and endosomal membranes, we used receiving Hek cells in which *alix* had been deleted using Crispr-Cas9 (C. Chatellard), as confirmed by western blot that demonstrated the absence of Alix protein expression in the lysate (Figure 26C). LgBit was expressed in Alix knockout (KO) and wild-type (WT) Hek cells followed by incubation with VSV-G^+ /HiBitCD63 EVs during 6h, 8h, and overnight. A time-dependent increase in luminescence was seen and comparable between both Alix KO and WT Hek cells (Figure 26D). This result reflects the absence effect of Alix in receiving cells for fusion.

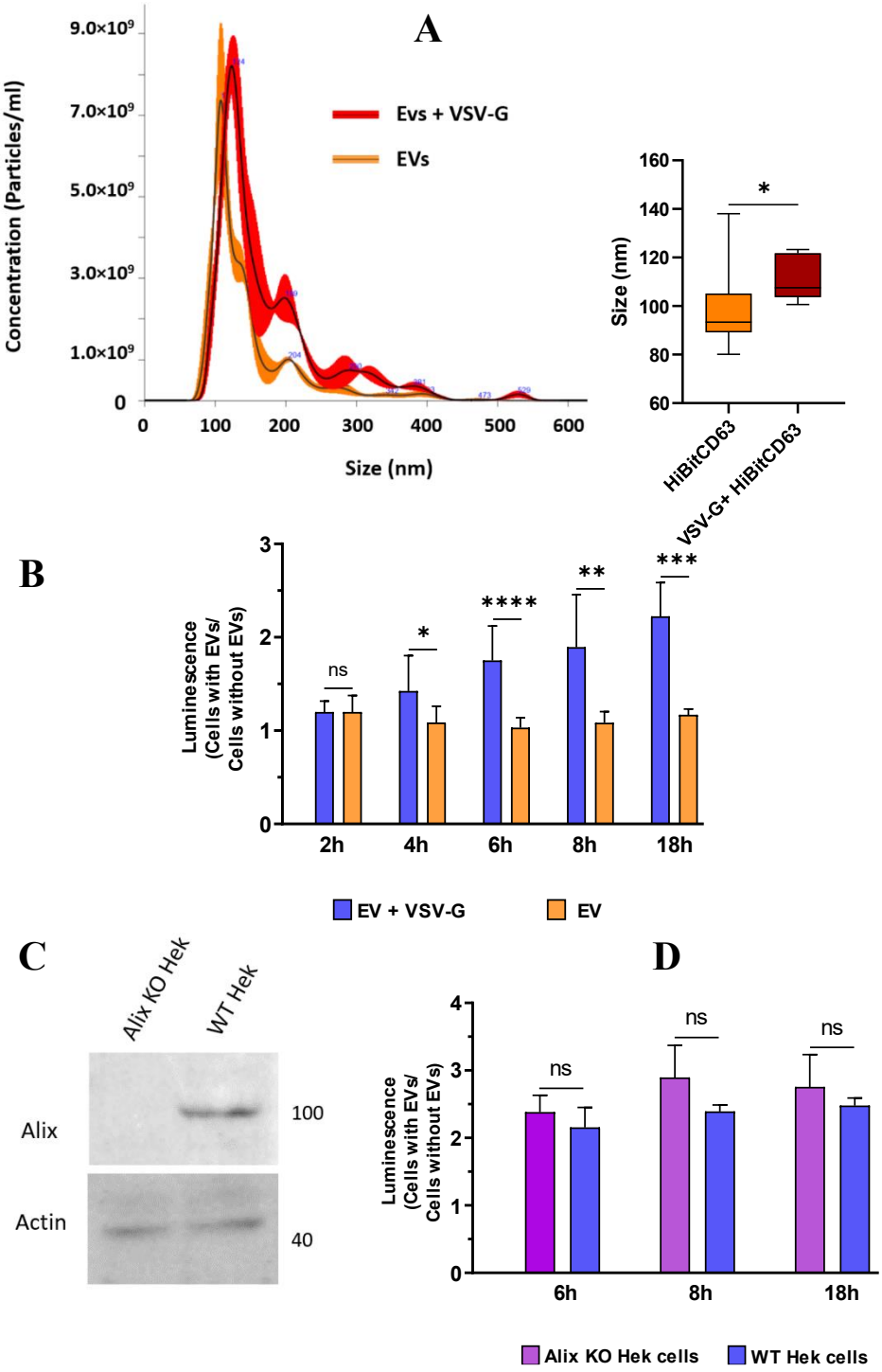

Figure 26: **Effect of VSV-G and Alix on membrane fusion.**

(A) NTA analysis of HiBitCD63-containing EVs and HiBitCD63-containing EVs bearing VSV-G+ obtained from Hek 48h condition medium, the black line represents mean values obtained from independent measurements (Red color), Particle size from NTA analysis was measured and compared in both groups, (Min and Max are represented, HiBitCD63 n=25, VSV-G$^+$ + HiBitCD63 n=5 independent experiments).

(B) Luminescence activity measurement after incubation of HiBitCD63-containing EVs bearing VSV-G$^+$ on LgBit-expressing cells and compared with HiBitCD63-containing EVs (Representative experiment, mean ±SD is represented, n=3 wells).

(C) Western blot showing the absence of Alix expression in the lysate of Alix knockout (KO) Hek cells using anti-Alix polyclonal antibody.

(D) Luminescence activity measurement after incubation of HiBitCD63-containing EVs bearing VSV-G$^+$ on LgBit-expressing wild-type (WT) Hek cells compared to LgBit-expressing Alix Knockout (Ko) Hek cells (Representative experiment, mean ±SD is represented, n=3 wells).

3.8 Cytosolic protein Hsp70 to track EVs' fate

There could be multiple reasons explaining the failure to detect reproducible fusion of EVs containing CD63 (see Discussion). Indeed, we reasoned that CD63 might incorporate into newly formed ILV directly after the fusion of the CD63 carrying EVs with the endosomal membrane, thereby decreasing the NanoLuc signal. We, therefore, chose Hsp70, a cytosolic protein known to concentrate inside EVs (Bonsergent et al., 2021). And which should be released into the cytosol after fusion. HiBit was fused with the N-terminal part of Hsp70 (Figure 27A). As expected, immunostaining on transfected cells by anti-myc antibodies demonstrated the cytoplasmic expression of HiBitHsp70 with little colocalization with GFP-CD63, which is expressed on the endosomal membrane and ILVs (Figure 27B). We next used NTA to quantify the number and the size distribution of the EVs secreted by Hsp70-expressing cells and compared them to those expressing CD63. As shown in Figure 27C, vesicles composed of a prominent population of 100 nm while a smaller population was observed within the range of 200-300 nm. Their size was comparable to those containing HiBitCD63 (Figure 27D).

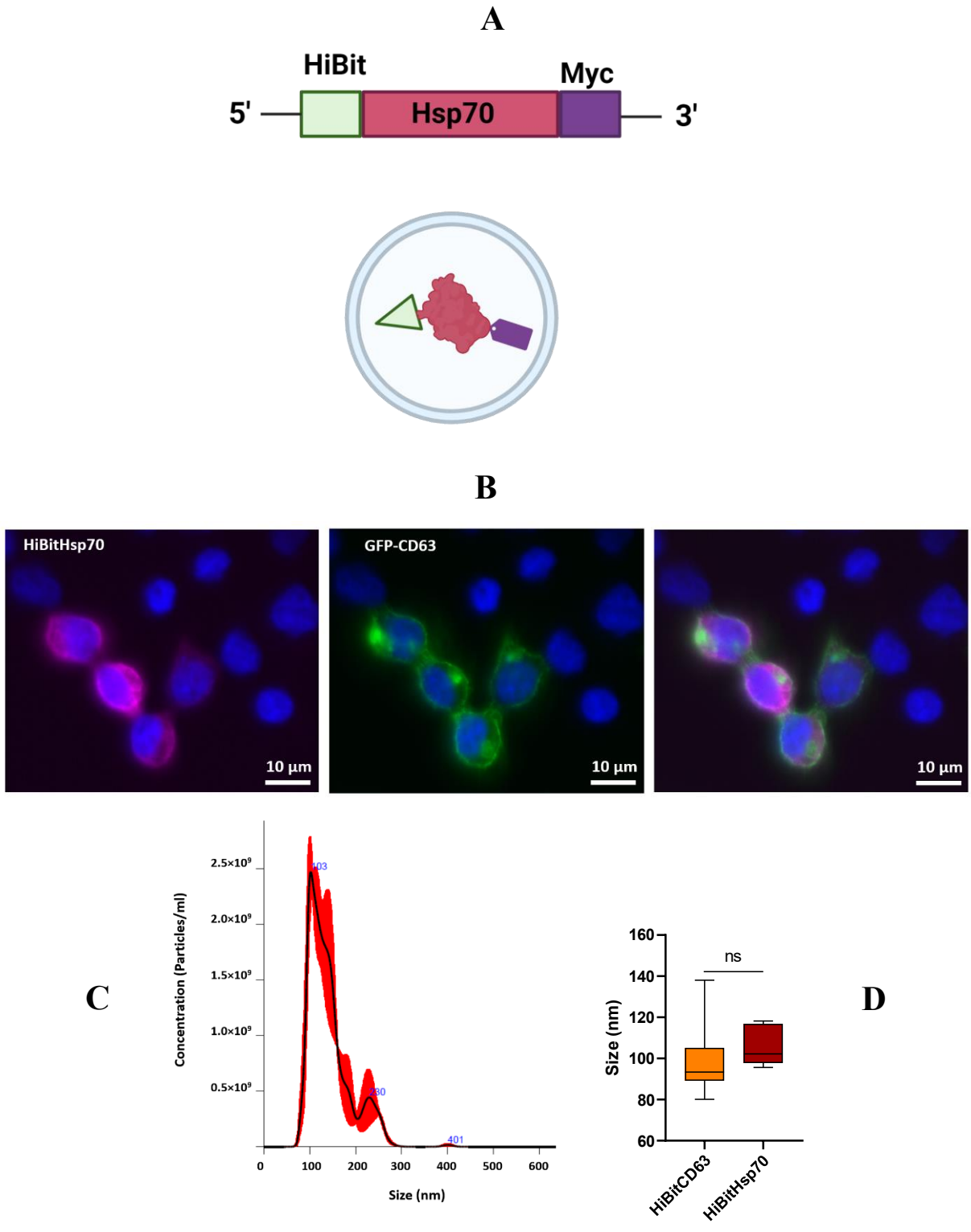

Figure 27: **The use of HiBitHsp70 labeled EVs.**

(A) Schematic representation of HiBit-tagged protein, and the protein localization inside EVs.

(B) Confocal fluorescence images of HiBitHsp70 co-expressing Hek cells with GFP-CD63, cells were labeled with anti-myc antibody (Scale bars, 10µm).

(C) NTA analysis of HiBitHsp70-containing EVs obtained from Hek 48h condition medium, the black line represents mean values obtained from independent measurements (Red colour).

(D) Particle size from NTA analysis was measured and compared between HiBitHsp70-containing EVs and HiBitCD63-containing EVs, (Min and Max are represented, HiBitCD63 n=25, HiBitHsp70 n=5 independent experiments).

3.9 CD63 enhances the secretion of vesicles by Hek cells

We noticed a significantly higher concentration of EVs secreted from cells overexpressing CD63 compared to cells overexpressing HiBitHsp70. One example of this is shown in Figure 28A where a majority of vesicles secreted from cells co-expressing HiBitHsp70 and HiBitCD63 are 97 nm and a majority of vesicles secreted from cells expressing HiBitHsp70 are 106 nm in diameter. A less abundant population is observed around 160 nm in both groups. However, statistical analysis revealed that the difference in size between the two groups is not significant (Figure 28B). Importantly, the number of vesicles showed a 3-fold increase in EV secretion when cells overexpressed CD63 (Figure 28A).

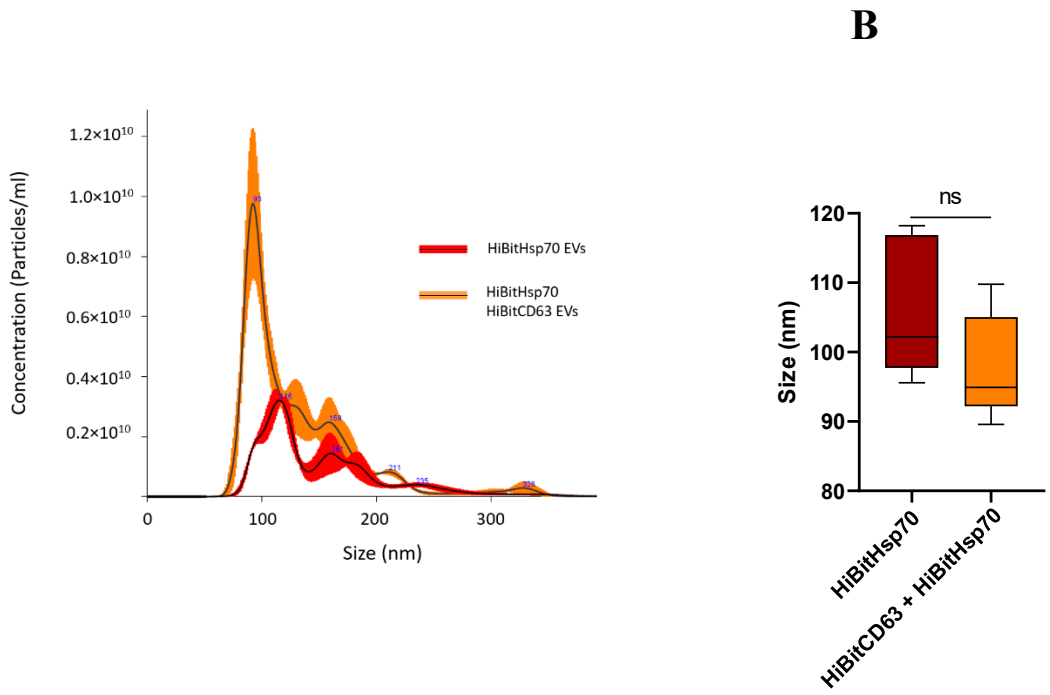

Figure 28: **Effect of overexpressed CD63 on the concentration and size of the vesicles.**

(A) NTA analysis of HiBitHsp70-containing EVs and HiBitCD63 + HiBitHsp70-containing EVs obtained from Hek 48h condition medium, the black line represents mean values obtained from independent measurements (Red color).

(B) Particle size from NTA analysis was measured and compared between HiBitHsp70-containing EVs and HiBitCD63 + HiBitHsp70-containing EVs, (Min and Max are represented, HiBitHsp70 n=5, HiBitCD63 + HiBitHsp70 n=5 independent experiments).

3.10 Enhancing EVs yield using suspension Hek cells

In our previous finding, we observed a low secretion of EVs from HiBitHsp70 overexpressing cells grown in monolayers. We next used Hek cells grown in suspension as an alternative approach to culture a higher cell density within a single flask and subsequently boost EV purification yield. Nevertheless, suspension Hek cells have the advantage of being cultured in a chemically defined medium, containing no serum.

In the first step, the size and concentration of vesicles purified from suspension Hek cells were checked by NTA. The analysis showed that most of the population was around 100 nm (Figure 29A). We next purified vesicles by ultracentrifugation of cell culture supernatants from Hek cells in suspension expressing HiBitCD63 after 72h and 96h. As depicted in Figure 29B, the expression of HiBitCD63 started after 24h post-transfection and increased until 3 days. The protein was highly enriched in EVs compared with flotillin. The EVs marker Alix was as expected also enriched in the purified EVs that support the validity and specificity of EV purification. All further experiments were performed with EVs purified from Hek cells in suspension.

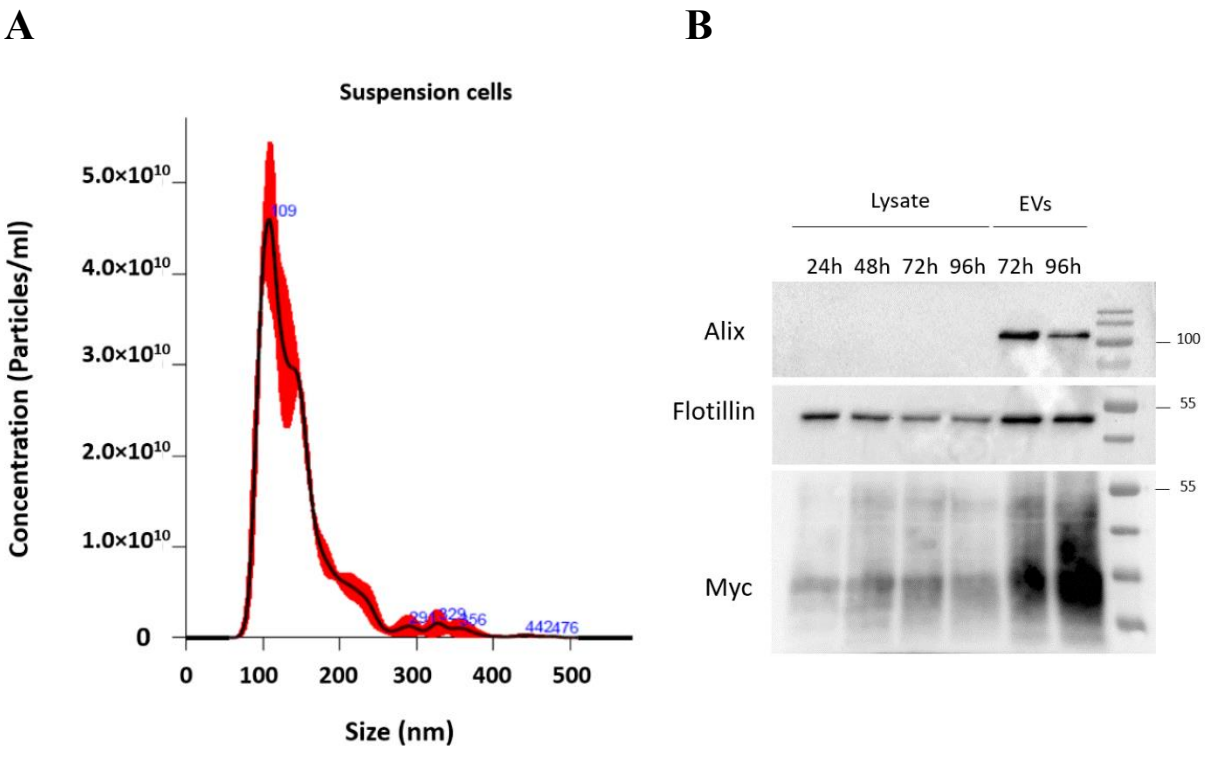

Figure 29: **Characterization of EVs secreted by Hek cells in suspension.**

(A) NTA analysis of EVs obtained from suspension Hek 72h condition medium, the black line represents mean values obtained from 3 independent measurements (Red color).

(B) Western blot showing the expression of HiBitCD63 for 4 days both in the lysate and in the EVs using anti-myc antibody, and the presence of Flotillin in the lysate and EVs using anti-flotillin antibody, and enrichment of Alix in EVs using anti-Alix polyclonal antibody.

3.11 Distinct set of vesicle secretion in cells expressing HiBitHsp70 or HiBitCD63

We next purified EVs from Hek cells expressing HiBitHsp70, HiBitCD63, or co-expressing HiBitHsp70 and HiBitCD63. As expected, both proteins were detected in both the lysates and EVs of the cells within all three experimental groups using anti-myc antibody (Figure 30A).

We then monitored the EVs fusion, by incubating the LgBit expressing cells with EVs purified from cells expressing HiBitHsp70 and HiBitCD63 individually as well as from cells co-expressing both for a duration of 3h. Following the incubation period, cells were washed two times with PBS and then luminescence was measured in the presence of the DrkBit peptide. The results showed no increase in luminescence, which indicates a lack of interaction between the HiBit of EVs and LgBit in the cytosol of receiving cells under these experimental conditions (Figure 30B).

The addition of 0.5% detergent (Triton X-100) led to a reduction in the level of luminescence in both the control group and the group incubated with EVs containing HiBitHsp70. This drop in background luminescence can be attributed to two factors. First, the presence of Triton X-100 which, as demonstrated before, massively decreases luminescence in our assays. Second, the presence of DrkBit effectively blocks all accessible LgBit sites upon solubilization. In contrast, no such decrease could be seen after Triton solubilization of cells incubated for 3h with EVs carrying HiBitCD63 or HiBitCD63 and HiBitHsp70. In this latter case, even a very slight but significant increase could be detected. In this assay, cells were washed, thus avoiding secreted LgBit and the measures were made in the presence of DrkBit, which is cell impermeable. Thus, the relative increase in luminescence detected after Triton addition to cells preincubated with HiBitCD63, or HiBitHsp70- and HiBitCD63- containing EVs, reveals the presence of HiBit-containing EVs on the surface or inside cells reacting with LgBit expressed by the cells upon membrane solubilization. This is in striking contrast with the lack of luminescence detected when cells were incubated with HiBitHsp70, demonstrating that EVs carrying Hsp70 alone are different from those carrying CD63. Our interpretation is that CD63-containing EVs can bind and perhaps be endocytosed by receiving cells without membrane fusion, which would allow the binding of HiBit with lgBit. The apparent lack of increase in luminescence induced by Triton in cells preincubated with EVs carrying HiBitHsp70 suggests that these EVs do not bind to or are not endocytosed by receiving cells (Figure 30B). This difference in behavior between EVs containing Hsp70 and those containing CD63 might reflect a different composition of EVs.

In order to further explore the difference in behavior between both types of EVs, we explored their vesicular characteristics. We checked the expression of CD9, a tetraspanin that is more

specific for ectosomes, which are vesicles released from the budding of the plasma membrane. We also tested Alix, which is more specific for exosomes, which are generated through the endocytic pathway. Actin was utilized as a commonly used marker for all EVs. Surprisingly both Alix and CD9 were enriched in vesicles secreted from cells expressing HiBitHsp70 compared to those from cells expressing HiBitCD63 alone or together with HiBitHsp70. This result suggests that the expression of HiBitHsp70 or CD63 differently influences the secretion of distinct EV populations (Figure 30C).

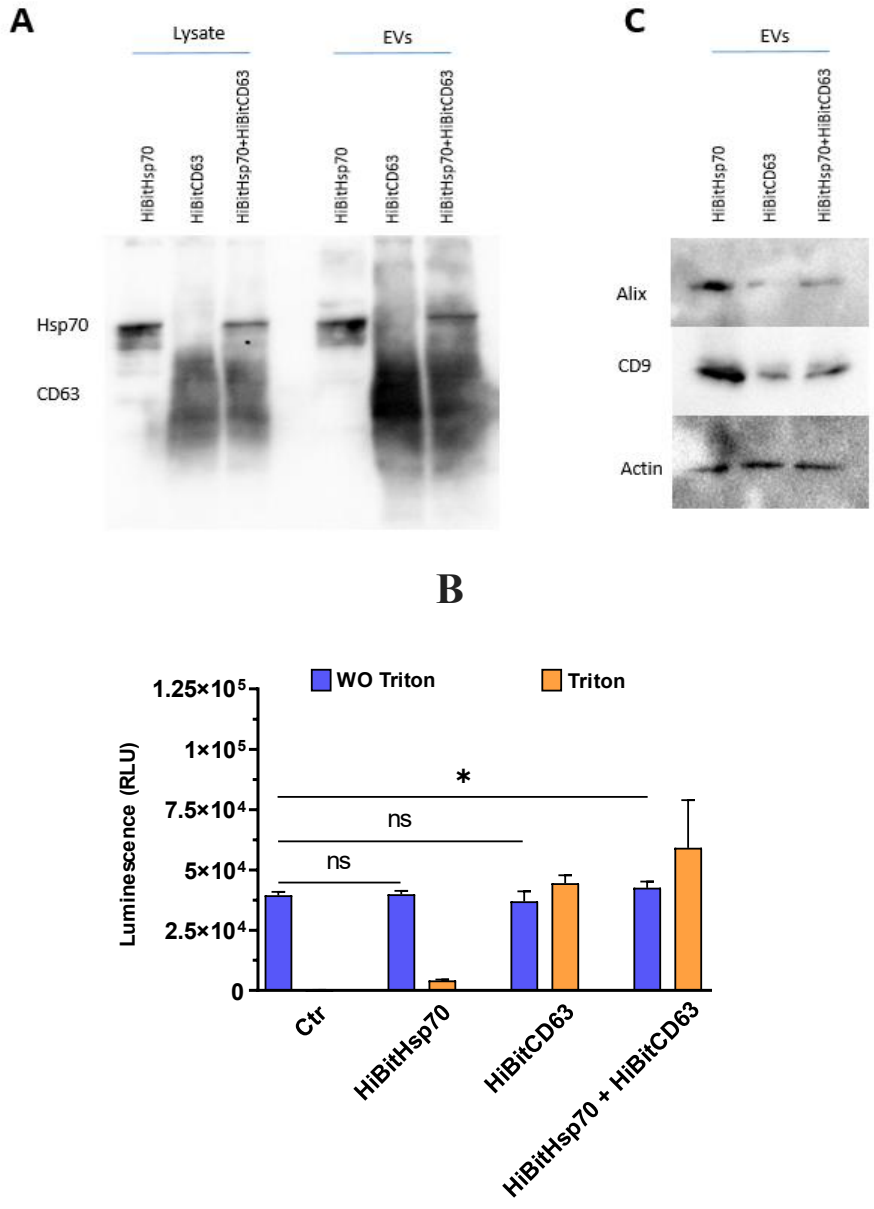

Figure 30: **Monitoring the expression of HiBitHsp70 and its presence in EVs.**

(A) Western blot showing the expression of HiBitHsp70 and HiBitCD63 in both the lysate and EVs using anti-myc antibody.

(B) Luminescence activity measurement after 3h incubation of EVs containing HiBitHsp70, HiBitCD63, and HiBitHsp70 +HiBitCD63 on the LgBit-expressing cells in the presence of DrkBiT peptide (Representative experiment, mean ±SD is represented, n=3 wells).

(C) Western blot showing the distribution of Alix and CD9 within EVs using anti-Alix polyclonal and anti-CD9 antibodies and normalized by the intensity of the actin band using anti-actin antibody.

Effect of low pH on Alix and EVs

As long as EVs are in the extracellular space, they are exposed to a neutral pH. Then upon internalization through endocytosis, EVs travel along the endocytic pathway, where the pH decreases down to 5.5 inside late endosomes or even 4.5 in the lysosomes. In the following parts of my thesis, we examined in vitro the effect of low pH on EVs and Alix behavior.

3.12 Role of pH in Alix interaction with EVs and liposomes

It has been shown that the Bro-1 domain on the Alix protein interacts with the artificial lipid membranes (Bissig et al., 2013). In this study, our objective was to explore the binding capacity of the Alix protein to the lipid bilayer of EVs or liposomes. In these analyses, we used recombinant Alix ΔPRD which lacks the long Proline-rich region but contains the Bro-1 which was shown to bind to lipids and the V domains necessary for dimerization of the protein. The monomeric form of Alix ΔPRD was incubated with liposomes composed of Sphingomyelin (SM), Phosphatidyl-serine (DOPS), and Cholesterol (Chol). Interaction with the liposomes was analyzed by sucrose flotation assay conducted at both neutral and acidic pH conditions. In this discontinuous gradient, liposomes incubated with Alix ΔPRD were diluted to 60% sucrose and overlaid with 40%, 30%, and 10% sucrose cushions (Figure 31A). After overnight centrifugation at 130 000 g, 5 fractions were collected and analyzed with a Coomassie gel. A white band corresponding to the liposomes could be detected in the upper part of the 30% fraction.

The main difference between the pH 7 and pH 5.5 conditions was the presence of Alix at the top of the gradient at pH5.5 although a portion of the protein remained in lower fractions. The presence of Alix ΔPRD in the 10 % sucrose fraction may be attributed to contamination from the lower fraction containing Liposomes (Figure 31B). This suggests that Alix ΔPRD has a stronger affinity for the liposomes at acidic pH conditions.

In order to investigate if the protein Alix can interact with the EVs membrane, we incubated the monomeric form of Alix ΔPRD with EVs at pH 7 and pH 5.5 and protein interaction was monitored by a continuous sucrose gradient floatation assay. Here a cushion of 60 % sucrose containing EVs preincubated with Alix ΔPRD was covered by a continuous sucrose gradient ranging from 55% to 8%. After overnight centrifugation at 130 000 g (Figure 31C), 10 fractions were collected and analyzed by western blot. The exosomal marker Syntenin was detected to fraction 5 corresponding to 29% sucrose, confirming the presence of exosomes. Alix ΔPRD was mainly detected in fractions 10-8 at pH 7 and detected up to fraction 5 at pH 5.5. Syntenin, which is enriched in EVs, was found in fractions 10 to 5. Thus, Alix interacts with the EVs at low pH (Figure 31D).

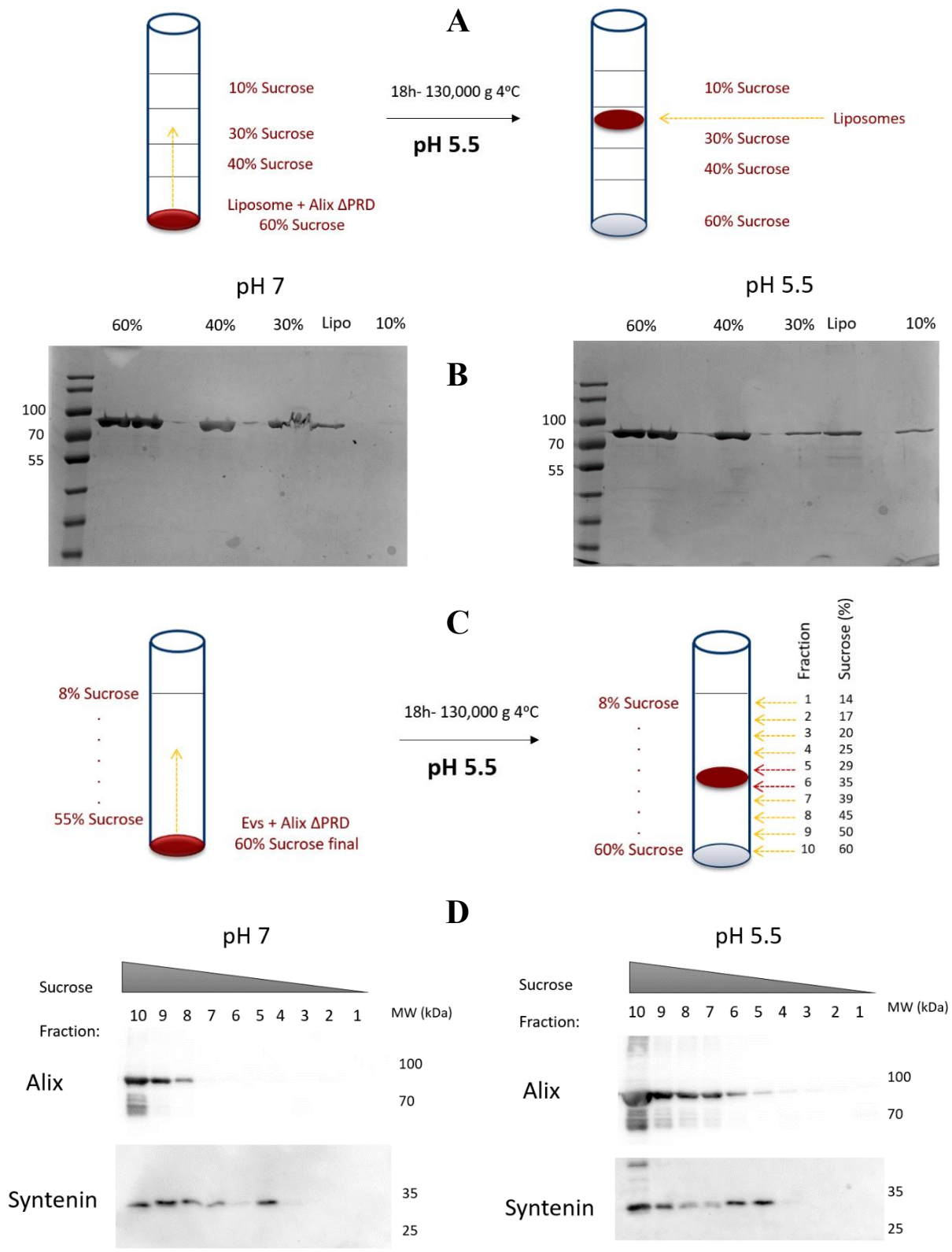

Figure 31: **Effect of pH on the interaction of Alix ΔPRD protein with membrane**.

(A) Sucrose cushion.

(B) Sucrose cushion centrifugation of liposomes incubated overnight with Alix ΔPRD at different pH. Samples from 5 fractions were analyzed by SDS-PAGE and the bands corresponding to the Alix ΔPRD protein (~ 79KDa) were detected by Coomassie blue staining.

(C) Continuous sucrose gradient.

(D) Sucrose gradient centrifugation of EVs incubated overnight with Alix ΔPRD at different pH. Samples from 10 fractions were analyzed by western blot and detected by anti-myc and anti-syntenin antibodies.

3.13 EVs fusion with liposomes at acidic pH in the presence of Alix

Thus, our results show that Alix can interact with the surface of EV membranes. To monitor if this interaction can lead to the fusion of EVs with other membranes mimicking endosomes, we set up a fluorescence assay. We used two lipophilic fluorophores, DiI (Ex:540, Em:570) as a donor and DiD (Ex:645, Em:665) as an acceptor analog (Figure 32A). Both dyes are incorporated in the lipid bilayers.

These two dyes were chosen because of their capability for fluorescence resonance energy transfer (FRET). When they are close enough, the fluorescence emitted by Dil excited at 540 nm is quenched as it is absorbed by DiD. The fluorescence will increase when both dyes are diluted (Figure 32B). Here the two fluorophores were used to label EVs and the labeled EVs were incubated with liposomes. The increase in fluorescence was measured as an index of EV fusion to the liposomes.

EVs were purified from Hek cells in suspension and labeled with DiI and DiD. Simultaneously, liposomes were prepared using a lipid composition of SM: DOPS: Chol (5:2.5:2.5) in order to mimick the lipid composition found in the endosome, where SM and Chol are known to be enriched.

NTA analysis showed a homogeneous population of liposomes with an average diameter of 100nm, the size of the EVs remained unchanged after the labeling process (Figure 32C). Labeled EVs and unlabeled liposomes were mixed at a final ratio of 1:300 and the fluorescence intensity was measured at 570 nm.

We first investigated the possible role of pH in the membrane fusion of EVs with liposomes. Liposomes were added after 5 min. In the presence of liposomes at neutral pH (pH 7), no increase in fluorescence intensity was observed. After 18 min, 20 mM MES was added to reach pH 5.5, simulating the acidic pH environment of late endosomes. MES is a recommended buffer for acidic pH which has a pKa of 6.1. The fluorescence intensity was not increased during the 95 min of the experiment (Figure 32D). The addition of Triton X-100 to the sample gave the maximum dequenching reachable with the labeled EVs. These findings show that a drop in pH similar to that occurring along endosome maturation does not noticeably influence the fusion of EVs to liposomes containing Chol, DOPS, and SM.

Nolwenn Miguet in our lab had shown that liposomes fuse together in the presence of Alix ΔPRD and that this fusion is pH dependent. This led us to investigate if Alix ΔPRD could trigger fusion between EVs and liposomes. As seen in Figure 32E, the presence of Alix ΔPRD at neutral pH (pH7), did not increase the fluorescence intensity, indicating a lack of fusion events. MES was then added to one group to lower the pH to 5.5. This pH change causes a

remarkable increase in fluorescence. This result shows that Alix is capable to promote membrane fusion under acidic pH conditions.

A

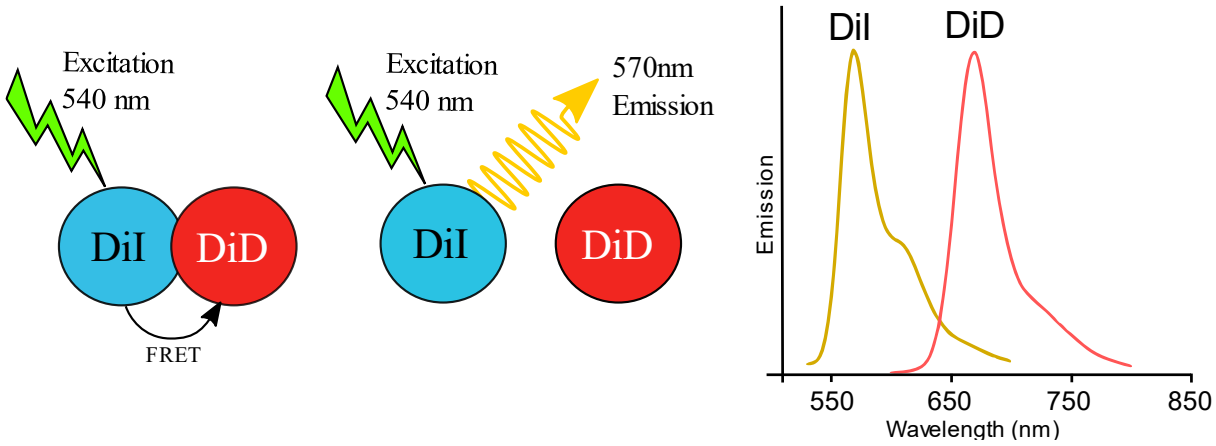

B

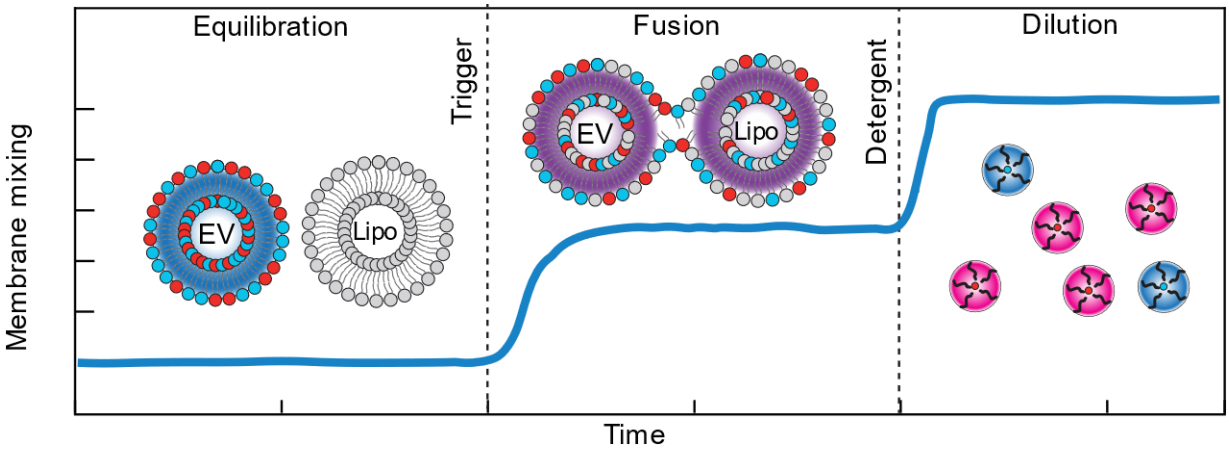

C

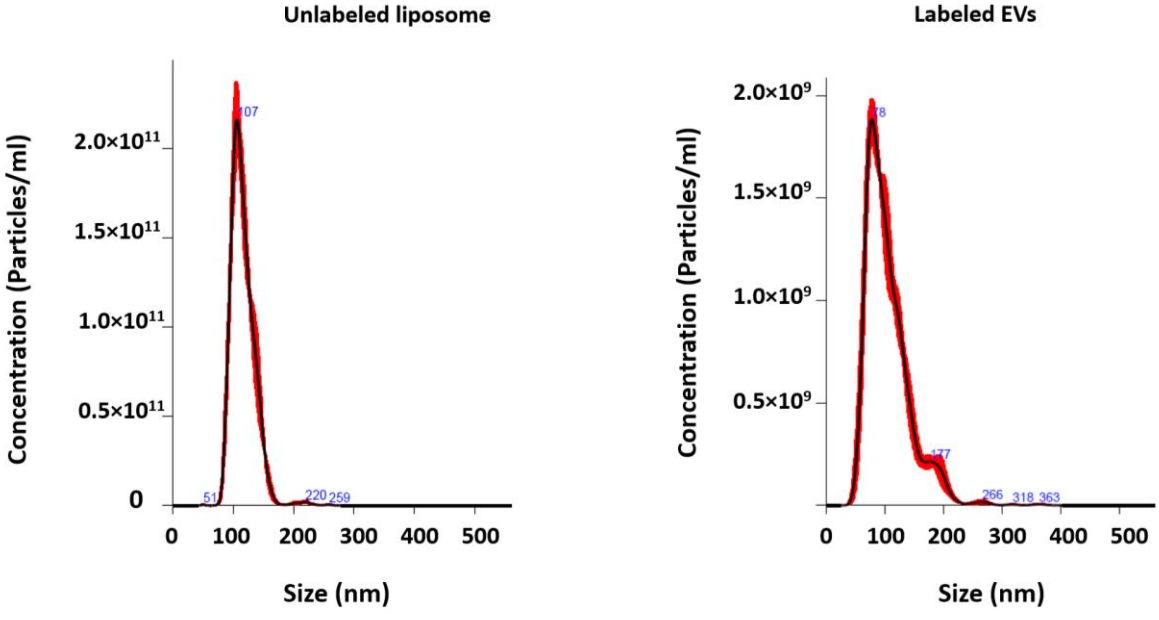

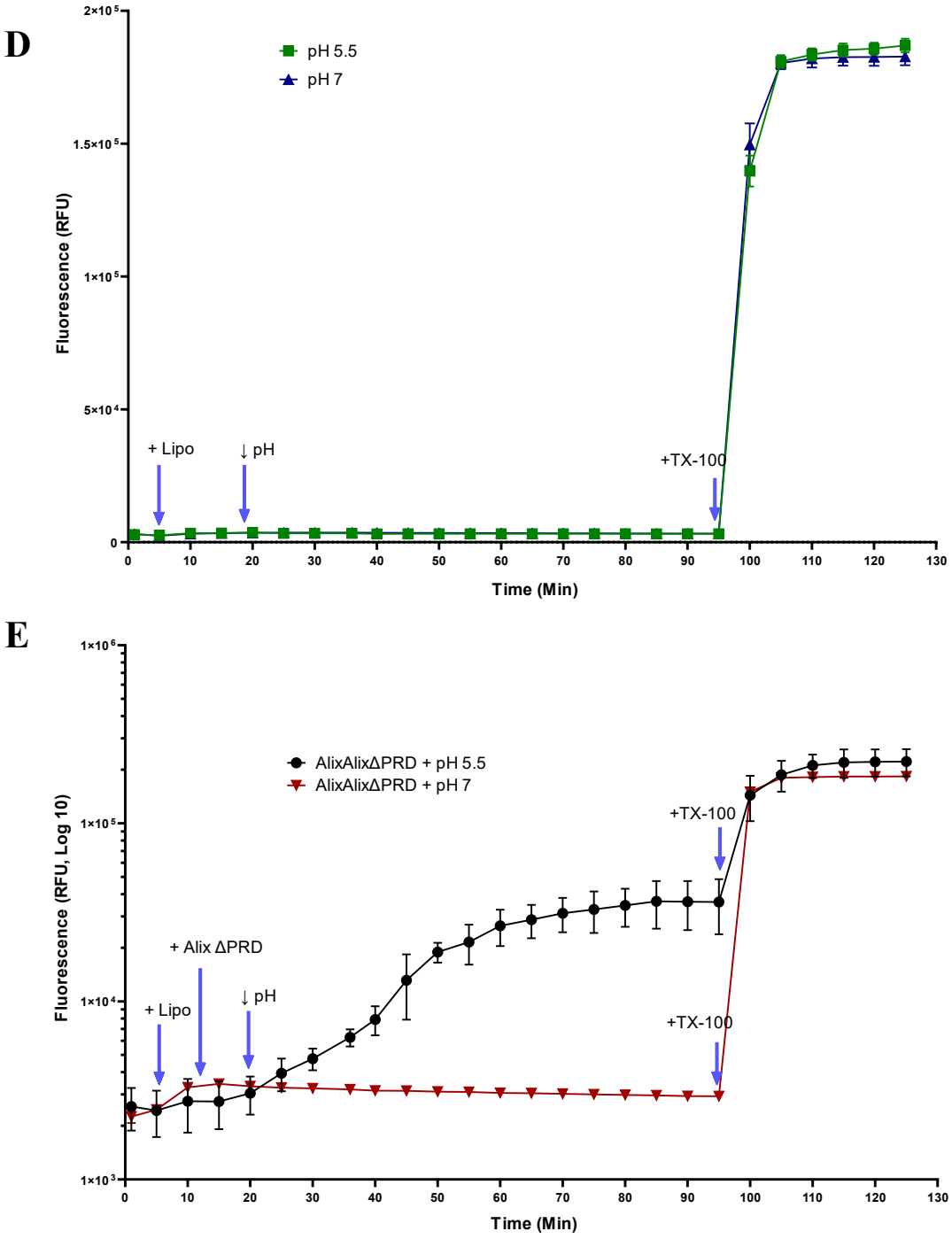

Figure 32: **Membrane fusion between EVs and liposomes in vitro**

(A) Fluorescence test principle: If the two fluorophores are very close, the DiI is excited at 540nm and the fluorescence emitted is absorbed by the DiD molecule (this is known as FRET); If the two fluorophores are far apart, the DiI is excited, and fluorescence emitted at 570nm.

(B) Illustration of the FRET-based membrane mixing assay used to quantify fusion between EVs and liposomes. Labeled EVs are incubated with non-labeled liposomes and their ability to fuse is monitored by donor fluorescent intensity. Adapted from (Morandi et al., 2022)

(C) NTA analysis of labeled EVs (right) and Liposomes (left), the black line represents mean values obtained from 3 independent measurements (Red color).

(D) Representative curves of membrane mixing for labeled EVs incubated with 300X unlabeled liposomes in pH7 (Blue) or pH 5.5 (Green), (Representative experiment, mean ±SD is represented, n=3 wells).

(E) Representative curves of membrane mixing for labeled EVs incubated with 300X unlabeled liposomes in the presence of monomeric Alix ΔPRD in pH7 (Red) or pH 5.5 (Black), (Representative experiment, mean ±SD is represented, n=3 wells).

3.14 Acidification of EVs lumen with changing external pH

Here, we investigated if the pH inside the EVs follows the drop in pH that EVs encounter after endocytosis. To address this question, we used a pH-sensitive derivative of GFP called, Super ecliptic pHluorin, the fluorescence of which decreases with the pH. This property of pHluorin makes it an ideal reporter for investigating pH changes. The SEP-pHluorin was fused to the C-terminal part of CD63, which sits inside the lumen of EVs. CD63pHluorin expressed in Hek cells was observed in the cytoplasm at the plasma membrane and in intracellular compartments. The detected fluorescence could correspond to ILVs accumulated inside endosomes with a neutral pH or to the cytosolic pHluorin of the C-terminal CD63 sitting at the limiting membrane of endosomes (Figure 33A). Indeed, some figures of round compartments decorated with fluorescence could be detected (arrows).

EVs were purified by ultracentrifugation of cell culture supernatants from Hek cells expressing CD63pHluorin and the NTA of these EVs showed the expected size distribution with a peak diameter of 117 nm (Figure 33B). Moreover, as we can see in Figure 33C, CD63pHluorin was detected in both the lysates and EVs on a western blot using an anti-myc antibody with strong enrichment in EVs.

For monitoring how the luminal pH of EVs is influenced by pH, we incubated purified EVs in PBS (pH 7) and fluorescence emission was collected using a 500–600-nm band-pass filter. As seen in Figure 33D, fluorescence first decreased with time reflecting the bleaching of pHluorin. After 8 min, MES was added to achieve a pH of 5.5. In the control, where PBS was added instead of MES, an immediate increase in fluorescence was measured suggesting dequenching due to dilution of the EVs, followed by a decrease due to bleaching of pHluorin. Note that the slower kinetic of bleaching also reflects the dilution of EV solution. Solubilization of EVs using Triton-X100 increased the fluorescence signal, probably due to dequenching of the pHluorin. In contrast, the fluorescence dropped within 1 min after the addition of MES demonstrating an immediate drop in pH in the EV lumen. No further drop was detected after solubilization of the EVs with Triton X-100. This demonstrates that EV membranes are permeable to protons at acidic pH and will therefore acidify after endocytosis. It will now be interesting to test at which pH this permeabilization to protons occurs and which channel is involved in this flux of protons.

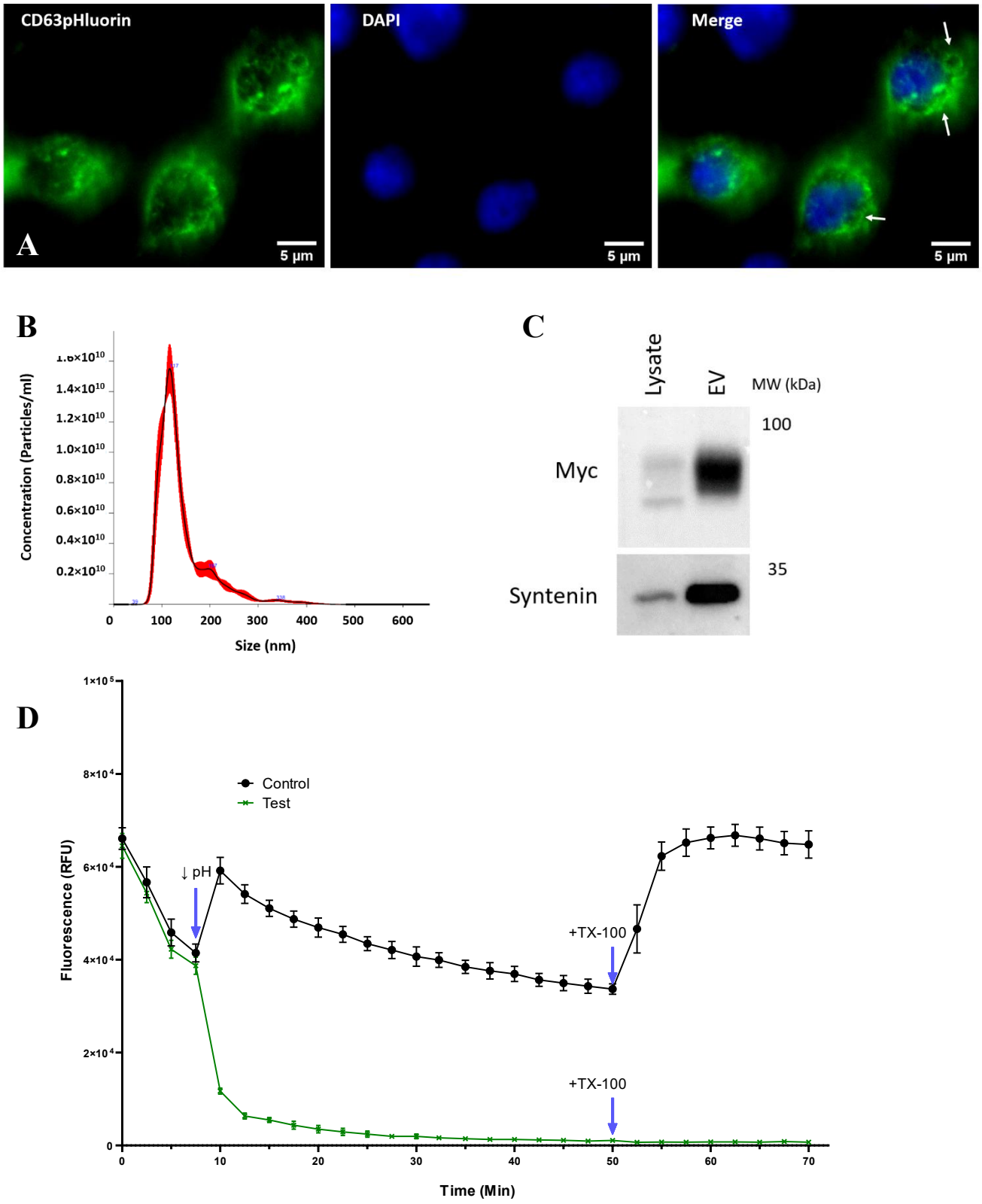

Figure 33: **Monitoring pH inside EVs.**

(A) Confocal fluorescence images of CD63pHluorin-expressing Hek cells (Scale bars, 5µm).

(B) NTA analysis of CD63pHluorin-containing EVs obtained from Hek 48h condition medium, the black line represents mean values obtained from independent measurements (Red color).

(C) Western blot showing the expression of CD63pHluorin in both the lysate and EVs using an anti-myc antibody and the enrichment of Syntenin in EVs using an anti-syntenin antibody.

(D) Representative fluorescence curves showing the pH variation inside the EVs during incubation at pH 7 (Black) or pH 5.5 (Green), (Representative experiment, mean±SD is represented, n=3 wells).

3.15 Lack of evidence for Alix translocation through the lipid bilayer of EVs

It has been observed that many cytosolic proteins are localized on the surface of EVs and may be connected to the surface by non-covalent binding. Some EV membrane proteins like SCAMP3 and STX4, or lipid-anchored molecules like most Rab proteins, were shown to have a reversed topology (inside-out topology). In other words, these proteins appear in a topologically reversed orientation compared to their annotations. It has been shown that some peptides and proteins can be both in the cytosolic and extracellular space like Fibroblast growth factor 2 (FGF2), HIV-Tat, and Tau. Also, many cytosolic proteins have extracellular functions and are secreted unconventionally. Some of these proteins are directly translocated across membranes (Sparn, Meyer, Saleppico, & Nickel, 2022).

Alix is cytosolic even though one study by Pan et al. demonstrated that the protein can be secreted into the extracellular milieu by an unknown mechanism (Pan et al., 2008). Also, some reports suggest that Alix associated with EVs is only partially protected from protease digestion, suggesting that part of the protein is present on the surface of the vesicles (Bonsergent et al., 2021).

These observations led us to hypothesize that Alix might cross the lipid bilayer. Specifically, we propose that once EVs come into the endocytic pathway, which features a pH range of 6.5 to 4.5, Alix could shift to the outside of the EVs thereby facilitating the fusion process of EVs with endosomal membranes.

The first approach to detect Alix translocation was the use of nanoluciferase. Here, EVs were purified from Hek cells expressing HiBitAlix and incubated at pH 7 or pH 5.5 for 1h. On the other hand, we prepared cytosolic extracts of LgBit-expressing cells as a source of soluble LgBit. Intact EVs containing HiBitAlix were incubated with the cytosolic LgBit and luminescence was measured. As shown in Figure 34A, there was no significant difference in the luminescence measured on EVs incubated at pH 7 or pH 5.5, which could suggest a possible translocation of the protein. In order to compare between experiments, we expressed the luminescence as the percentage of the maximum luminescence measured after solubilization of EVs, we used 0.5% detergent (Triton X-100), to allow HiBit to bind to LgBit. This allowed us to show that the luminescence measured from EVs containing HiBitAlix is almost 95% of the luminescence detected in the presence of Triton (Figure 34A), indicating that the vast majority of HiBit is found outside of the EVs. In comparison, we also used EVs containing HiBitCD63, where HiBit is at the NT part of the protein which is located inside the EVs. In this case, the luminescence measured on intact EVs was only 2% of that measured after Triton-solubilization showing that, as expected, the vast majority of the N-terminal part of CD63 sits inside EVs

(Figure 34A). Also expected was the lack of effect of lowering the pH on the orientation of CD63.

We then tested the Proteinase K (PK) protection assay of overexpressed HiBitAlix. Here, proteins contained inside the vesicle are preserved and only surface-accessible proteins are digested by PK. EVs purified from cells expressing HiBitAlix were treated with or without PK and the level of protein Alix was analyzed by western blot using an anti-Alix polyclonal antibody. Interestingly, PK was able to digest more than 50% of the protein confirming that a significant amount of overexpressed Alix is present on the outer surface of EVs (Figure 34B). Two (or more) Alix-associated bands were observed on the western blot analysis. One band with a molecular mass of 93kDa (predicted size of Alix according to UniProt), while another band at 75kDa was also observed in the cell lysates as well as in EVs (Figure 34B). This latter band might correspond to that characterized by Lopes-Rodrigues et al., which lacks the CT peptide due to the proteolytic cleavage mediated by cathepsins (Vanessa et al., 2019).

As we had shown that soluble Alix could bind to the surface of EVs, we tested if the culture medium of transfected cells contains HiBitAlix. Here the culture medium was centrifuged at 100 000g to eliminate EVs. The full-length HiBitAlix was revealed in the supernatant using western blot, whereas the cell lysates contained mainly the 75kDa band, which might correspond to the cathepsin cleavage product. In addition, soluble Alix was fully digested by PK showing that is not protected by any membrane. This suggests that Alix associated with the EV's surface, may originate from the supernatant of the cells.

This finding of HiBitAlix on the surface of EVs encouraged us to test if endogenous Alix can also be present on the EV surface and if this might be influenced by the pH. As shown in Figure 34C, 2 bands of 95 and 75 kD can be detected by an anti-Alix polyclonal antibody. Only the upper band is found associated with EVs. Unlike previous findings from other labs (Bonsergent et al., 2021), Alix was fully protected from PK at neutral pH when the EVs were incubated with PK. The protein was completely digested in the presence of Triton, confirming the functionality of the protease under our experimental condition and reinforcing our finding that Alix is protected by a lipid membrane. This result demonstrates that endogenous Alix is only present in the lumen of EVs and that the presence of the protein on the surface of EVs is due to its overexpression (Figure 34D).

We next tested using PK protection if Alix could be translocated toward the outside of EVs. EVs were first incubated at neutral or acidic pH for 1h before the addition of PK. Following this, we analyzed by western blot the level of Alix, as well as Flotillin-1 and Syntenin which were both already shown to be present inside EVs (Chivet et al., 2014; Mathieu et al., 2021). Noteworthy here, is that Syntenin was also chosen because it is a demonstrated interactor of Alix (Figure 34E). Unexpectedly, we observed that the level of all proteins was reduced

following the 1h incubation at pH 5.5 (lanes on the far right in both graphs). This decrease is likely due to intraluminal proteases activated at low pH since the addition during the 1h incubation at pH 5.5 of a cocktail of membrane-impermeable protease inhibitors (Roche) did not block the decrease. Noteworthy is that the protease inhibitors even decreased the amount of Alix upon incubation at pH 7 (Figure 34E, left graph).

In good agreement with their intraluminal localization, Alix, flotillin, and Syntenin were not degraded by PK incubation with EVs. Furthermore, the degree of protection against PK activity was not drastically changed upon incubation at pH 5.5 (Figure 34E, right graph). Suggesting once more that Alix is not translocated through the membrane of EVs at acidic pH.

To control the integrity of the vesicles in acidic pH and the presence of PK, we used cryo-electron microscopy (cryo-EM) imaging, a technique that allows good preservation of the membrane. In general, most EVs visualized were round with a diameter of 100-120 nm. The EV membranes were clearly visible and continuous in all groups, which revealed that neither acidification nor PK treatment affected the integrity or morphology of EVs. However, the striking aspect of EVs incubated at pH 5.5 was the presence of dark densities, probably proteins, bound to the inner and outer leaflet of the membrane (Figure 34F).

The possible translocation of Alix was also tested using immunoprecipitation of intact EVs, which should precipitate the protein outside of the EVs. EVs were incubated at neutral and acidic pH for 1h and were then immunoprecipitated using an anti-Alix antibody. As we can see in Figure 34G, Alix could be only immunoprecipitated from EVs in the presence of 0.5% Triton X-100. However, the protein was not precipitated from intact EVs incubated at pH 7 or pH 5.5, suggesting again that no translocation occurs. One note of caution is that the low pH used here could affect Alix's immunoprecipitation. Furthermore, only 25% of Alix could be immunoprecipitated from solubilized EVs challenging our capacity to detect a small quantity of translocated proteins.

Thus, our different approaches have not allowed us to give any evidence for the translocation of Alix through EV membranes at low pH.

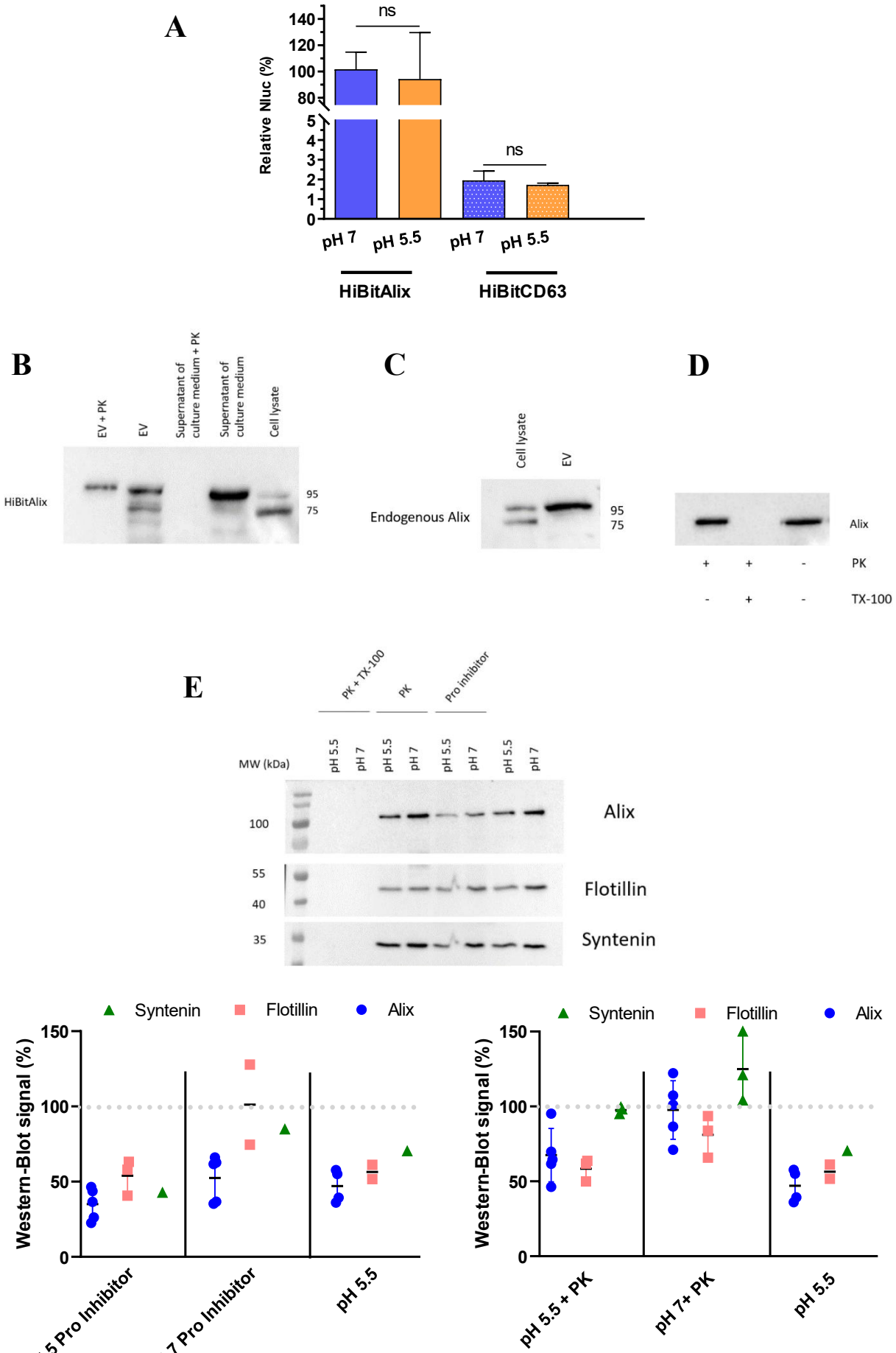
A
Relative Nluc (%)
ns
ns
pH 7
pH 5.5
pH 7
pH 5.5
HiBitAlix
HiBitCD63
B
EV + PK
EV
Supernatant of culture medium + PK
Supernatant of culture medium
Cell lysate
HiBitAlix
95
75
C
Cell lysate
EV
Endogenous Alix
95
75
D
Alix
PK
TX-100
E
PK + TX-100
PK
Pro inhibitor
MW (kDa)
pH 5.5
pH 7
100
55
40
35
Alix
Flotillin
Syntenin
Syntenin
Flotillin
Alix
Western-Blot signal (%)
pH 5.5 Pro Inhibitor
pH 7 Pro Inhibitor
pH 5.5
pH 5.5 + PK
pH 7+ PK
pH 5.5

F

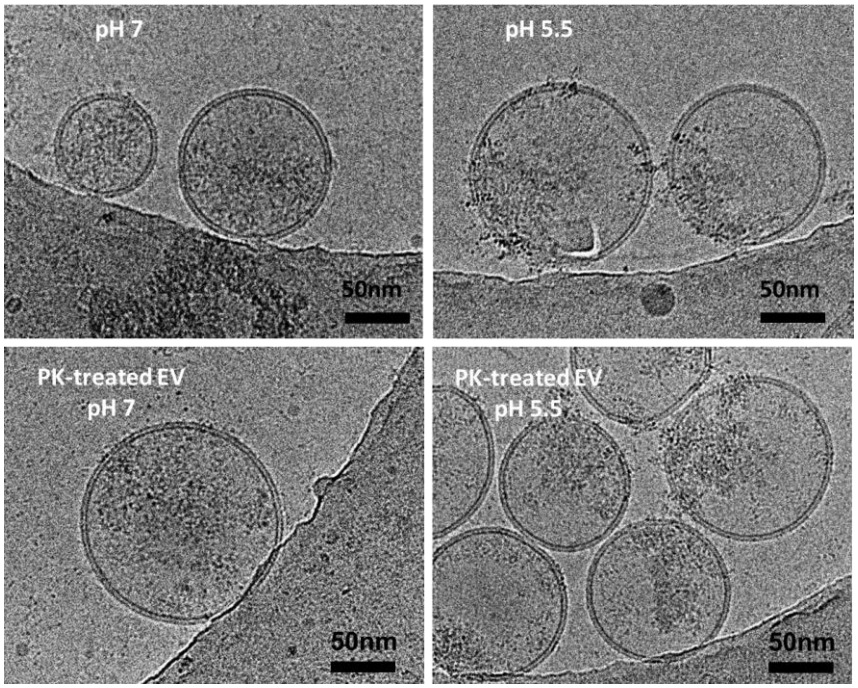

G

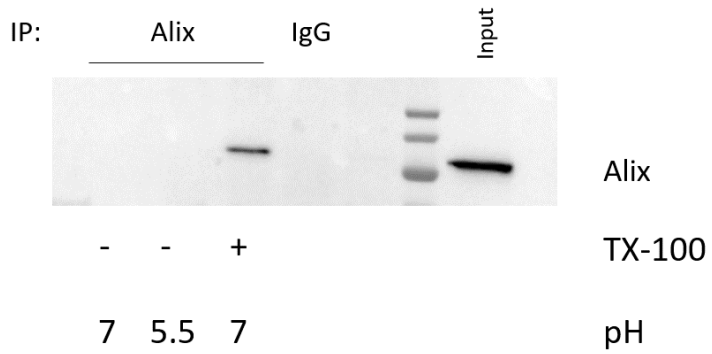

Figure 34: **Monitoring Alix orientation at natural and acidic pH within EVs**.

(A) Quantification of HiBitAlix and HiBitCD63 EVs incubated with cytosol of cells expressing LgBit at pH 7 and pH 5.5. Treated or not with detergent. Triton X-100 solubilization EVs were set to 100% (Representative experiment, mean±SD is represented, n=3 wells).

(B) Western blot showing the presence of Alix in the supernatant of EVs containing HiBitAlix using anti-Alix polyclonal antibody.

(C) Western blot showing the presence of Alix in the lysate and EVs using anti-Alix polyclonal antibody.

(D) Western blot showing the protection of Alix within EVs in the presence of PK, using anti-Alix polyclonal antibody.

(E) Western blot analysis of non-treated and PK-treated EVs at different pH (Right graph), in the presence or absence of protease inhibitor (Left graph) with different EVs marker (EVs at pH 7 were set to 100% for each protein, mean ±SD is represented, Independent experiments).

(F) Cryo-EM shows the size and integrity of the lipid bilayer of the EVs at different pHs, treated or not with PK.

(G) Western blot of the pull-down and input of the immunoprecipitation with anti-Alix antibody (1A12).

Chapter 4 DISCUSSION

Given the limited understanding of EV uptake and the molecular mechanisms underlying cargo transfer, this area of study holds great significance in advancing our knowledge in this field.

4.1 EVs cargo delivery and membrane fusion

EVs can enter cells through fusion with the plasma membrane or endocytosis. Although there is some evidence that shows the fusion between EVs and the plasma membrane of recipient cells (Montecalvo et al., 2012), endocytosis is the main pathway for EV uptake. EV cargo needs to be released from the endosomal compartment to keep its biological activities. There are several possible mechanisms by which cargo is released from endosomes, including kiss-and-run fusion with the endoplasmic reticulum, membrane fusion between EVs and endosomes, and endosomal permeabilization. Until now, some evidence suggests cytosolic delivery of EV cargo, however, the mechanism by which EVs can deliver their cargo into the cytosol remains obscure.

In 2016, Heusermann et al., demonstrated that EVs use filopodia to actively surf along the cell surface to reach specific regions known as endocytic hotspots. At these hotspots, EVs are grabbed and internalized through interactions with filopodia. Furthermore, they revealed that EV-containing endosomes undergo stop-and-go (kiss and run) movement along filamentous and mesh-like structures within cells. These structures were identified as the endoplasmic reticulum (ER), which serves as entry sites for EV cargo. TEM images demonstrated the uptake of CD63-Apex2 tagged exosomes by receiving cells, typically within vesicles in close proximity to the rough ER (Heusermann et al., 2016).

In 2018, a study successfully demonstrated the interaction between EVs and endosomes/MVBs using GFP-carrying EVs labeled with quenching R18 probes. However, they encountered challenges in detecting the release of GFP into the cytosol, most likely due to the rapid dilution of the soluble GFP cargo upon entry into the cytosol (Yao et al., 2018). Building upon these findings, in 2020, Joshi et al. provided evidence for the delivery of GFP-CD63 EV cargo to the cytosol. They used molecular tools with correlative light and electron microscopy (CLEM) to demonstrate the fusion of EVs with endosomes/lysosomes. In this experiment, GFP inside the EVs became accessible to the anti-GFP fluobody upon reaching the cytosol of receiving cell. While they revealed that endosomal permeabilization does not occur during the EV internalization process (Joshi et al., 2020).

Toribio et al. used EVs containing EGFP-luciferase-tagged tetraspanin to monitor the uptake of EVs by receiving cells. This investigation was facilitated by preloading the receiving cells with coelenterazine substrate, which can cross EV membranes. Notably, Only the EVs that were

taken up by receiving cells could access the substrate (Toribio et al., 2019). However, their assay lacked the ability to differentiate between the EV uptake and the actual delivery of functional cargo.

In light of this limitation, the core of our study tried to develop a NanoBiT luminescence-based method capable of showing the cargo release of EVs into the receiving cells through membrane fusion with intracellular membranes. This technique has been previously used in virus infectious studies. For instance, research conducted in 2020 on SARS-CoV-2 showed the virus's capability to infect VeroE6/TMPRSS2 through the interaction of the viral spike with the TMPRSS2 receptor present in VeroE6 cells. Treating HiBitVLP-SARS2 with LgBiT-expressing VeroE6/TMPRSS2 cells for 3h showed a significant increase in Nanoluc luminescence, suggesting a successful viral release (Miyakawa et al., 2020).

Our studies provided evidence that luminescence was occasionally detected when LgBit-expressing cells were incubated with EVs carrying HiBitCD63. This observation suggests that HiBit from HiBitCD63 EVs comes in contact with LgBit in the cytosol of the recipient cell. However, our findings also revealed a major limitation of this experimental design as we demonstrated that LgBit leaked from the recipient cells into the medium. Additionally, we discovered that the little fraction of EVs containing very low amounts of non-encapsulated HiBit was sufficient to significantly impact the accuracy of the luminescence assay.

During the course of our experiments, Somyia et al., published a paper, in which they faced similar artifacts while monitoring the fusion of EVs to cells using a similar approach to ours. Taking inspiration from their innovative solution, DrkBit was used during the luminescence measurement to prevent unwanted interactions and enhance the specificity of our assay. Their group had previously confirmed the membrane-impermeability of DrkBit and demonstrated that the addition of up to 1 μM of this peptide had no noticeable impact on the activity of NanoLuc in living cells (Somiya & Kuroda, 2021). Therefore, by using this peptide in our experimental setup, we were able to confirm that the occasional increase in luminescence over time in LgBit cells incubated with HiBitCD63-EV was indeed attributed to nonspecific binding between non-encapsulated HiBit and extracellular LgBit. Using DrkBit greatly influenced our approach and provided a practical solution to overcome the challenges we encountered during our study.

As we were unable to show EVs mediated fusion and cargo delivery, particularly in the case of Hek-derived EVs in recipient Hek cells. Perhaps, the nature of Hek cells, their little adhesion properties, their lipid and protein membrane composition, their efficient cellular trafficking could be at the origin of the complex data obtained on the uptake of EVs. Considering this limitation, we hypothesized that the efficiency and specificity of EV-mediated cargo delivery might improve when using different combinations of EVs and recipient cells, particularly those

with distinct cellular origins from the donor cells. However, the use of other cells (N2A, Hela and MCF7) as receiver gave negative results.

Despite our efforts, our observation did not reveal any evidence of fusion between EVs and the endosomal membrane. This lack of fusion was apparent not only when HiBitCD63-containing EVs were incubated with receiving cells expressing cytosolic LgBit, but also when incubated with receiving cells expressing LgBit specifically localized on the endosomal membrane. We used endosomal proteins, such as CD63 and Rab proteins, as potential markers for our experiments. Rab proteins, a family of small GTPases, are commonly used as markers to study the endocytic pathway. For example, Rab5 and Rab7, are two known proteins associated with EEs and LEs, respectively (Chavrier, Parton, Hauri, Simons, & Zerial, 1990). Our rationale was that the incorporation of these proteins into LgBit could help in identifying cargo release specifically at the fusion site. Therefore, we fused LgBit to the N-terminal or C-terminal of CD63, as well as the N-terminal of Rab5 or Rab7 in receiving cells and incubated with HiBitCD63-EVs. Unfortunately, none of these approaches succeeds in showing the fusion.

The decision to focus on Hsp70, one of the recognized generic EV markers, instead of CD63, was driven by the specific goal of assessing the cytosolic release of Hsp70, making it a good applicant compared to membrane-associated markers. Moreover, Hsp70 has been validated as an EV-encapsulated cargo in a study conducted by Bonsergent et al, (Bonsergent et al., 2021). Another hypothesis stemmed from the fact that the lipids and proteins present on the limiting membrane of endosomes are incorporated into ILV during EV formation. This is particularly true for CD63 which is concentrated in ILVs. Consequently, HiBitCD63 might transiently reside on the limiting membrane of the endosome after EV fusion and may reincorporate into newly formed EVs. However, our data using HiBitHsp70-containing EVs incubated with cytosolic LgBit receiving cells also failed to show the desired cargo release.

Although we did not detect any fusion event between EVs and endosomal membrane, regardless of whether we used HiBitCD63 or HiBitHsp70, an interesting observation was made upon the addition of detergent. This revealed an increase in luminescence in cells preincubated with HiBitCD63-containing EVs, while the lack of luminescence was detected in cells preincubated with HiBitHsp70. This allowed us to detect the differential behavior of both types of EVs in receiving cells. The observation revealed that the expression of HiBitHsp70 or HiBitCD63 differentially influenced the secretion of distinct EV populations. In all cases, HiBitCD63 EVs exhibited binding to or internalization by LgBit-expressing cells, while no incorporation of HiBitHsp70 vesicles was observed in the recipient cells. These results suggested the presence of two populations of EVs.

Further validation of these differences was obtained through western blot analysis, which showed distinct enrichment patterns of CD9 and Alix in each EV population. In one population,

EVs exhibited a higher abundance of CD63 on their membranes, leading to enhanced interactions and internalization by the receiving cells. While in a study by Tognoli et al., suggested that tetraspanins may not be required for the EV uptake and delivery process. They made this conclusion by comparing CD63 knockout, CD9 knockout, and wild-type cells as both donors and acceptors in their experiments (Tognoli et al., 2023).

Figure 27B presents the cytosolic expression of HiBitHsp70, revealing no colocalization with GFP-CD63. The lack of colocalization between HiBitHsp70 and GFP-CD63, which is known to be present in EVs derived from endosomal pathways, indicated that EVs containing Hsp70 do not originate from this particular cellular pathway. These findings confirm that EVs can be generated from distinct sources within the cell, supporting our previous data that suggest the existence of subpopulations of EVs with distinct cargo compositions and functions.

Based on some research, there is evidence suggesting that EVs may not be able to effectively transport cargo due to their limited cargo delivery capacity. Recent studies developed methods to improve EV cargo delivery through the use of fusogenic proteins. Some studies have incorporated viral fusogenic protein VSV-G (Somiya & Kuroda, 2021) or Syncytin-1, an endogenous retroviral envelope protein with fusogenic properties (Bui, Dancourt, & Lavieu, 2023). Recent findings provided by the group of Ina Vorberg emphasized the significant role of VSV-G in the uptake and fusion process of EVs and the intercellular propagation of prions. In their investigations, they focused on inducible protein aggregation using Sup35 NM as a model protein. They isolated EVs derived from NM-HA^{agg} and exposed them with NM-GFP^{sol} cells as a recipient cell. Their research revealed that EVs decorated with VSV-G showed a remarkable ability to enhance NM-GFP aggregation within recipient cells. This enhancement was attributed to their capacity to mediate efficient cellular membrane contact and fusion, both between EVs and target cells and among cellular membranes themselves. This internalization was preferentially facilitated by clathrin-mediated endocytosis, while fusion of EVs with receiving cells and escape from endosomes were found to be pH-dependent processes (Liu et al., 2021).

In our experiment, the incorporated VSV-G bearing EVs resulted in a 2-fold increase in membrane fusion. Despite the high sensitivity of the Nano-Luc assay, we were unable to observe the membrane fusion of EVs without co-expressing VSV-G for up to 18h. Our results indicate that EVs lacking known fusion proteins may not effectively deliver cargo, at least in the case of Hek-derived EVs in recipient Hek cells. Most studies of EV cargo delivery including ours, highlight the importance of fusogenic proteins in enhancing the fusion efficiency of EVs with endosomal membranes.

In a separate experiment conducted by Somiya et al., they demonstrated that EVs containing HiBit-tagged EPN-01 were delivered to LgBit recipient cells, but only in the presence of VSV-

G. This result shows a 5 to 8-fold increase in delivery efficiency after 90min and 24h, respectively. EPN-01 is a de novo-designed protein that forms a 60-mer self-assembled nanocage, allowing 60 HiBit tags to accumulate within a single nanocage. This design significantly enhances the sensitivity of the cargo delivery assay compared to ours. They also fused HiBit to the N-terminal of tetraspanin proteins like CD9, CD63, and CD81 as EV cargo. However, they did not present the results of using these cargo proteins, possibly suggesting their lower efficiency compared to EPN-01 (Somiya & Kuroda, 2021).

Additionally, in 2023, Bui et al., compared EVs containing Nluc-Hsp70 with either VSV-G or Syncytin-1 in the fusion/delivery system. They observed that Both VSV-G and Syncytin-1 strongly increased EV uptake and cargo release, with a 3-fold and 5-fold enhancement, respectively. These fusogenic proteins have the potential to continue to be explored in the context of EV-mediated cargo delivery to advance the field of EV-based therapeutics (Bui et al., 2023).

In the case of VSV virus infection, VSV fusion with the endosome depends on the cytosolic protein Alix and its interacting phospholipid (LBPA) (Bissig & Gruenberg, 2014). Following virus endocytosis, the viral envelope undergoes fusion with the ILV membrane thereby the capsid is delivered into the protective ILV lumen. Then, the capsids are released into the host-cell cytoplasm through the back-fusion of ILV membranes with late endosome membranes (Bissig et al., 2013; Le Blanc et al., 2005; Luyet et al., 2008). This process is the reverse of the ILV formation process. Thus, Alix is implicated in both the formation and the back-fusion of ILVs (Baietti et al., 2012; Gruenberg, 2020; Matsuo et al., 2004).

In agreement with Alix being a major actor in ILV back-fusion and viral infection (Bissig & Gruenberg, 2014; Bissig et al., 2013), our interpretation is that EVs containing VSV-G might not fuse with the endosomal membrane of Alix knockout cells. However, the comparison of EVs containing VSV-G incubated with Alix knockout receiving cells compared to wild-type receiving cells suggests that Alix may not be a critical factor for the fusion of EVs containing VSV-G in the receiving cells. However, despite the presence of the fusogenic protein VSV-G, we have been unable to achieve more than a twofold increase in membrane fusion in WT receiving cells. This limitation could make challenges when trying to compare it with Alix KO receiving cells. Other explanation for the disparity in our findings may arise from the fundamental differences between membrane of viruses and EVs carrying virus-derived fusogenic proteins. Further studies are required to elucidate other factors that may be involved in this fusion in the absence of Alix.

4.2 Alix membrane interaction

Alix has been shown to interact with liposomes containing LBPA through its calcium-bound Bro-1 domain, after membrane interaction, it could partially insert its hydrophobic loop into lipid bilayers, inducing a local conformational change and dimerization. The presence of LBPA is crucial for this interaction, as its absence resulted in an approximately 80% reduction in Alix binding. They further explored Alix's binding with other lipids individually, like PC, PS, PA, PI, and PE. In each case, Alix revealed a much lower binding capacity, with less than 40% compared to its interaction with LBPA. (Bissig et al., 2013).

In our study, we aimed to investigate the membrane binding capacity of the Alix further, we tested its interaction with EVs derived from Hek cells and liposomes containing other lipids like Sphingomyelin (SM) and Cholesterol (Chol), which have been shown to play a crucial role in the fusion of viruses with the plasma membrane (S. T. Yang, Kiessling, Simmons, White, & Tamm, 2015). SM is known to be enriched in the plasma membrane, as well as it is presented in endosomes (Koivusalo, Jansen, Somerharju, & Ikonen, 2007).

Our in vitro experiments successfully demonstrated the ability of Alix ΔPRD to bind to liposomes and EVs, with a stronger interaction observed at acidic pH. This result indicated a pH-dependent interaction between Alix and membrane, suggesting that Alix's binding affinity may be regulated depending on the cellular environment during endosomal maturation.

Upon EVs interaction with Alix ΔPRD, a considerable increase in the presence of EVs in lower fractions was observed. This observation suggests that the interaction of Alix with the EVs' membrane may affect its density, potentially influencing the protein-to-lipid ratio. Exosomes are typically described as having a density of 1.1-1.2 g/ml (fraction 5-6 in Figure 31D). While the observed presence of EVs in a lower fraction might be attributed to a higher density resulting from the interaction with the protein Alix, possibly affecting their flotation properties. Further studies could explore the significance of different lipid compositions in liposomes regarding the membrane binding of Alix.

4.3 pH regulation inside the lumen of EVs

EVs are exposed to a neutral pH when they are in the extracellular space. However, upon internalization into cells via endocytosis, the pH in the endosome gradually decreased from EE to LE and finally reaches pH 4.5 at the lysosome. The pH inside the EVs and the way it varies after EVs have been endocytosed is currently unknown.

A recent study by Riazaniski et al. focused on the luminal pH of EVs using Acridine orange (AO) as a pH indicator. To capture single EVs within a specific size range, they employed a

nanoporous silicon nitride (NPN) membrane. They demonstrated that when AO-loaded vesicles were exposed to low pH conditions, no decrease in fluorescence was observed, suggesting that EVs are capable to maintain a neutral pH environment in spite of external acidification. They also identified the presence of the epithelial sodium-hydrogen exchanger, NHE1, which could maintenance pH neutrality within EVs, even in the presence of a varying biological fluid composition. However, it is important to note that the presence of functional NHE1 on EVs varied significantly between different cell types. Specifically, in Hek cells only 40-45% of the total EVs were found to have functional NHE1. Their results confirmed that vesicles derived from the plasma membrane (Ectosome) had a higher percentage of the NHE1 transport protein compared to vesicles derived from MVBs (Exosome) (Riazanski et al., 2022). The limitation of their study was started with a heterogeneous population of EVs. And from these EVs, they selected the ones which were able to maintain a neutral pH when incubated at low pH.

Our study focused on EVs that contain CD63. And CD63pHluorin was used as a pH reporter within the lumen of EVs to investigate their pH dynamics. Interestingly, we observed that the luminal pH of EV drops within 1 min once exposed to an acidic environment. This rapid change in the permeability of EV membranes to protons led us to hypothesize the presence of a pH-sensitive channel in EV membranes. Notably, lysosomal membranes contain specific channels, which maintain a steady-state pH of the lysosomal lumen and balance the activity of V-ATPase. One such channel is TMEM175, which is associated with a genetic risk factor for Parkinson's disease (PD). TMEM175 acts as a proton-activated, proton-selective channel on the lysosomal membrane (LyPAP). it becomes active when the luminal face of a lysosome is exposed to a pH of 4.6, near the lower limit of the optimal pH range for lysosomes. TMEM175 selectively allows protons and potassium ions to permeate, facilitating the lysosomal "H^+ leak" and maintaining lysosome pH homeostasis (Hu et al., 2022). We propose a hypothesis that similar proton-activated channels might be present on the membranes of EVs, which allows protons entry into the lumen of EVs. As EVs are endocytosed, they are exposed to an acidic pH, these channels could be triggered to open, leading to the rapid acidification of the EV lumen.

Further analysis is warranted to determine the presence and functionality of proton channels within EVs. To achieve this, we propose using nonspecific protons or potassium channel inhibitors to monitor whether the observed drop in pH within the lumen is affected or not. In the next step, we aim to gain deeper insights into the kinetics of pH changes within the vesicles. Real-time fluorescence assays will be used to measure pH changes over time. This enables us to explore the optimal pH range required for the activation of the channels. Another interesting aspect is the use of CD9pHluorin EVs, which are known to be released more from the plasma membrane and might contain a higher proportion of functional NHE1 to maintain a neutral pH. By comparing the pH dynamics of CD9pHluorin EVs with our current result, we can obtain a better understanding of the mechanisms underlying vesicular pH regulation.

Furthermore, CD63pHluorin is suitable for advanced investigations into the pH dynamics of CD63-positive vesicles that accumulate inside endosomes. As we can see in Figure 33A, the expression of CD63pHluorin is detected on both the plasma membrane and intracellular compartment. In this latter case, the fluorescence delineates the compartment. This may be due to the C-terminal part of CD63 of the endosome membrane, which resides in the cytosol, and they are exposed to a neutral pH environment. This would also explain why the protein is also fluorescent at the plasma membrane. Moreover, it is known that the pH within MVBs plays a crucial role in determining whether they undergo degradation or secretion (Parolini et al., 2009). Secretory MVBs (sMVBs) are committed to releasing their ILVs as exosomes while maintaining a neutral pH. Consequently, the use of high-resolution microscopy could allow observing the CD63-positive vesicles within the endosome and thereby correspond to sMVBs, follow the plasma membrane, and release EVs containing CD63pHluorin.

4.4 In vitro membrane fusion

Within eukaryotic cells, EV fusion seems to be triggered by low pH which may occur inside endosomes (Bonsergent & Lavieu, 2019). This is analogous to the case of some viruses, which require endosome acidification, and the presence of Alix to enter the cytosol (Le Blanc et al., 2005).

Our work on membrane fusion of EVs with liposomes at pH 5 in the presence of protein Alix, suggests that Alix ΔPRD controls the fusion process between EVs and liposomes at low pH in vitro. The acidic pH serves as a trigger for Alix ΔPRD, increasing its ability to interact with the lipid bilayers of EVs and induce fusion.

A significant question regarding endosome topology remains unanswered, focusing on the mechanism underlying the position of the cytosolic protein Alix on the limiting membrane of late endosomes and control membrane fusion. One potential hypothesis is that Alix may serve as a mediator for the formation of fusion hotspots at the limiting membrane of endosomes or may control the redistribution of lipids within the endosomal membrane favoring budding and fusion of ILVs, in a pH-dependent manner. This could involve changing the lipid composition or organization within the membrane, promoting membrane curvature, and facilitating the fusion process (Figure 35A)(Bissig & Gruenberg, 2014).

Another possibility is that the protein translocates towards the outside of EVs (Figure 35B). A study by Pan et al. showed that the protein Alix can be secreted into the extracellular space in order to regulate integrin-dependent cell adhesion (Pan et al., 2008). Since then, the idea that Alix would be able to cross the plasma membrane has remained largely unexplored. However, a recent study conducted by Nolwenn Miguet in our lab has shed new light on this matter.

Similarly, to our results with EVs and liposomes, she observed that fusion of liposomes could occur at acidic pH, but only in the presence of protein Alix. Using cryo-EM, she demonstrated the presence of Alix on the surface of small liposomes. Interestingly, she noticed that the protein was absent from fused liposomes. This suggests that Alix might undergo translocation through the membrane during the process of fusion in vitro.

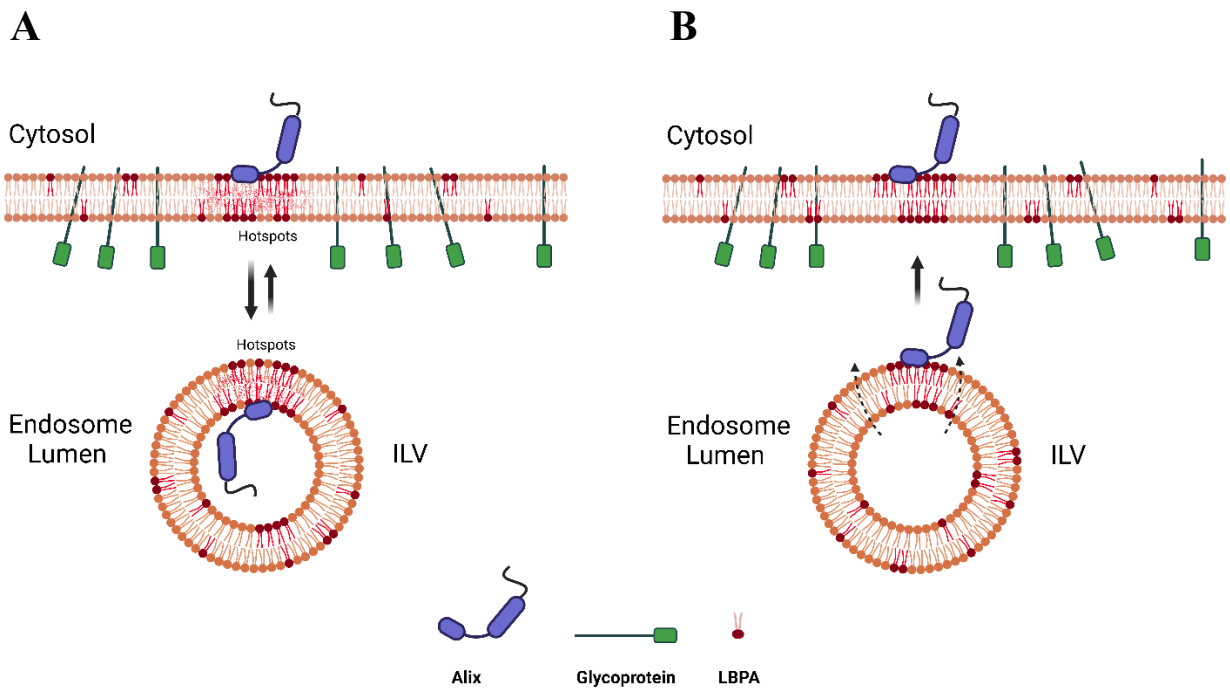

Figure 35: **Two hypothesis of the Alix's role in the ILV fusion.**

(A) The Role of Alix-LBPA interactions in facilitating Lipid-Rich ILV Docking and Fusion: Generating endosomal limiting membrane perturbations.
(B) Alix translocates towards the luminal side of endosomes and outside of ILVs. Bridging endosomal and ILV membranes for fusion.

So far, few mechanisms have been identified for transporting cytoplasmic proteins across the plasma membrane, including ectocytosis (Mehul & Hughes, 1997; Stein & Luzio, 1991) and membrane flip-flop (Denny, Gokool, Russell, Field, & Smith, 2000; Nickel, 2003). Annexins, for example, have been shown to translocate across the membrane depending on bilateral lipid movements (Stewart, Ashkenazi, Williamson, Rubinsztein, & Moreau, 2018).

Our experiments demonstrated a drop in pH inside EVs exposed to low pH, strongly suggesting that when EVs pass through late endosomes, Alix inside EVs is exposed to low pH. This may lead to the recruitment of Alix to the EV membrane and possibly translocation. To test this, we conducted a range of experimental techniques, using Immunoprecipitation, Nanolucifrase, and Protein protection assay. However, we have not been able to demonstrate Alix translocation at low pH. It is important to recognize the limitations faced in all experiments. The low efficiency

of the immunoprecipitation technique may have affected the detection of translocated protein. In the case of the luminescence assay, our approach involved overexpressing Alix, which did not display the expected topology within EVs, since it was present both inside and outside of EVs, contrary to endogenous Alix, which was only found inside. These results reveal that it is important to be cautious when using overexpressed Alix-containing EVs, since it may not accurately represent the endogenous Alix behavior and localization.

In the proteinase K protection assay, all examined proteins, including Alix, showed a decrease in abundance in EVs exposed to pH 5.5. The fact that PK did not noticeably decrease the amount of proteins demonstrates that this decrease concerns proteins inside EVs. Such a decrease might be due to the activation of proteases inside EVs which become active at acidic pH. This possibility was further suggested by the fact that a similar reduction in protein levels was observed despite the addition of protease inhibitors, which are membrane impermeable.

Moreover, our study confirmed the intact integrity of EVs' membrane under acidic pH and in the presence of PK using Cryo-EM microscopy. The only observed difference in the aspect of EVs at pH 5.5 was the presence of dark densities suggests that there might be alterations in the protein composition and interactions within the EV membrane at the acidic pH environment, which is recommended for additional quantification using Cryo-EM.

Consequently, it would be interesting to further investigate the protein profile of the EVs under both acidic and neutral pH conditions in order to better understand protein stability and degradation mechanisms within EVs.

Chapter 5 REFERENCES

Abdullah, M., Nakamura, T., Ferdous, T., Gao, Y., Chen, Y., Zou, K., & Michikawa, M. (2021). Cholesterol Regulates Exosome Release in Cultured Astrocytes. *Front Immunol, 12*, 722581. doi:10.3389/fimmu.2021.722581

Abrami, L., Lindsay, M., Parton, R. G., Leppla, S. H., & van der Goot, F. G. (2004). Membrane insertion of anthrax protective antigen and cytoplasmic delivery of lethal factor occur at different stages of the endocytic pathway. *J Cell Biol, 166*(5), 645-651. doi:10.1083/jcb.200312072

Albacete-Albacete, L., Navarro-Lérida, I., López, J. A., Martín-Padura, I., Astudillo, A. M., Ferrarini, A., . . . Del Pozo, M. (2020). ECM deposition is driven by caveolin-1-dependent regulation of exosomal biogenesis and cargo sorting. *J Cell Biol, 219*(11). doi:10.1083/jcb.202006178

Alderson, T. R., Kim, J. H., & Markley, J. L. (2016). Dynamical Structures of Hsp70 and Hsp70-Hsp40 Complexes. *Structure, 24*(7), 1014-1030. doi:10.1016/j.str.2016.05.011

Amara, A., & Mercer, J. (2015). Viral apoptotic mimicry. *Nat Rev Microbiol, 13*(8), 461-469. doi:10.1038/nrmicro3469

Andrews, N. W., Almeida, P. E., & Corrotte, M. (2014). Damage control: cellular mechanisms of plasma membrane repair. *Trends Cell Biol, 24*(12), 734-742. doi:10.1016/j.tcb.2014.07.008

Baietti, M. F., Zhang, Z., Mortier, E., Melchior, A., Degeest, G., Geeraerts, A., . . . David, G. (2012). Syndecan-syntenin-ALIX regulates the biogenesis of exosomes. *Nat Cell Biol, 14*(7), 677-685. doi:10.1038/ncb2502

Barrès, C., Blanc, L., Bette-Bobillo, P., André, S., Mamoun, R., Gabius, H. J., & Vidal, M. (2010). Galectin-5 is bound onto the surface of rat reticulocyte exosomes and modulates vesicle uptake by macrophages. *Blood, 115*(3), 696-705. doi:10.1182/blood-2009-07-231449

Behzadi, S., Serpooshan, V., Tao, W., Hamaly, M. A., Alkawareek, M. Y., Dreaden, E. C., . . . Mahmoudi, M. (2017). Cellular uptake of nanoparticles: journey inside the cell. *Chem Soc Rev, 46*(14), 4218-4244. doi:10.1039/c6cs00636a

Benlimame, N., Le, P. U., & Nabi, I. R. (1998). Localization of autocrine motility factor receptor to caveolae and clathrin-independent internalization of its ligand to smooth endoplasmic reticulum. *Mol Biol Cell, 9*(7), 1773-1786. doi:10.1091/mbc.9.7.1773

Berg, T. O., Fengsrud, M., Strømhaug, P. E., Berg, T., & Seglen, P. O. (1998). Isolation and characterization of rat liver amphisomes. Evidence for fusion of autophagosomes with both early and late endosomes. *J Biol Chem, 273*(34), 21883-21892. doi:10.1074/jbc.273.34.21883

Bissig, C., & Gruenberg, J. (2014). ALIX and the multivesicular endosome: ALIX in Wonderland. *Trends Cell Biol, 24*(1), 19-25. doi:10.1016/j.tcb.2013.10.009

Bissig, C., Lenoir, M., Velluz, M. C., Kufareva, I., Abagyan, R., Overduin, M., & Gruenberg, J. (2013). Viral infection controlled by a calcium-dependent lipid-binding module in ALIX. *Dev Cell, 25*(4), 364-373. doi:10.1016/j.devcel.2013.04.003

Blum, D., Hemming, F. J., Galas, M. C., Torch, S., Cuvelier, L., Schiffmann, S. N., & Sadoul, R. (2004). Increased Alix (apoptosis-linked gene-2 interacting protein X) immunoreactivity in the degenerating striatum of rats chronically treated by 3-nitropropionic acid. *Neurosci Lett, 368*(3), 309-313. doi:10.1016/j.neulet.2004.07.046

Bobrie, A., Colombo, M., Raposo, G., & Théry, C. (2011). Exosome secretion: molecular mechanisms and roles in immune responses. *Traffic, 12*(12), 1659-1668. doi:10.1111/j.1600-0854.2011.01225.x

Bonifacino, J. S., & Glick, B. S. (2004). The mechanisms of vesicle budding and fusion. *Cell, 116*(2), 153-166. doi:10.1016/s0092-8674(03)01079-1

Bonjoch, L., Gironella, M., Iovanna, J. L., & Closa, D. (2017). REG3β modifies cell tumor function by impairing extracellular vesicle uptake. *Sci Rep, 7*(1), 3143. doi:10.1038/s41598-017-03244-4

Bonsergent, E., Grisard, E., Buchrieser, J., Schwartz, O., Théry, C., & Lavieu, G. (2021). Quantitative characterization of extracellular vesicle uptake and content delivery within mammalian cells. *Nat Commun, 12*(1), 1864. doi:10.1038/s41467-021-22126-y

Bonsergent, E., & Lavieu, G. (2019). Content release of extracellular vesicles in a cell-free extract. *FEBS Lett, 593*(15), 1983-1992. doi:10.1002/1873-3468.13472

Booth, A. M., Fang, Y., Fallon, J. K., Yang, J. M., Hildreth, J. E., & Gould, S. J. (2006). Exosomes and HIV Gag bud from endosome-like domains of the T cell plasma membrane. *J Cell Biol, 172*(6), 923-935. doi:10.1083/jcb.200508014

Bröcker, C., Engelbrecht-Vandré, S., & Ungermann, C. (2010). Multisubunit tethering complexes and their role in membrane fusion. *Curr Biol, 20*(21), R943-952. doi:10.1016/j.cub.2010.09.015

Bucci, C., Thomsen, P., Nicoziani, P., McCarthy, J., & van Deurs, B. (2000). Rab7: a key to lysosome biogenesis. *Mol Biol Cell, 11*(2), 467-480. doi:10.1091/mbc.11.2.467

Buckley, C. M., & King, J. S. (2017). Drinking problems: mechanisms of macropinosome formation and maturation. *Febs j, 284*(22), 3778-3790. doi:10.1111/febs.14115

Bui, S., Dancourt, J., & Lavieu, G. (2023). Virus-Free Method to Control and Enhance Extracellular Vesicle Cargo Loading and Delivery. *ACS Appl Bio Mater, 6*(3), 1081-1091. doi:10.1021/acsabm.2c00955

Buschow, S. I., Nolte-'t Hoen, E. N., van Niel, G., Pols, M. S., ten Broeke, T., Lauwen, M., . . . Stoorvogel, W. (2009). MHC II in dendritic cells is targeted to lysosomes or T cell-induced exosomes via distinct multivesicular body pathways. *Traffic, 10*(10), 1528-1542. doi:10.1111/j.1600-0854.2009.00963.x

Butreddy, A., Kommineni, N., & Dudhipala, N. (2021). Exosomes as Naturally Occurring Vehicles for Delivery of Biopharmaceuticals: Insights from Drug Delivery to Clinical Perspectives. *Nanomaterials (Basel), 11*(6). doi:10.3390/nano11061481

Cabezas, A., Bache, K. G., Brech, A., & Stenmark, H. (2005). Alix regulates cortical actin and the spatial distribution of endosomes. *J Cell Sci, 118*(Pt 12), 2625-2635. doi:10.1242/jcs.02382

Calabia-Linares, C., Robles-Valero, J., de la Fuente, H., Perez-Martinez, M., Martín-Cofreces, N., Alfonso-Pérez, M., . . . Veiga, E. (2011). Endosomal clathrin drives actin accumulation at the immunological synapse. *J Cell Sci, 124*(Pt 5), 820-830. doi:10.1242/jcs.078832

Carlton, J. G., Agromayor, M., & Martin-Serrano, J. (2008). Differential requirements for Alix and ESCRT-III in cytokinesis and HIV-1 release. *Proc Natl Acad Sci U S A, 105*(30), 10541-10546. doi:10.1073/pnas.0802008105

Chanda, D., Otoupalova, E., Hough, K. P., Locy, M. L., Bernard, K., Deshane, J. S., . . . Thannickal, V. J. (2019). Fibronectin on the Surface of Extracellular Vesicles Mediates Fibroblast Invasion. *Am J Respir Cell Mol Biol, 60*(3), 279-288. doi:10.1165/rcmb.2018-0062OC

Chatellard-Causse, C., Blot, B., Cristina, N., Torch, S., Missotten, M., & Sadoul, R. (2002). Alix (ALG-2-interacting protein X), a protein involved in apoptosis, binds to endophilins and induces cytoplasmic vacuolization. *J Biol Chem, 277*(32), 29108-29115. doi:10.1074/jbc.M204019200

Chavrier, P., Parton, R. G., Hauri, H. P., Simons, K., & Zerial, M. (1990). Localization of low molecular weight GTP binding proteins to exocytic and endocytic compartments. *Cell, 62*(2), 317-329. doi:10.1016/0092-8674(90)90369-p

Chen, Y., Li, J., Ma, B., Li, N., Wang, S., Sun, Z., . . . Zhao, R. C. (2020). MSC-derived exosomes promote recovery from traumatic brain injury via microglia/macrophages in rat. *Aging (Albany NY), 12*(18), 18274-18296. doi:10.18632/aging.103692

Chivet, M., Hemming, F., Pernet-Gallay, K., Fraboulet, S., & Sadoul, R. (2012). Emerging role of neuronal exosomes in the central nervous system. *Front Physiol, 3*, 145. doi:10.3389/fphys.2012.00145

Chivet, M., Javalet, C., Laulagnier, K., Blot, B., Hemming, F. J., & Sadoul, R. (2014). Exosomes secreted by cortical neurons upon glutamatergic synapse activation specifically interact with neurons. *J Extracell Vesicles, 3*, 24722. doi:10.3402/jev.v3.24722

Christianson, H. C., & Belting, M. (2014). Heparan sulfate proteoglycan as a cell-surface endocytosis receptor. *Matrix Biol, 35*, 51-55. doi:10.1016/j.matbio.2013.10.004

Cocucci, E., Gaudin, R., & Kirchhausen, T. (2014). Dynamin recruitment and membrane scission at the neck of a clathrin-coated pit. *Mol Biol Cell, 25*(22), 3595-3609. doi:10.1091/mbc.E14-07-1240

Colombo, M., Raposo, G., & Théry, C. (2014). Biogenesis, secretion, and intercellular interactions of exosomes and other extracellular vesicles. *Annu Rev Cell Dev Biol, 30*, 255-289. doi:10.1146/annurev-cellbio-101512-122326

Corbeil, D., Santos, M. F., Karbanová, J., Kurth, T., Rappa, G., & Lorico, A. (2020). Uptake and Fate of Extracellular Membrane Vesicles: Nucleoplasmic Reticulum-Associated Late Endosomes as a New Gate to Intercellular Communication. *Cells, 9*(9). doi:10.3390/cells9091931

Cossart, P., & Helenius, A. (2014). Endocytosis of viruses and bacteria. *Cold Spring Harb Perspect Biol, 6*(8). doi:10.1101/cshperspect.a016972

Costafreda, M. I., Abbasi, A., Lu, H., & Kaplan, G. (2020). Exosome mimicry by a HAVCR1-NPC1 pathway of endosomal fusion mediates hepatitis A virus infection. *Nat Microbiol, 5*(9), 1096-1106. doi:10.1038/s41564-020-0740-y

Cox, R. G., Mainou, B. A., Johnson, M., Hastings, A. K., Schuster, J. E., Dermody, T. S., & Williams, J. V. (2015). Human Metapneumovirus Is Capable of Entering Cells by Fusion with Endosomal Membranes. *PLoS Pathog, 11*(12), e1005303. doi:10.1371/journal.ppat.1005303

D'Avino, P. P., Giansanti, M. G., & Petronczki, M. (2015). Cytokinesis in animal cells. *Cold Spring Harb Perspect Biol, 7*(4), a015834. doi:10.1101/cshperspect.a015834

Dawson, G. (2021). Isolation of Lipid Rafts (Detergent-Resistant Microdomains) and Comparison to Extracellular Vesicles (Exosomes). *Methods Mol Biol, 2187*, 99-112. doi:10.1007/978-1-0716-0814-2_6

de Gassart, A., Geminard, C., Fevrier, B., Raposo, G., & Vidal, M. (2003). Lipid raft-associated protein sorting in exosomes. *Blood, 102*(13), 4336-4344. doi:10.1182/blood-2003-03-0871

Deb, A., Gupta, S., & Mazumder, P. B. (2021). Exosomes: A new horizon in modern medicine. *Life Sci, 264*, 118623. doi:10.1016/j.lfs.2020.118623

Dejournett, R. E., Kobayashi, R., Pan, S., Wu, C., Etkin, L. D., Clark, R. B., . . . Kuang, J. (2007). Phosphorylation of the proline-rich domain of Xp95 modulates Xp95 interaction with partner proteins. *Biochem J, 401*(2), 521-531. doi:10.1042/bj20061287

Denny, P. W., Gokool, S., Russell, D. G., Field, M. C., & Smith, D. F. (2000). Acylation-dependent protein export in Leishmania. *J Biol Chem, 275*(15), 11017-11025. doi:10.1074/jbc.275.15.11017

Diaz, A., Zhang, J., Ollwerther, A., Wang, X., & Ahlquist, P. (2015). Host ESCRT proteins are required for bromovirus RNA replication compartment assembly and function. *PLoS Pathog, 11*(3), e1004742. doi:10.1371/journal.ppat.1004742

Dixon, C. L., Mekhail, K., & Fairn, G. D. (2021). Examining the Underappreciated Role of S-Acylated Proteins as Critical Regulators of Phagocytosis and Phagosome Maturation in Macrophages. *Front Immunol, 12*, 659533. doi:10.3389/fimmu.2021.659533

Doherty, G. J., & McMahon, H. T. (2009). Mechanisms of endocytosis. *Annu Rev Biochem, 78*, 857-902. doi:10.1146/annurev.biochem.78.081307.110540

Dolcetti, E., Bruno, A., Guadalupi, L., Rizzo, F. R., Musella, A., Gentile, A., . . . Mandolesi, G. (2020). Emerging Role of Extracellular Vesicles in the Pathophysiology of Multiple Sclerosis. *Int J Mol Sci, 21*(19). doi:10.3390/ijms21197336

Donahue, N. D., Acar, H., & Wilhelm, S. (2019). Concepts of nanoparticle cellular uptake, intracellular trafficking, and kinetics in nanomedicine. *Adv Drug Deliv Rev, 143*, 68-96. doi:10.1016/j.addr.2019.04.008

Donoso-Quezada, J., Ayala-Mar, S., & González-Valdez, J. (2021). The role of lipids in exosome biology and intercellular communication: Function, analytics and applications. *Traffic, 22*(7), 204-220. doi:10.1111/tra.12803

Dores, M. R., Chen, B., Lin, H., Soh, U. J., Paing, M. M., Montagne, W. A., . . . Trejo, J. (2012). ALIX binds a YPX(3)L motif of the GPCR PAR1 and mediates ubiquitin-independent ESCRT-III/MVB sorting. *J Cell Biol, 197*(3), 407-419. doi:10.1083/jcb.201110031

Dores, M. R., Grimsey, N. J., Mendez, F., & Trejo, J. (2016). ALIX Regulates the Ubiquitin-Independent Lysosomal Sorting of the P2Y1 Purinergic Receptor via a YPX3L Motif. *PLoS One, 11*(6), e0157587. doi:10.1371/journal.pone.0157587

Dowlatshahi, D. P., Sandrin, V., Vivona, S., Shaler, T. A., Kaiser, S. E., Melandri, F., . . . Kopito, R. R. (2012). ALIX is a Lys63-specific polyubiquitin binding protein that functions in retrovirus budding. *Dev Cell, 23*(6), 1247-1254. doi:10.1016/j.devcel.2012.10.023

Eden, E. R., Sanchez-Heras, E., Tsapara, A., Sobota, A., Levine, T. P., & Futter, C. E. (2016). Annexin A1 Tethers Membrane Contact Sites that Mediate ER to Endosome Cholesterol Transport. *Dev Cell, 37*(5), 473-483. doi:10.1016/j.devcel.2016.05.005

Edgar, J. R. (2016). Q&A: What are exosomes, exactly? *BMC Biol, 14*, 46. doi:10.1186/s12915-016-0268-z

Eguchi, S., Takefuji, M., Sakaguchi, T., Ishihama, S., Mori, Y., Tsuda, T., . . . Murohara, T. (2019). Cardiomyocytes capture stem cell-derived, anti-apoptotic microRNA-214 via clathrin-mediated endocytosis in acute myocardial infarction. *J Biol Chem, 294*(31), 11665-11674. doi:10.1074/jbc.RA119.007537

Ehrlich, M., Boll, W., Van Oijen, A., Hariharan, R., Chandran, K., Nibert, M. L., & Kirchhausen, T. (2004). Endocytosis by random initiation and stabilization of clathrin-coated pits. *Cell, 118*(5), 591-605. doi:10.1016/j.cell.2004.08.017

El-Sayed, A., & Harashima, H. (2013). Endocytosis of gene delivery vectors: from clathrin-dependent to lipid raft-mediated endocytosis. *Mol Ther, 21*(6), 1118-1130. doi:10.1038/mt.2013.54

Elia, N., Sougrat, R., Spurlin, T. A., Hurley, J. H., & Lippincott-Schwartz, J. (2011). Dynamics of endosomal sorting complex required for transport (ESCRT) machinery during cytokinesis and its role in abscission. *Proc Natl Acad Sci U S A, 108*(12), 4846-4851. doi:10.1073/pnas.1102714108

Elmore, S. (2007). Apoptosis: a review of programmed cell death. *Toxicol Pathol, 35*(4), 495-516. doi:10.1080/01926230701320337

Emam, S. E., Abu Lila, A. S., Elsadek, N. E., Ando, H., Shimizu, T., Okuhira, K., . . . Ishida, T. (2019). Cancer cell-type tropism is one of crucial determinants for the efficient systemic delivery of cancer cell-derived exosomes to tumor tissues. *Eur J Pharm Biopharm, 145*, 27-34. doi:10.1016/j.ejpb.2019.10.005

Emam, S. E., Ando, H., Lila, A. S. A., Shimizu, T., Okuhira, K., Ishima, Y., . . . Ishida, T. (2018). Liposome co-incubation with cancer cells secreted exosomes (extracellular vesicles) with different proteins expressions and different uptake pathways. *Sci Rep, 8*(1), 14493. doi:10.1038/s41598-018-32861-w

Erb, U., Hikel, J., Meyer, S., Ishikawa, H., Worst, T. S., Nitschke, K., . . . Karremann, M. (2020). The Impact of Small Extracellular Vesicles on Lymphoblast Trafficking across the Blood-Cerebrospinal Fluid Barrier In Vitro. *Int J Mol Sci, 21*(15). doi:10.3390/ijms21155491

Escola, J. M., Kleijmeer, M. J., Stoorvogel, W., Griffith, J. M., Yoshie, O., & Geuze, H. J. (1998). Selective enrichment of tetraspan proteins on the internal vesicles of multivesicular endosomes and on

exosomes secreted by human B-lymphocytes. *J Biol Chem, 273*(32), 20121-20127. doi:10.1074/jbc.273.32.20121

Escrevente, C., Keller, S., Altevogt, P., & Costa, J. (2011). Interaction and uptake of exosomes by ovarian cancer cells. *BMC Cancer, 11*, 108. doi:10.1186/1471-2407-11-108

Estadella, I., Pedrós-Gámez, O., Colomer-Molera, M., Bosch, M., Sorkin, A., & Felipe, A. (2020). Endocytosis: A Turnover Mechanism Controlling Ion Channel Function. *Cells, 9*(8). doi:10.3390/cells9081833

Falguières, T., Luyet, P. P., Bissig, C., Scott, C. C., Velluz, M. C., & Gruenberg, J. (2008). In vitro budding of intralumenal vesicles into late endosomes is regulated by Alix and Tsg101. *Mol Biol Cell, 19*(11), 4942-4955. doi:10.1091/mbc.e08-03-0239

Fan, S. J., Kroeger, B., Marie, P. P., Bridges, E. M., Mason, J. D., McCormick, K., . . . Goberdhan, D. C. (2020). Glutamine deprivation alters the origin and function of cancer cell exosomes. *Embo j, 39*(16), e103009. doi:10.15252/embj.2019103009

Feng, D., Zhao, W. L., Ye, Y. Y., Bai, X. C., Liu, R. Q., Chang, L. F., . . . Sui, S. F. (2010). Cellular internalization of exosomes occurs through phagocytosis. *Traffic, 11*(5), 675-687. doi:10.1111/j.1600-0854.2010.01041.x

Ferreira, J. V., da Rosa Soares, A., Ramalho, J., Máximo Carvalho, C., Cardoso, M. H., Pintado, P., . . . Pereira, P. (2022). LAMP2A regulates the loading of proteins into exosomes. *Sci Adv, 8*(12), eabm1140. doi:10.1126/sciadv.abm1140

Filipe, V., Hawe, A., & Jiskoot, W. (2010). Critical evaluation of Nanoparticle Tracking Analysis (NTA) by NanoSight for the measurement of nanoparticles and protein aggregates. *Pharm Res, 27*(5), 796-810. doi:10.1007/s11095-010-0073-2

Foroozandeh, P., & Aziz, A. A. (2018). Insight into Cellular Uptake and Intracellular Trafficking of Nanoparticles. *Nanoscale Res Lett, 13*(1), 339. doi:10.1186/s11671-018-2728-6

Friand, V., David, G., & Zimmermann, P. (2015). Syntenin and syndecan in the biogenesis of exosomes. *Biol Cell, 107*(10), 331-341. doi:10.1111/boc.201500010

Fuller, N., & Rand, R. P. (2001). The influence of lysolipids on the spontaneous curvature and bending elasticity of phospholipid membranes. *Biophys J, 81*(1), 243-254. doi:10.1016/s0006-3495(01)75695-0

Gagescu, R., Demaurex, N., Parton, R. G., Hunziker, W., Huber, L. A., & Gruenberg, J. (2000). The recycling endosome of Madin-Darby canine kidney cells is a mildly acidic compartment rich in raft components. *Mol Biol Cell, 11*(8), 2775-2791. doi:10.1091/mbc.11.8.2775

Gao, Y., Qin, Y., Wan, C., Sun, Y., Meng, J., Huang, J., . . . Yang, K. (2021). Small Extracellular Vesicles: A Novel Avenue for Cancer Management. *Front Oncol, 11*, 638357. doi:10.3389/fonc.2021.638357

Garrus, J. E., von Schwedler, U. K., Pornillos, O. W., Morham, S. G., Zavitz, K. H., Wang, H. E., . . . Sundquist, W. I. (2001). Tsg101 and the vacuolar protein sorting pathway are essential for HIV-1 budding. *Cell, 107*(1), 55-65. doi:10.1016/s0092-8674(01)00506-2

Ge, L., Zhang, N., Li, D., Wu, Y., Wang, H., & Wang, J. (2020). Circulating exosomal small RNAs are promising non-invasive diagnostic biomarkers for gastric cancer. *J Cell Mol Med, 24*(24), 14502-14513. doi:10.1111/jcmm.16077

Geuze, H. J., Slot, J. W., Strous, G. J., Hasilik, A., & von Figura, K. (1985). Possible pathways for lysosomal enzyme delivery. *J Cell Biol, 101*(6), 2253-2262. doi:10.1083/jcb.101.6.2253

Ghossoub, R., Lembo, F., Rubio, A., Gaillard, C. B., Bouchet, J., Vitale, N., . . . Zimmermann, P. (2014). Syntenin-ALIX exosome biogenesis and budding into multivesicular bodies are controlled by ARF6 and PLD2. *Nat Commun, 5*, 3477. doi:10.1038/ncomms4477

Gillooly, D. J., Simonsen, A., & Stenmark, H. (2001). Phosphoinositides and phagocytosis. *J Cell Biol, 155*(1), 15-17. doi:10.1083/jcb.200109001

Gräßel, L., Fast, L. A., Scheffer, K. D., Boukhallouk, F., Spoden, G. A., Tenzer, S., . . . Florin, L. (2016). The CD63-Syntenin-1 Complex Controls Post-Endocytic Trafficking of Oncogenic Human Papillomaviruses. *Sci Rep, 6*, 32337. doi:10.1038/srep32337

Groot, M., & Lee, H. (2020). Sorting Mechanisms for MicroRNAs into Extracellular Vesicles and Their Associated Diseases. *Cells, 9*(4). doi:10.3390/cells9041044

Gross, J. C., Chaudhary, V., Bartscherer, K., & Boutros, M. (2012). Active Wnt proteins are secreted on exosomes. *Nat Cell Biol, 14*(10), 1036-1045. doi:10.1038/ncb2574

Grove, J., & Marsh, M. (2011). The cell biology of receptor-mediated virus entry. *J Cell Biol, 195*(7), 1071-1082. doi:10.1083/jcb.201108131

Gruenberg, J. (2009). Viruses and endosome membrane dynamics. *Curr Opin Cell Biol, 21*(4), 582-588. doi:10.1016/j.ceb.2009.03.008

Gruenberg, J. (2020). Life in the lumen: The multivesicular endosome. *Traffic, 21*(1), 76-93. doi:10.1111/tra.12715

Gruenberg, J., Griffiths, G., & Howell, K. E. (1989). Characterization of the early endosome and putative endocytic carrier vesicles in vivo and with an assay of vesicle fusion in vitro. *J Cell Biol, 108*(4), 1301-1316. doi:10.1083/jcb.108.4.1301

Guduric-Fuchs, J., O'Connor, A., Camp, B., O'Neill, C. L., Medina, R. J., & Simpson, D. A. (2012). Selective extracellular vesicle-mediated export of an overlapping set of microRNAs from multiple cell types. *BMC Genomics, 13*, 357. doi:10.1186/1471-2164-13-357

Guix, F. X., Sannerud, R., Berditchevski, F., Arranz, A. M., Horré, K., Snellinx, A., . . . De Strooper, B. (2017). Tetraspanin 6: a pivotal protein of the multiple vesicular body determining exosome release and lysosomal degradation of amyloid precursor protein fragments. *Mol Neurodegener, 12*(1), 25. doi:10.1186/s13024-017-0165-0

Guizetti, J., Schermelleh, L., Mäntler, J., Maar, S., Poser, I., Leonhardt, H., . . . Gerlich, D. W. (2011). Cortical constriction during abscission involves helices of ESCRT-III-dependent filaments. *Science, 331*(6024), 1616-1620. doi:10.1126/science.1201847

Guo, H., Chitiprolu, M., Roncevic, L., Javalet, C., Hemming, F. J., Trung, M. T., . . . Gibbings, D. (2017). Atg5 Disassociates the V(1)V(0)-ATPase to Promote Exosome Production and Tumor Metastasis Independent of Canonical Macroautophagy. *Dev Cell, 43*(6), 716-730.e717. doi:10.1016/j.devcel.2017.11.018

Guo, H., Sadoul, R., & Gibbings, D. (2018). Autophagy-independent effects of autophagy-related-5 (Atg5) on exosome production and metastasis. *Mol Cell Oncol, 5*(3), e1445941. doi:10.1080/23723556.2018.1445941

Gurung, S., Perocheau, D., Touramanidou, L., & Baruteau, J. (2021). The exosome journey: from biogenesis to uptake and intracellular signalling. *Cell Commun Signal, 19*(1), 47. doi:10.1186/s12964-021-00730-1

Hamzah, R. N., Alghazali, K. M., Biris, A. S., & Griffin, R. J. (2021). Exosome Traceability and Cell Source Dependence on Composition and Cell-Cell Cross Talk. *Int J Mol Sci, 22*(10). doi:10.3390/ijms22105346

Han, Q. F., Li, W. J., Hu, K. S., Gao, J., Zhai, W. L., Yang, J. H., & Zhang, S. J. (2022). Exosome biogenesis: machinery, regulation, and therapeutic implications in cancer. *Mol Cancer, 21*(1), 207. doi:10.1186/s12943-022-01671-0

Hao, S., Bai, O., Li, F., Yuan, J., Laferte, S., & Xiang, J. (2007). Mature dendritic cells pulsed with exosomes stimulate efficient cytotoxic T-lymphocyte responses and antitumour immunity. *Immunology, 120*(1), 90-102. doi:10.1111/j.1365-2567.2006.02483.x

Harding, C., Heuser, J., & Stahl, P. (1983). Receptor-mediated endocytosis of transferrin and recycling of the transferrin receptor in rat reticulocytes. *J Cell Biol, 97*(2), 329-339. doi:10.1083/jcb.97.2.329

Hazan-Halevy, I., Rosenblum, D., Weinstein, S., Bairey, O., Raanani, P., & Peer, D. (2015). Cell-specific uptake of mantle cell lymphoma-derived exosomes by malignant and non-malignant B-lymphocytes. *Cancer Lett, 364*(1), 59-69. doi:10.1016/j.canlet.2015.04.026

Hazawa, M., Tomiyama, K., Saotome-Nakamura, A., Obara, C., Yasuda, T., Gotoh, T., . . . Tajima, K. (2014). Radiation increases the cellular uptake of exosomes through CD29/CD81 complex formation. *Biochem Biophys Res Commun, 446*(4), 1165-1171. doi:10.1016/j.bbrc.2014.03.067

Helenius, A., Kartenbeck, J., Simons, K., & Fries, E. (1980). On the entry of Semliki forest virus into BHK-21 cells. *J Cell Biol, 84*(2), 404-420. doi:10.1083/jcb.84.2.404

Helms, J. B., & Zurzolo, C. (2004). Lipids as targeting signals: lipid rafts and intracellular trafficking. *Traffic, 5*(4), 247-254. doi:10.1111/j.1600-0854.2004.0181.x

Hemler, M. E. (2003). Tetraspanin proteins mediate cellular penetration, invasion, and fusion events and define a novel type of membrane microdomain. *Annu Rev Cell Dev Biol, 19*, 397-422. doi:10.1146/annurev.cellbio.19.111301.153609

Hemming, F. J., Fraboulet, S., Blot, B., & Sadoul, R. (2004). Early increase of apoptosis-linked gene-2 interacting protein X in areas of kainate-induced neurodegeneration. *Neuroscience, 123*(4), 887-895. doi:10.1016/j.neuroscience.2003.10.036

Henley, J. R., Krueger, E. W., Oswald, B. J., & McNiven, M. A. (1998). Dynamin-mediated internalization of caveolae. *J Cell Biol, 141*(1), 85-99. doi:10.1083/jcb.141.1.85

Henne, W. M., Buchkovich, N. J., & Emr, S. D. (2011). The ESCRT pathway. *Dev Cell, 21*(1), 77-91. doi:10.1016/j.devcel.2011.05.015

Hessvik, N. P., & Llorente, A. (2018). Current knowledge on exosome biogenesis and release. *Cell Mol Life Sci, 75*(2), 193-208. doi:10.1007/s00018-017-2595-9

Hessvik, N. P., Øverbye, A., Brech, A., Torgersen, M. L., Jakobsen, I. S., Sandvig, K., & Llorente, A. (2016). PIKfyve inhibition increases exosome release and induces secretory autophagy. *Cell Mol Life Sci, 73*(24), 4717-4737. doi:10.1007/s00018-016-2309-8

Heusermann, W., Hean, J., Trojer, D., Steib, E., von Bueren, S., Graff-Meyer, A., . . . Meisner-Kober, N. C. (2016). Exosomes surf on filopodia to enter cells at endocytic hot spots, traffic within endosomes, and are targeted to the ER. *J Cell Biol, 213*(2), 173-184. doi:10.1083/jcb.201506084

Hikita, T., Kuwahara, A., Watanabe, R., Miyata, M., & Oneyama, C. (2019). Src in endosomal membranes promotes exosome secretion and tumor progression. *Sci Rep, 9*(1), 3265. doi:10.1038/s41598-019-39882-z

Hoshino, A., Costa-Silva, B., Shen, T. L., Rodrigues, G., Hashimoto, A., Tesic Mark, M., . . . Lyden, D. (2015). Tumour exosome integrins determine organotropic metastasis. *Nature, 527*(7578), 329-335. doi:10.1038/nature15756

Hosseini, M., Khatamianfar, S., Hassanian, S. M., Nedaeinia, R., Shafiee, M., Maftouh, M., . . . Avan, A. (2017). Exosome-Encapsulated microRNAs as Potential Circulating Biomarkers in Colon Cancer. *Curr Pharm Des, 23*(11), 1705-1709. doi:10.2174/1381612822666161201144634

Hsu, C., Morohashi, Y., Yoshimura, S., Manrique-Hoyos, N., Jung, S., Lauterbach, M. A., . . . Simons, M. (2010). Regulation of exosome secretion by Rab35 and its GTPase-activating proteins TBC1D10A-C. *J Cell Biol, 189*(2), 223-232. doi:10.1083/jcb.200911018

Hu, M., Li, P., Wang, C., Feng, X., Geng, Q., Chen, W., . . . Xu, H. (2022). Parkinson's disease-risk protein TMEM175 is a proton-activated proton channel in lysosomes. *Cell, 185*(13), 2292-2308.e2220. doi:10.1016/j.cell.2022.05.021

Huotari, J., & Helenius, A. (2011). Endosome maturation. *Embo j, 30*(17), 3481-3500. doi:10.1038/emboj.2011.286

Hurley, J. H., & Emr, S. D. (2006). The ESCRT complexes: structure and mechanism of a membrane-trafficking network. *Annu Rev Biophys Biomol Struct, 35*, 277-298. doi:10.1146/annurev.biophys.35.040405.102126

Hynes, R. O. (2002). Integrins: bidirectional, allosteric signaling machines. *Cell, 110*(6), 673-687. doi:10.1016/s0092-8674(02)00971-6

Iavello, A., Frech, V. S., Gai, C., Deregibus, M. C., Quesenberry, P. J., & Camussi, G. (2016). Role of Alix in miRNA packaging during extracellular vesicle biogenesis. *Int J Mol Med, 37*(4), 958-966. doi:10.3892/ijmm.2016.2488

Im, E. J., Lee, C. H., Moon, P. G., Rangaswamy, G. G., Lee, B., Lee, J. M., . . . Baek, M. C. (2019). Sulfisoxazole inhibits the secretion of small extracellular vesicles by targeting the endothelin receptor A. *Nat Commun, 10*(1), 1387. doi:10.1038/s41467-019-09387-4

Imjeti, N. S., Menck, K., Egea-Jimenez, A. L., Lecointre, C., Lembo, F., Bouguenina, H., . . . Zimmermann, P. (2017). Syntenin mediates SRC function in exosomal cell-to-cell communication. *Proc Natl Acad Sci U S A, 114*(47), 12495-12500. doi:10.1073/pnas.1713433114

Izquierdo-Useros, N., Naranjo-Gómez, M., Archer, J., Hatch, S. C., Erkizia, I., Blanco, J., . . . Martinez-Picado, J. (2009). Capture and transfer of HIV-1 particles by mature dendritic cells converges with the exosome-dissemination pathway. *Blood, 113*(12), 2732-2741. doi:10.1182/blood-2008-05-158642

Jahn, R., & Scheller, R. H. (2006). SNAREs--engines for membrane fusion. *Nat Rev Mol Cell Biol, 7*(9), 631-643. doi:10.1038/nrm2002

Jeppesen, D. K., Fenix, A. M., Franklin, J. L., Higginbotham, J. N., Zhang, Q., Zimmerman, L. J., . . . Coffey, R. J. (2019). Reassessment of Exosome Composition. *Cell, 177*(2), 428-445.e418. doi:10.1016/j.cell.2019.02.029

Jia, S., Zhang, Q., Wang, Y., Wang, Y., Liu, D., He, Y., . . . Yuan, Z. (2021). PIWI-interacting RNA sequencing profiles in maternal plasma-derived exosomes reveal novel non-invasive prenatal biomarkers for the early diagnosis of nonsyndromic cleft lip and palate. *EBioMedicine, 65*, 103253. doi:10.1016/j.ebiom.2021.103253

Jimenez, A. J., Maiuri, P., Lafaurie-Janvore, J., Divoux, S., Piel, M., & Perez, F. (2014). ESCRT machinery is required for plasma membrane repair. *Science, 343*(6174), 1247136. doi:10.1126/science.1247136

Johannes, L., Wunder, C., & Shafaq-Zadah, M. (2016). Glycolipids and Lectins in Endocytic Uptake Processes. *J Mol Biol*. doi:10.1016/j.jmb.2016.10.027

Johannsdottir, H. K., Mancini, R., Kartenbeck, J., Amato, L., & Helenius, A. (2009). Host cell factors and functions involved in vesicular stomatitis virus entry. *J Virol, 83*(1), 440-453. doi:10.1128/jvi.01864-08

Johnson, J. L., He, J., Ramadass, M., Pestonjamasp, K., Kiosses, W. B., Zhang, J., & Catz, S. D. (2016). Munc13-4 Is a Rab11-binding Protein That Regulates Rab11-positive Vesicle Trafficking and Docking at the Plasma Membrane. *J Biol Chem, 291*(7), 3423-3438. doi:10.1074/jbc.M115.705871

Johnstone, R. M., Adam, M., Hammond, J. R., Orr, L., & Turbide, C. (1987). Vesicle formation during reticulocyte maturation. Association of plasma membrane activities with released vesicles (exosomes). *J Biol Chem, 262*(19), 9412-9420.

Joseph, J. G., & Liu, A. P. (2020). Mechanical Regulation of Endocytosis: New Insights and Recent Advances. *Adv Biosyst, 4*(5), e1900278. doi:10.1002/adbi.201900278

Joshi, B. S., de Beer, M. A., Giepmans, B. N. G., & Zuhorn, I. S. (2020). Endocytosis of Extracellular Vesicles and Release of Their Cargo from Endosomes. *ACS Nano, 14*(4), 4444-4455. doi:10.1021/acsnano.9b10033

Joshi, B. S., & Zuhorn, I. S. (2021). Heparan sulfate proteoglycan-mediated dynamin-dependent transport of neural stem cell exosomes in an in vitro blood-brain barrier model. *Eur J Neurosci, 53*(3), 706-719. doi:10.1111/ejn.14974

Ju, Y., Guo, H., Edman, M., & Hamm-Alvarez, S. F. (2020). Application of advances in endocytosis and membrane trafficking to drug delivery. *Adv Drug Deliv Rev, 157*, 118-141. doi:10.1016/j.addr.2020.07.026

Jurgielewicz, B. J., Yao, Y., & Stice, S. L. (2020). Kinetics and Specificity of HEK293T Extracellular Vesicle Uptake using Imaging Flow Cytometry. *Nanoscale Res Lett, 15*(1), 170. doi:10.1186/s11671-020-03399-6

Kadlecova, Z., Spielman, S. J., Loerke, D., Mohanakrishnan, A., Reed, D. K., & Schmid, S. L. (2017). Regulation of clathrin-mediated endocytosis by hierarchical allosteric activation of AP2. *J Cell Biol, 216*(1), 167-179. doi:10.1083/jcb.201608071

Kadry, Y. A., & Calderwood, D. A. (2020). Chapter 22: Structural and signaling functions of integrins. *Biochim Biophys Acta Biomembr, 1862*(5), 183206. doi:10.1016/j.bbamem.2020.183206

Kaksonen, M., & Roux, A. (2018). Mechanisms of clathrin-mediated endocytosis. *Nat Rev Mol Cell Biol, 19*(5), 313-326. doi:10.1038/nrm.2017.132

Kalluri, R., & LeBleu, V. S. (2020). The biology, function, and biomedical applications of exosomes. *Science, 367*(6478). doi:10.1126/science.aau6977

Kashyap, R., Balzano, M., Lechat, B., Lambaerts, K., Egea-Jimenez, A. L., Lembo, F., . . . Zimmermann, P. (2021). Syntenin-knock out reduces exosome turnover and viral transduction. *Sci Rep, 11*(1), 4083. doi:10.1038/s41598-021-81697-4

Kavsan, V. M., Iershov, A. V., & Balynska, O. V. (2011). Immortalized cells and one oncogene in malignant transformation: old insights on new explanation. *BMC Cell Biol, 12*, 23. doi:10.1186/1471-2121-12-23

Kawamoto, T., Ohga, N., Akiyama, K., Hirata, N., Kitahara, S., Maishi, N., . . . Hida, K. (2012). Tumor-derived microvesicles induce proangiogenic phenotype in endothelial cells via endocytosis. *PLoS One, 7*(3), e34045. doi:10.1371/journal.pone.0034045

Kerr, M. C., & Teasdale, R. D. (2009). Defining macropinocytosis. *Traffic, 10*(4), 364-371. doi:10.1111/j.1600-0854.2009.00878.x

Kielian, M. C., & Helenius, A. (1984). Role of cholesterol in fusion of Semliki Forest virus with membranes. *J Virol, 52*(1), 281-283. doi:10.1128/jvi.52.1.281-283.1984

Kielian, M. C., Marsh, M., & Helenius, A. (1986). Kinetics of endosome acidification detected by mutant and wild-type Semliki Forest virus. *Embo j, 5*(12), 3103-3109. doi:10.1002/j.1460-2075.1986.tb04616.x

Kleinfelter, L. M., Jangra, R. K., Jae, L. T., Herbert, A. S., Mittler, E., Stiles, K. M., . . . Chandran, K. (2015). Haploid Genetic Screen Reveals a Profound and Direct Dependence on Cholesterol for Hantavirus Membrane Fusion. *mBio, 6*(4), e00801. doi:10.1128/mBio.00801-15

Kobayashi, T., Beuchat, M. H., Chevallier, J., Makino, A., Mayran, N., Escola, J. M., . . . Gruenberg, J. (2002). Separation and characterization of late endosomal membrane domains. *J Biol Chem, 277*(35), 32157-32164. doi:10.1074/jbc.M202838200

Kobayashi, T., Stang, E., Fang, K. S., de Moerloose, P., Parton, R. G., & Gruenberg, J. (1998). A lipid associated with the antiphospholipid syndrome regulates endosome structure and function. *Nature, 392*(6672), 193-197. doi:10.1038/32440

Kobayashi, T., Vischer, U. M., Rosnoblet, C., Lebrand, C., Lindsay, M., Parton, R. G., . . . Gruenberg, J. (2000). The tetraspanin CD63/lamp3 cycles between endocytic and secretory compartments in human endothelial cells. *Mol Biol Cell, 11*(5), 1829-1843. doi:10.1091/mbc.11.5.1829

Koike, S., & Jahn, R. (2019). SNAREs define targeting specificity of trafficking vesicles by combinatorial interaction with tethering factors. *Nat Commun, 10*(1), 1608. doi:10.1038/s41467-019-09617-9

Koivusalo, M., Jansen, M., Somerharju, P., & Ikonen, E. (2007). Endocytic trafficking of sphingomyelin depends on its acyl chain length. *Mol Biol Cell, 18*(12), 5113-5123. doi:10.1091/mbc.e07-04-0330

Kosaka, N., Iguchi, H., Yoshioka, Y., Takeshita, F., Matsuki, Y., & Ochiya, T. (2010). Secretory mechanisms and intercellular transfer of microRNAs in living cells. *J Biol Chem, 285*(23), 17442-17452. doi:10.1074/jbc.M110.107821

Koumangoye, R. B., Sakwe, A. M., Goodwin, J. S., Patel, T., & Ochieng, J. (2011). Detachment of breast tumor cells induces rapid secretion of exosomes which subsequently mediate cellular adhesion and spreading. *PLoS One, 6*(9), e24234. doi:10.1371/journal.pone.0024234

Krylova, S. V., & Feng, D. (2023). The Machinery of Exosomes: Biogenesis, Release, and Uptake. *Int J Mol Sci, 24*(2). doi:10.3390/ijms24021337

Kumar, A., Sundaram, K., Mu, J., Dryden, G. W., Sriwastva, M. K., Lei, C., . . . Zhang, H. G. (2021). High-fat diet-induced upregulation of exosomal phosphatidylcholine contributes to insulin resistance. *Nat Commun, 12*(1), 213. doi:10.1038/s41467-020-20500-w

Kummer, D., Steinbacher, T., Schwietzer, M. F., Thölmann, S., & Ebnet, K. (2020). Tetraspanins: integrating cell surface receptors to functional microdomains in homeostasis and disease. *Med Microbiol Immunol, 209*(4), 397-405. doi:10.1007/s00430-020-00673-3

Lajoie, P., & Nabi, I. R. (2007). Regulation of raft-dependent endocytosis. *J Cell Mol Med, 11*(4), 644-653. doi:10.1111/j.1582-4934.2007.00083.x

Larios, J., Mercier, V., Roux, A., & Gruenberg, J. (2020). ALIX- and ESCRT-III-dependent sorting of tetraspanins to exosomes. *J Cell Biol, 219*(3). doi:10.1083/jcb.201904113

Latifkar, A., Ling, L., Hingorani, A., Johansen, E., Clement, A., Zhang, X., . . . Antonyak, M. A. (2019). Loss of Sirtuin 1 Alters the Secretome of Breast Cancer Cells by Impairing Lysosomal Integrity. *Dev Cell, 49*(3), 393-408.e397. doi:10.1016/j.devcel.2019.03.011

Latysheva, N., Muratov, G., Rajesh, S., Padgett, M., Hotchin, N. A., Overduin, M., & Berditchevski, F. (2006). Syntenin-1 is a new component of tetraspanin-enriched microdomains: mechanisms and consequences of the interaction of syntenin-1 with CD63. *Mol Cell Biol, 26*(20), 7707-7718. doi:10.1128/mcb.00849-06

Le Blanc, I., Luyet, P. P., Pons, V., Ferguson, C., Emans, N., Petiot, A., . . . Gruenberg, J. (2005). Endosome-to-cytosol transport of viral nucleocapsids. *Nat Cell Biol, 7*(7), 653-664. doi:10.1038/ncb1269

Levin, R., Grinstein, S., & Canton, J. (2016). The life cycle of phagosomes: formation, maturation, and resolution. *Immunol Rev, 273*(1), 156-179. doi:10.1111/imr.12439

Li, B., Antonyak, M. A., Zhang, J., & Cerione, R. A. (2012). RhoA triggers a specific signaling pathway that generates transforming microvesicles in cancer cells. *Oncogene, 31*(45), 4740-4749. doi:10.1038/onc.2011.636

Li, H., Pinilla-Macua, I., Ouyang, Y., Sadovsky, E., Kajiwara, K., Sorkin, A., & Sadovsky, Y. (2020). Internalization of trophoblastic small extracellular vesicles and detection of their miRNA cargo in P-bodies. *J Extracell Vesicles, 9*(1), 1812261. doi:10.1080/20013078.2020.1812261

Li, J., Chen, X., Yi, J., Liu, Y., Li, D., Wang, J., . . . Zhang, Y. (2016). Identification and Characterization of 293T Cell-Derived Exosomes by Profiling the Protein, mRNA and MicroRNA Components. *PLoS One, 11*(9), e0163043. doi:10.1371/journal.pone.0163043

Li, X., Chen, R., Kemper, S., & Brigstock, D. R. (2021). Structural and Functional Characterization of Fibronectin in Extracellular Vesicles From Hepatocytes. *Front Cell Dev Biol, 9*, 640667. doi:10.3389/fcell.2021.640667

Lim, J. P., & Gleeson, P. A. (2011). Macropinocytosis: an endocytic pathway for internalising large gulps. *Immunol Cell Biol, 89*(8), 836-843. doi:10.1038/icb.2011.20

Lim, J. P., Gosavi, P., Mintern, J. D., Ross, E. M., & Gleeson, P. A. (2015). Sorting nexin 5 selectively regulates dorsal-ruffle-mediated macropinocytosis in primary macrophages. *J Cell Sci, 128*(23), 4407-4419. doi:10.1242/jcs.174359

Lima, L. G., Ham, S., Shin, H., Chai, E. P. Z., Lek, E. S. H., Lobb, R. J., . . . Möller, A. (2021). Tumor microenvironmental cytokines bound to cancer exosomes determine uptake by cytokine receptor-expressing cells and biodistribution. *Nat Commun, 12*(1), 3543. doi:10.1038/s41467-021-23946-8

Lin, X. P., Mintern, J. D., & Gleeson, P. A. (2020). Macropinocytosis in Different Cell Types: Similarities and Differences. *Membranes (Basel), 10*(8). doi:10.3390/membranes10080177

Liu, S., Hossinger, A., Heumüller, S. E., Hornberger, A., Buravlova, O., Konstantoulea, K., . . . Vorberg, I. M. (2021). Highly efficient intercellular spreading of protein misfolding mediated by viral ligand-receptor interactions. *Nat Commun, 12*(1), 5739. doi:10.1038/s41467-021-25855-2

Luhtala, N., & Odorizzi, G. (2004). Bro1 coordinates deubiquitination in the multivesicular body pathway by recruiting Doa4 to endosomes. *J Cell Biol, 166*(5), 717-729. doi:10.1083/jcb.200403139

Luo, M., Lewik, G., Ratcliffe, J. C., Choi, C. H. J., Mäkilä, E., Tong, W. Y., & Voelcker, N. H. (2019). Systematic Evaluation of Transferrin-Modified Porous Silicon Nanoparticles for Targeted Delivery of Doxorubicin to Glioblastoma. *ACS Appl Mater Interfaces, 11*(37), 33637-33649. doi:10.1021/acsami.9b10787

Luyet, P. P., Falguières, T., Pons, V., Pattnaik, A. K., & Gruenberg, J. (2008). The ESCRT-I subunit TSG101 controls endosome-to-cytosol release of viral RNA. *Traffic, 9*(12), 2279-2290. doi:10.1111/j.1600-0854.2008.00820.x

Ma, S., Mangala, L. S., Hu, W., Bayaktar, E., Yokoi, A., Hu, W., . . . Sood, A. K. (2021). CD63-mediated cloaking of VEGF in small extracellular vesicles contributes to anti-VEGF therapy resistance. *Cell Rep, 36*(7), 109549. doi:10.1016/j.celrep.2021.109549

Macia, E., Ehrlich, M., Massol, R., Boucrot, E., Brunner, C., & Kirchhausen, T. (2006). Dynasore, a cell-permeable inhibitor of dynamin. *Dev Cell, 10*(6), 839-850. doi:10.1016/j.devcel.2006.04.002

Mahul-Mellier, A. L., Strappazzon, F., Petiot, A., Chatellard-Causse, C., Torch, S., Blot, B., . . . Sadoul, R. (2008). Alix and ALG-2 are involved in tumor necrosis factor receptor 1-induced cell death. *J Biol Chem, 283*(50), 34954-34965. doi:10.1074/jbc.M803140200

Majumder, P., & Chakrabarti, O. (2015). Mahogunin regulates fusion between amphisomes/MVBs and lysosomes via ubiquitination of TSG101. *Cell Death Dis, 6*(11), e1970. doi:10.1038/cddis.2015.257

Marshansky, V., & Futai, M. (2008). The V-type H+-ATPase in vesicular trafficking: targeting, regulation and function. *Curr Opin Cell Biol, 20*(4), 415-426. doi:10.1016/j.ceb.2008.03.015

Martín-Cófreces, N. B., Baixauli, F., & Sánchez-Madrid, F. (2014). Immune synapse: conductor of orchestrated organelle movement. *Trends Cell Biol, 24*(1), 61-72. doi:10.1016/j.tcb.2013.09.005

Martin-Serrano, J., Yarovoy, A., Perez-Caballero, D., & Bieniasz, P. D. (2003). Divergent retroviral late-budding domains recruit vacuolar protein sorting factors by using alternative adaptor proteins. *Proc Natl Acad Sci U S A, 100*(21), 12414-12419. doi:10.1073/pnas.2133846100

Más, V., & Melero, J. A. (2013). Entry of enveloped viruses into host cells: membrane fusion. *Subcell Biochem, 68*, 467-487. doi:10.1007/978-94-007-6552-8_16

Masola, V., Zaza, G., Gambaro, G., Franchi, M., & Onisto, M. (2020). Role of heparanase in tumor progression: Molecular aspects and therapeutic options. *Semin Cancer Biol, 62*, 86-98. doi:10.1016/j.semcancer.2019.07.014

Mathew, A., Bell, A., & Johnstone, R. M. (1995). Hsp-70 is closely associated with the transferrin receptor in exosomes from maturing reticulocytes. *Biochem J, 308 (Pt 3)*(Pt 3), 823-830. doi:10.1042/bj3080823

Mathieu, M., Martin-Jaular, L., Lavieu, G., & Théry, C. (2019). Specificities of secretion and uptake of exosomes and other extracellular vesicles for cell-to-cell communication. *Nat Cell Biol, 21*(1), 9-17. doi:10.1038/s41556-018-0250-9

Mathieu, M., Névo, N., Jouve, M., Valenzuela, J. I., Maurin, M., Verweij, F. J., . . . Théry, C. (2021). Specificities of exosome versus small ectosome secretion revealed by live intracellular tracking of CD63 and CD9. *Nat Commun, 12*(1), 4389. doi:10.1038/s41467-021-24384-2

Matlin, K. S., Reggio, H., Helenius, A., & Simons, K. (1982). Pathway of vesicular stomatitis virus entry leading to infection. *J Mol Biol, 156*(3), 609-631. doi:10.1016/0022-2836(82)90269-8

Matos, P. M., Marin, M., Ahn, B., Lam, W., Santos, N. C., & Melikyan, G. B. (2013). Anionic lipids are required for vesicular stomatitis virus G protein-mediated single particle fusion with supported lipid bilayers. *J Biol Chem, 288*(18), 12416-12425. doi:10.1074/jbc.M113.462028

Matsuo, H., Chevallier, J., Mayran, N., Le Blanc, I., Ferguson, C., Fauré, J., . . . Gruenberg, J. (2004). Role of LBPA and Alix in multivesicular liposome formation and endosome organization. *Science, 303*(5657), 531-534. doi:10.1126/science.1092425

Maxfield, F. R., & Yamashiro, D. J. (1987). Endosome acidification and the pathways of receptor-mediated endocytosis. *Adv Exp Med Biol, 225*, 189-198. doi:10.1007/978-1-4684-5442-0_16

Mazumdar, S., Chitkara, D., & Mittal, A. (2021). Exploration and insights into the cellular internalization and intracellular fate of amphiphilic polymeric nanocarriers. *Acta Pharm Sin B, 11*(4), 903-924. doi:10.1016/j.apsb.2021.02.019

McConnell, R. E., Higginbotham, J. N., Shifrin, D. A., Jr., Tabb, D. L., Coffey, R. J., & Tyska, M. J. (2009). The enterocyte microvillus is a vesicle-generating organelle. *J Cell Biol, 185*(7), 1285-1298. doi:10.1083/jcb.200902147

Meher, G., & Chakraborty, H. (2019). Membrane Composition Modulates Fusion by Altering Membrane Properties and Fusion Peptide Structure. *J Membr Biol, 252*(4-5), 261-272. doi:10.1007/s00232-019-00064-7

Mehul, B., & Hughes, R. C. (1997). Plasma membrane targetting, vesicular budding and release of galectin 3 from the cytoplasm of mammalian cells during secretion. *J Cell Sci, 110 (Pt 10)*, 1169-1178. doi:10.1242/jcs.110.10.1169

Melo, S. A., Luecke, L. B., Kahlert, C., Fernandez, A. F., Gammon, S. T., Kaye, J., . . . Kalluri, R. (2015). Glypican-1 identifies cancer exosomes and detects early pancreatic cancer. *Nature, 523*(7559), 177-182. doi:10.1038/nature14581

Mercer, J., & Helenius, A. (2012). Gulping rather than sipping: macropinocytosis as a way of virus entry. *Curr Opin Microbiol, 15*(4), 490-499. doi:10.1016/j.mib.2012.05.016

Mercer, J., Schelhaas, M., & Helenius, A. (2010). Virus entry by endocytosis. *Annu Rev Biochem, 79*, 803-833. doi:10.1146/annurev-biochem-060208-104626

Mercier, V., Laporte, M. H., Destaing, O., Blot, B., Blouin, C. M., Pernet-Gallay, K., . . . Sadoul, R. (2016). ALG-2 interacting protein-X (Alix) is essential for clathrin-independent endocytosis and signaling. *Sci Rep, 6*, 26986. doi:10.1038/srep26986

Merrifield, C. J., Perrais, D., & Zenisek, D. (2005). Coupling between clathrin-coated-pit invagination, cortactin recruitment, and membrane scission observed in live cells. *Cell, 121*(4), 593-606. doi:10.1016/j.cell.2005.03.015

Messenger, S. W., Woo, S. S., Sun, Z., & Martin, T. F. J. (2018). A Ca(2+)-stimulated exosome release pathway in cancer cells is regulated by Munc13-4. *J Cell Biol, 217*(8), 2877-2890. doi:10.1083/jcb.201710132

Miaczynska, M., & Stenmark, H. (2008). Mechanisms and functions of endocytosis. *J Cell Biol, 180*(1), 7-11. doi:10.1083/jcb.200711073

Mindell, J. A. (2012). Lysosomal acidification mechanisms. *Annu Rev Physiol, 74*, 69-86. doi:10.1146/annurev-physiol-012110-142317

Missotten, M., Nichols, A., Rieger, K., & Sadoul, R. (1999). Alix, a novel mouse protein undergoing calcium-dependent interaction with the apoptosis-linked-gene 2 (ALG-2) protein. *Cell Death Differ, 6*(2), 124-129. doi:10.1038/sj.cdd.4400456

Miyakawa, K., Jeremiah, S. S., Ohtake, N., Matsunaga, S., Yamaoka, Y., Nishi, M., . . . Ryo, A. (2020). Rapid quantitative screening assay for SARS-CoV-2 neutralizing antibodies using HiBiT-tagged virus-like particles. *J Mol Cell Biol, 12*(12), 987-990. doi:10.1093/jmcb/mjaa047

Miyauchi, K., Kim, Y., Latinovic, O., Morozov, V., & Melikyan, G. B. (2009). HIV enters cells via endocytosis and dynamin-dependent fusion with endosomes. *Cell, 137*(3), 433-444. doi:10.1016/j.cell.2009.02.046

Möbius, W., Ohno-Iwashita, Y., van Donselaar, E. G., Oorschot, V. M., Shimada, Y., Fujimoto, T., . . . Slot, J. W. (2002). Immunoelectron microscopic localization of cholesterol using biotinylated and non-cytolytic perfringolysin O. *J Histochem Cytochem, 50*(1), 43-55. doi:10.1177/002215540205000105

Möbius, W., van Donselaar, E., Ohno-Iwashita, Y., Shimada, Y., Heijnen, H. F., Slot, J. W., & Geuze, H. J. (2003). Recycling compartments and the internal vesicles of multivesicular bodies harbor most of the cholesterol found in the endocytic pathway. *Traffic, 4*(4), 222-231. doi:10.1034/j.1600-0854.2003.00072.x

Montecalvo, A., Larregina, A. T., Shufesky, W. J., Stolz, D. B., Sullivan, M. L., Karlsson, J. M., . . . Morelli, A. E. (2012). Mechanism of transfer of functional microRNAs between mouse dendritic cells via exosomes. *Blood, 119*(3), 756-766. doi:10.1182/blood-2011-02-338004

Morandi, M. I., Busko, P., Ozer-Partuk, E., Khan, S., Zarfati, G., Elbaz-Alon, Y., . . . Avinoam, O. (2022). Extracellular vesicle fusion visualized by cryo-EM. *bioRxiv*, 2022.2003.2028.486013. doi:10.1101/2022.03.28.486013

Morishita, M., Horita, M., Higuchi, A., Marui, M., Katsumi, H., & Yamamoto, A. (2021). Characterizing Different Probiotic-Derived Extracellular Vesicles as a Novel Adjuvant for Immunotherapy. *Mol Pharm, 18*(3), 1080-1092. doi:10.1021/acs.molpharmaceut.0c01011

Morita, E., Sandrin, V., Chung, H. Y., Morham, S. G., Gygi, S. P., Rodesch, C. K., & Sundquist, W. I. (2007). Human ESCRT and ALIX proteins interact with proteins of the midbody and function in cytokinesis. *Embo j, 26*(19), 4215-4227. doi:10.1038/sj.emboj.7601850

Mukherjee, S., Ghosh, R. N., & Maxfield, F. R. (1997). Endocytosis. *Physiol Rev, 77*(3), 759-803. doi:10.1152/physrev.1997.77.3.759

Mulcahy, L. A., Pink, R. C., & Carter, D. R. (2014). Routes and mechanisms of extracellular vesicle uptake. *J Extracell Vesicles, 3*. doi:10.3402/jev.v3.24641

Munich, S., Sobo-Vujanovic, A., Buchser, W. J., Beer-Stolz, D., & Vujanovic, N. L. (2012). Dendritic cell exosomes directly kill tumor cells and activate natural killer cells via TNF superfamily ligands. *Oncoimmunology, 1*(7), 1074-1083. doi:10.4161/onci.20897

Murk, J. L., Stoorvogel, W., Kleijmeer, M. J., & Geuze, H. J. (2002). The plasticity of multivesicular bodies and the regulation of antigen presentation. *Semin Cell Dev Biol, 13*(4), 303-311. doi:10.1016/s1084952102000605

Nabhan, J. F., Hu, R., Oh, R. S., Cohen, S. N., & Lu, Q. (2012). Formation and release of arrestin domain-containing protein 1-mediated microvesicles (ARMMs) at plasma membrane by recruitment of TSG101 protein. *Proc Natl Acad Sci U S A, 109*(11), 4146-4151. doi:10.1073/pnas.1200448109

Nguyen, J. A., & Yates, R. M. (2021). Better Together: Current Insights Into Phagosome-Lysosome Fusion. *Front Immunol, 12*, 636078. doi:10.3389/fimmu.2021.636078

Nichols, B. J., Kenworthy, A. K., Polishchuk, R. S., Lodge, R., Roberts, T. H., Hirschberg, K., . . . Lippincott-Schwartz, J. (2001). Rapid cycling of lipid raft markers between the cell surface and Golgi complex. *J Cell Biol, 153*(3), 529-541. doi:10.1083/jcb.153.3.529

Nickel, W. (2003). The mystery of nonclassical protein secretion. A current view on cargo proteins and potential export routes. *Eur J Biochem, 270*(10), 2109-2119. doi:10.1046/j.1432-1033.2003.03577.x

Nieva, J. L., Bron, R., Corver, J., & Wilschut, J. (1994). Membrane fusion of Semliki Forest virus requires sphingolipids in the target membrane. *Embo j, 13*(12), 2797-2804. doi:10.1002/j.1460-2075.1994.tb06573.x

Nolte, M. A., Nolte-'t Hoen, E. N. M., & Margadant, C. (2021). Integrins Control Vesicular Trafficking; New Tricks for Old Dogs. *Trends Biochem Sci, 46*(2), 124-137. doi:10.1016/j.tibs.2020.09.001

O'Dea, K. P., Tan, Y. Y., Shah, S., B, V. P., K, C. T., Wilson, M. R., . . . Takata, M. (2020). Monocytes mediate homing of circulating microvesicles to the pulmonary vasculature during low-grade systemic inflammation. *J Extracell Vesicles, 9*(1), 1706708. doi:10.1080/20013078.2019.1706708

Odorizzi, G. (2006). The multiple personalities of Alix. *J Cell Sci, 119*(Pt 15), 3025-3032. doi:10.1242/jcs.03072

Ostrowski, M., Carmo, N. B., Krumeich, S., Fanget, I., Raposo, G., Savina, A., . . . Thery, C. (2010). Rab27a and Rab27b control different steps of the exosome secretion pathway. *Nat Cell Biol, 12*(1), 19-30; sup pp 11-13. doi:10.1038/ncb2000

Pan, S., Wang, R., Zhou, X., Corvera, J., Kloc, M., Sifers, R., . . . Kuang, J. (2008). Extracellular Alix regulates integrin-mediated cell adhesions and extracellular matrix assembly. *Embo j, 27*(15), 2077-2090. doi:10.1038/emboj.2008.134

Pan, S., Wang, R., Zhou, X., He, G., Koomen, J., Kobayashi, R., . . . Kuang, J. (2006). Involvement of the conserved adaptor protein Alix in actin cytoskeleton assembly. *J Biol Chem, 281*(45), 34640-34650. doi:10.1074/jbc.M602263200

Parolini, I., Federici, C., Raggi, C., Lugini, L., Palleschi, S., De Milito, A., . . . Fais, S. (2009). Microenvironmental pH is a key factor for exosome traffic in tumor cells. *J Biol Chem, 284*(49), 34211-34222. doi:10.1074/jbc.M109.041152

Parton, R. G., McMahon, K. A., & Wu, Y. (2020). Caveolae: Formation, dynamics, and function. *Curr Opin Cell Biol, 65*, 8-16. doi:10.1016/j.ceb.2020.02.001

Peak, T. C., Panigrahi, G. K., Praharaj, P. P., Su, Y., Shi, L., Chyr, J., . . . Deep, G. (2020). Syntaxin 6-mediated exosome secretion regulates enzalutamide resistance in prostate cancer. *Mol Carcinog, 59*(1), 62-72. doi:10.1002/mc.23129

Pegtel, D. M., & Gould, S. J. (2019). Exosomes. *Annu Rev Biochem, 88*, 487-514. doi:10.1146/annurev-biochem-013118-111902

Peinado, H., Alečković, M., Lavotshkin, S., Matei, I., Costa-Silva, B., Moreno-Bueno, G., . . . Lyden, D. (2012). Melanoma exosomes educate bone marrow progenitor cells toward a pro-metastatic phenotype through MET. *Nat Med, 18*(6), 883-891. doi:10.1038/nm.2753

Pelkmans, L., Kartenbeck, J., & Helenius, A. (2001). Caveolar endocytosis of simian virus 40 reveals a new two-step vesicular-transport pathway to the ER. *Nat Cell Biol, 3*(5), 473-483. doi:10.1038/35074539

Peng, X., Yang, L., Ma, Y., Li, Y., & Li, H. (2020). Focus on the morphogenesis, fate and the role in tumor progression of multivesicular bodies. *Cell Commun Signal, 18*(1), 122. doi:10.1186/s12964-020-00619-5

Perrin, P., Janssen, L., Janssen, H., van den Broek, B., Voortman, L. M., van Elsland, D., . . . Neefjes, J. (2021). Retrofusion of intralumenal MVB membranes parallels viral infection and coexists with exosome release. *Curr Biol, 31*(17), 3884-3893.e3884. doi:10.1016/j.cub.2021.06.022

Petrany, M. J., & Millay, D. P. (2019). Cell Fusion: Merging Membranes and Making Muscle. *Trends Cell Biol, 29*(12), 964-973. doi:10.1016/j.tcb.2019.09.002

Phuyal, S., Hessvik, N. P., Skotland, T., Sandvig, K., & Llorente, A. (2014). Regulation of exosome release by glycosphingolipids and flotillins. *Febs j, 281*(9), 2214-2227. doi:10.1111/febs.12775

Pilliod, J., Desjardins, A., Pernègre, C., Jamann, H., Larochelle, C., Fon, E. A., & Leclerc, N. (2020). Clearance of intracellular tau protein from neuronal cells via VAMP8-induced secretion. *J Biol Chem, 295*(51), 17827-17841. doi:10.1074/jbc.RA120.013553

Pires, R., Hartlieb, B., Signor, L., Schoehn, G., Lata, S., Roessle, M., . . . Weissenhorn, W. (2009). A crescent-shaped ALIX dimer targets ESCRT-III CHMP4 filaments. *Structure, 17*(6), 843-856. doi:10.1016/j.str.2009.04.007

Plebanek, M. P., Mutharasan, R. K., Volpert, O., Matov, A., Gatlin, J. C., & Thaxton, C. S. (2015). Nanoparticle Targeting and Cholesterol Flux Through Scavenger Receptor Type B-1 Inhibits Cellular Exosome Uptake. *Sci Rep, 5*, 15724. doi:10.1038/srep15724

Polo, S., Sigismund, S., Faretta, M., Guidi, M., Capua, M. R., Bossi, G., . . . Di Fiore, P. P. (2002). A single motif responsible for ubiquitin recognition and monoubiquitination in endocytic proteins. *Nature, 416*(6879), 451-455. doi:10.1038/416451a

Poteryaev, D., Datta, S., Ackema, K., Zerial, M., & Spang, A. (2010). Identification of the switch in early-to-late endosome transition. *Cell, 141*(3), 497-508. doi:10.1016/j.cell.2010.03.011

Radulovic, M., & Stenmark, H. (2018). ESCRTs in membrane sealing. *Biochem Soc Trans, 46*(4), 773-778. doi:10.1042/bst20170435

Raiborg, C., & Stenmark, H. (2009). The ESCRT machinery in endosomal sorting of ubiquitylated membrane proteins. *Nature, 458*(7237), 445-452. doi:10.1038/nature07961

Rana, S., Yue, S., Stadel, D., & Zöller, M. (2012). Toward tailored exosomes: the exosomal tetraspanin web contributes to target cell selection. *Int J Biochem Cell Biol, 44*(9), 1574-1584. doi:10.1016/j.biocel.2012.06.018

Rao, S. K., Huynh, C., Proux-Gillardeaux, V., Galli, T., & Andrews, N. W. (2004). Identification of SNAREs involved in synaptotagmin VII-regulated lysosomal exocytosis. *J Biol Chem, 279*(19), 20471-20479. doi:10.1074/jbc.M400798200

Raposo, G., Nijman, H. W., Stoorvogel, W., Liejendekker, R., Harding, C. V., Melief, C. J., & Geuze, H. J. (1996). B lymphocytes secrete antigen-presenting vesicles. *J Exp Med, 183*(3), 1161-1172. doi:10.1084/jem.183.3.1161

Raposo, G., & Stoorvogel, W. (2013). Extracellular vesicles: exosomes, microvesicles, and friends. *J Cell Biol, 200*(4), 373-383. doi:10.1083/jcb.201211138

Ratajczak, M. Z., & Ratajczak, J. (2020). Extracellular microvesicles/exosomes: discovery, disbelief, acceptance, and the future? *Leukemia, 34*(12), 3126-3135. doi:10.1038/s41375-020-01041-z

Reddy, V. S., Madala, S. K., Trinath, J., & Reddy, G. B. (2018). Extracellular small heat shock proteins: exosomal biogenesis and function. *Cell Stress Chaperones, 23*(3), 441-454. doi:10.1007/s12192-017-0856-z

Ren, H., Elgner, F., Himmelsbach, K., Akhras, S., Jiang, B., Medvedev, R., . . . Hildt, E. (2017). Identification of syntaxin 4 as an essential factor for the hepatitis C virus life cycle. *Eur J Cell Biol, 96*(6), 542-552. doi:10.1016/j.ejcb.2017.06.002

Riazanski, V., Mauleon, G., Lucas, K., Walker, S., Zimnicka, A. M., McGrath, J. L., & Nelson, D. J. (2022). Real time imaging of single extracellular vesicle pH regulation in a microfluidic cross-flow filtration platform. *Commun Biol, 5*(1), 13. doi:10.1038/s42003-021-02965-7

Rieu, S., Géminard, C., Rabesandratana, H., Sainte-Marie, J., & Vidal, M. (2000). Exosomes released during reticulocyte maturation bind to fibronectin via integrin alpha4beta1. *Eur J Biochem, 267*(2), 583-590. doi:10.1046/j.1432-1327.2000.01036.x

Rink, J., Ghigo, E., Kalaidzidis, Y., & Zerial, M. (2005). Rab conversion as a mechanism of progression from early to late endosomes. *Cell, 122*(5), 735-749. doi:10.1016/j.cell.2005.06.043

Roberts-Dalton, H. D., Cocks, A., Falcon-Perez, J. M., Sayers, E. J., Webber, J. P., Watson, P., . . . Jones, A. T. (2017). Fluorescence labelling of extracellular vesicles using a novel thiol-based strategy for quantitative analysis of cellular delivery and intracellular traffic. *Nanoscale, 9*(36), 13693-13706. doi:10.1039/c7nr04128d

Ruiz-Martinez, M., Navarro, A., Marrades, R. M., Viñolas, N., Santasusagna, S., Muñoz, C., . . . Monzo, M. (2016). YKT6 expression, exosome release, and survival in non-small cell lung cancer. *Oncotarget, 7*(32), 51515-51524. doi:10.18632/oncotarget.9862

S, E. L. A., Mäger, I., Breakefield, X. O., & Wood, M. J. (2013). Extracellular vesicles: biology and emerging therapeutic opportunities. *Nat Rev Drug Discov, 12*(5), 347-357. doi:10.1038/nrd3978

Saeed, M. F., Kolokoltsov, A. A., & Davey, R. A. (2006). Novel, rapid assay for measuring entry of diverse enveloped viruses, including HIV and rabies. *J Virol Methods, 135*(2), 143-150. doi:10.1016/j.jviromet.2006.02.011

Sancho-Albero, M., Navascués, N., Mendoza, G., Sebastián, V., Arruebo, M., Martín-Duque, P., & Santamaría, J. (2019). Exosome origin determines cell targeting and the transfer of therapeutic nanoparticles towards target cells. *J Nanobiotechnology, 17*(1), 16. doi:10.1186/s12951-018-0437-z

Sardar, A., Dewangan, N., Panda, B., Bhowmick, D., & Tarafdar, P. K. (2022). Lipid and Lipidation in Membrane Fusion. *J Membr Biol, 255*(6), 691-703. doi:10.1007/s00232-022-00267-5

Scheffer, L. L., Sreetama, S. C., Sharma, N., Medikayala, S., Brown, K. J., Defour, A., & Jaiswal, J. K. (2014). Mechanism of Ca^{2+}-triggered ESCRT assembly and regulation of cell membrane repair. *Nat Commun, 5*, 5646. doi:10.1038/ncomms6646

Schmidt, M. H. H., Chen, B., Randazzo, L. M., & Bogler, O. (2003). SETA/CIN85/Ruk and its binding partner AIP1 associate with diverse cytoskeletal elements, including FAKs, and modulate cell adhesion. *J Cell Sci, 116*(Pt 14), 2845-2855. doi:10.1242/jcs.00522

Schmidt, M. H. H., Dikic, I., & Bögler, O. (2005). Src phosphorylation of Alix/AIP1 modulates its interaction with binding partners and antagonizes its activities. *J Biol Chem, 280*(5), 3414-3425. doi:10.1074/jbc.M409839200

Schmidt, M. H. H., Hoeller, D., Yu, J., Furnari, F. B., Cavenee, W. K., Dikic, I., & Bögler, O. (2004). Alix/AIP1 antagonizes epidermal growth factor receptor downregulation by the Cbl-SETA/CIN85 complex. *Mol Cell Biol, 24*(20), 8981-8993. doi:10.1128/mcb.24.20.8981-8993.2004

Schmidt, O., & Teis, D. (2012). The ESCRT machinery. *Curr Biol, 22*(4), R116-120. doi:10.1016/j.cub.2012.01.028

Schöneberg, J., Lee, I. H., Iwasa, J. H., & Hurley, J. H. (2017). Reverse-topology membrane scission by the ESCRT proteins. *Nat Rev Mol Cell Biol, 18*(1), 5-17. doi:10.1038/nrm.2016.121

Scott, C. C., & Gruenberg, J. (2011). Ion flux and the function of endosomes and lysosomes: pH is just the start: the flux of ions across endosomal membranes influences endosome function not only through regulation of the luminal pH. *Bioessays, 33*(2), 103-110. doi:10.1002/bies.201000108

Scott, C. C., Vacca, F., & Gruenberg, J. (2014). Endosome maturation, transport and functions. *Semin Cell Dev Biol, 31*, 2-10. doi:10.1016/j.semcdb.2014.03.034

Segura, E., Nicco, C., Lombard, B., Véron, P., Raposo, G., Batteux, F., . . . Théry, C. (2005). ICAM-1 on exosomes from mature dendritic cells is critical for efficient naive T-cell priming. *Blood, 106*(1), 216-223. doi:10.1182/blood-2005-01-0220

Sette, P., Dussupt, V., & Bouamr, F. (2012). Identification of the HIV-1 NC binding interface in Alix Bro1 reveals a role for RNA. *J Virol, 86*(21), 11608-11615. doi:10.1128/jvi.01260-12

Shimoda, A., Tahara, Y., Sawada, S. I., Sasaki, Y., & Akiyoshi, K. (2017). Glycan profiling analysis using evanescent-field fluorescence-assisted lectin array: Importance of sugar recognition for cellular uptake of exosomes from mesenchymal stem cells. *Biochem Biophys Res Commun, 491*(3), 701-707. doi:10.1016/j.bbrc.2017.07.126

Shin, E. Y., Soung, N. K., Schwartz, M. A., & Kim, E. G. (2021). Altered endocytosis in cellular senescence. *Ageing Res Rev, 68*, 101332. doi:10.1016/j.arr.2021.101332

Showalter, M. R., Berg, A. L., Nagourney, A., Heil, H., Carraway, K. L., 3rd, & Fiehn, O. (2020). The Emerging and Diverse Roles of Bis(monoacylglycero) Phosphate Lipids in Cellular Physiology and Disease. *Int J Mol Sci, 21*(21). doi:10.3390/ijms21218067

Shukla, S., Larsen, K. P., Ou, C., Rose, K., & Hurley, J. H. (2022). In vitro reconstitution of calcium-dependent recruitment of the human ESCRT machinery in lysosomal membrane repair. *Proc Natl Acad Sci U S A, 119*(35), e2205590119. doi:10.1073/pnas.2205590119

Simpson, R. J., Lim, J. W., Moritz, R. L., & Mathivanan, S. (2009). Exosomes: proteomic insights and diagnostic potential. *Expert Rev Proteomics, 6*(3), 267-283. doi:10.1586/epr.09.17

Skotland, T., Hessvik, N. P., Sandvig, K., & Llorente, A. (2019). Exosomal lipid composition and the role of ether lipids and phosphoinositides in exosome biology. *J Lipid Res, 60*(1), 9-18. doi:10.1194/jlr.R084343

Skryabin, G. O., Komelkov, A. V., Savelyeva, E. E., & Tchevkina, E. M. (2020). Lipid Rafts in Exosome Biogenesis. *Biochemistry (Mosc), 85*(2), 177-191. doi:10.1134/s0006297920020054

Smyth, T. J., Redzic, J. S., Graner, M. W., & Anchordoquy, T. J. (2014). Examination of the specificity of tumor cell derived exosomes with tumor cells in vitro. *Biochim Biophys Acta, 1838*(11), 2954-2965. doi:10.1016/j.bbamem.2014.07.026

Somiya, M., & Kuroda, S. (2021). Real-Time Luminescence Assay for Cytoplasmic Cargo Delivery of Extracellular Vesicles. *Anal Chem, 93*(13), 5612-5620. doi:10.1021/acs.analchem.1c00339

Soubeyran, P., Kowanetz, K., Szymkiewicz, I., Langdon, W. Y., & Dikic, I. (2002). Cbl-CIN85-endophilin complex mediates ligand-induced downregulation of EGF receptors. *Nature, 416*(6877), 183-187. doi:10.1038/416183a

Sparn, C., Meyer, A., Saleppico, R., & Nickel, W. (2022). Unconventional secretion mediated by direct protein self-translocation across the plasma membranes of mammalian cells. *Trends Biochem Sci, 47*(8), 699-709. doi:10.1016/j.tibs.2022.04.001

Stein, J. M., & Luzio, J. P. (1991). Ectocytosis caused by sublytic autologous complement attack on human neutrophils. The sorting of endogenous plasma-membrane proteins and lipids into shed vesicles. *Biochem J, 274 (Pt 2)*(Pt 2), 381-386. doi:10.1042/bj2740381

Stenmark, H. (2009). Rab GTPases as coordinators of vesicle traffic. *Nat Rev Mol Cell Biol, 10*(8), 513-525. doi:10.1038/nrm2728

Stewart, S. E., Ashkenazi, A., Williamson, A., Rubinsztein, D. C., & Moreau, K. (2018). Transbilayer phospholipid movement facilitates the translocation of annexin across membranes. *J Cell Sci, 131*(14). doi:10.1242/jcs.217034

Stow, J. L., Hung, Y., & Wall, A. A. (2020). Macropinocytosis: Insights from immunology and cancer. *Curr Opin Cell Biol, 65*, 131-140. doi:10.1016/j.ceb.2020.06.005

Strack, B., Calistri, A., Craig, S., Popova, E., & Göttlinger, H. G. (2003). AIP1/ALIX is a binding partner for HIV-1 p6 and EIAV p9 functioning in virus budding. *Cell, 114*(6), 689-699. doi:10.1016/s0092-8674(03)00653-6

Strauss, K., Goebel, C., Runz, H., Möbius, W., Weiss, S., Feussner, I., . . . Schneider, A. (2010). Exosome secretion ameliorates lysosomal storage of cholesterol in Niemann-Pick type C disease. *J Biol Chem, 285*(34), 26279-26288. doi:10.1074/jbc.M110.134775

Sundquist, W. I., & Kräusslich, H. G. (2012). HIV-1 assembly, budding, and maturation. *Cold Spring Harb Perspect Med, 2*(7), a006924. doi:10.1101/cshperspect.a006924

Sung, B. H., Parent, C. A., & Weaver, A. M. (2021). Extracellular vesicles: Critical players during cell migration. *Dev Cell, 56*(13), 1861-1874. doi:10.1016/j.devcel.2021.03.020

Sung, P. S., & Hsieh, S. L. (2021). C-type lectins and extracellular vesicles in virus-induced NETosis. *J Biomed Sci, 28*(1), 46. doi:10.1186/s12929-021-00741-7

Sung, P. S., Huang, T. F., & Hsieh, S. L. (2019). Extracellular vesicles from CLEC2-activated platelets enhance dengue virus-induced lethality via CLEC5A/TLR2. *Nat Commun, 10*(1), 2402. doi:10.1038/s41467-019-10360-4

Takahashi, A., Okada, R., Nagao, K., Kawamata, Y., Hanyu, A., Yoshimoto, S., . . . Hara, E. (2017). Exosomes maintain cellular homeostasis by excreting harmful DNA from cells. *Nat Commun, 8*, 15287. doi:10.1038/ncomms15287

Takeuchi, T., Suzuki, M., Fujikake, N., Popiel, H. A., Kikuchi, H., Futaki, S., . . . Nagai, Y. (2015). Intercellular chaperone transmission via exosomes contributes to maintenance of protein homeostasis at the organismal level. *Proc Natl Acad Sci U S A, 112*(19), E2497-2506. doi:10.1073/pnas.1412651112

Tarafdar, P. K., Chakraborty, H., Bruno, M. J., & Lentz, B. R. (2015). Phosphatidylserine-Dependent Catalysis of Stalk and Pore Formation by Synaptobrevin JMR-TMD Peptide. *Biophys J, 109*(9), 1863-1872. doi:10.1016/j.bpj.2015.08.051

Tarasenko, D., & Meinecke, M. (2021). Protein-dependent membrane remodeling in mitochondrial morphology and clathrin-mediated endocytosis. *Eur Biophys J, 50*(2), 295-306. doi:10.1007/s00249-021-01501-z

Teng, Y., Ren, Y., Hu, X., Mu, J., Samykutty, A., Zhuang, X., . . . Zhang, H. G. (2017). MVP-mediated exosomal sorting of miR-193a promotes colon cancer progression. *Nat Commun, 8*, 14448. doi:10.1038/ncomms14448

Théry, C., Boussac, M., Véron, P., Ricciardi-Castagnoli, P., Raposo, G., Garin, J., & Amigorena, S. (2001). Proteomic analysis of dendritic cell-derived exosomes: a secreted subcellular compartment distinct from apoptotic vesicles. *J Immunol, 166*(12), 7309-7318. doi:10.4049/jimmunol.166.12.7309

Tkach, M., Kowal, J., Zucchetti, A. E., Enserink, L., Jouve, M., Lankar, D., . . . Théry, C. (2017). Qualitative differences in T-cell activation by dendritic cell-derived extracellular vesicle subtypes. *Embo j, 36*(20), 3012-3028. doi:10.15252/embj.201696003

Tognoli, M. L., Dancourt, J., Bonsergent, E., Palmulli, R., de Jong, O. G., Van Niel, G., . . . Lavieu, G. (2023). Lack of involvement of CD63 and CD9 tetraspanins in the extracellular vesicle content delivery process. *Commun Biol, 6*(1), 532. doi:10.1038/s42003-023-04911-1

Toribio, V., Morales, S., López-Martín, S., Cardeñes, B., Cabañas, C., & Yáñez-Mó, M. (2019). Development of a quantitative method to measure EV uptake. *Sci Rep, 9*(1), 10522. doi:10.1038/s41598-019-47023-9

Torralba, D., Baixauli, F., Villarroya-Beltri, C., Fernández-Delgado, I., Latorre-Pellicer, A., Acín-Pérez, R., . . . Sánchez-Madrid, F. (2018). Priming of dendritic cells by DNA-containing extracellular vesicles from activated T cells through antigen-driven contacts. *Nat Commun, 9*(1), 2658. doi:10.1038/s41467-018-05077-9

Trajkovic, K., Hsu, C., Chiantia, S., Rajendran, L., Wenzel, D., Wieland, F., . . . Simons, M. (2008). Ceramide triggers budding of exosome vesicles into multivesicular endosomes. *Science, 319*(5867), 1244-1247. doi:10.1126/science.1153124

Trioulier, Y., Torch, S., Blot, B., Cristina, N., Chatellard-Causse, C., Verna, J. M., & Sadoul, R. (2004). Alix, a protein regulating endosomal trafficking, is involved in neuronal death. *J Biol Chem, 279*(3), 2046-2052. doi:10.1074/jbc.M309243200

Tseng, C. C., Dean, S., Davies, B. A., Azmi, I. F., Pashkova, N., Payne, J. A., . . . Katzmann, D. J. (2021). Bro1 stimulates Vps4 to promote intralumenal vesicle formation during multivesicular body biogenesis. *J Cell Biol, 220*(8). doi:10.1083/jcb.202102070

Tu, C., Du, Z., Zhang, H., Feng, Y., Qi, Y., Zheng, Y., . . . Wang, J. (2021). Endocytic pathway inhibition attenuates extracellular vesicle-induced reduction of chemosensitivity to bortezomib in multiple myeloma cells. *Theranostics, 11*(5), 2364-2380. doi:10.7150/thno.47996

Urabe, F., Kosaka, N., Ito, K., Kimura, T., Egawa, S., & Ochiya, T. (2020). Extracellular vesicles as biomarkers and therapeutic targets for cancer. *Am J Physiol Cell Physiol, 318*(1), C29-c39. doi:10.1152/ajpcell.00280.2019

Valadi, H., Ekström, K., Bossios, A., Sjöstrand, M., Lee, J. J., & Lötvall, J. O. (2007). Exosome-mediated transfer of mRNAs and microRNAs is a novel mechanism of genetic exchange between cells. *Nat Cell Biol, 9*(6), 654-659. doi:10.1038/ncb1596

van der Goot, F. G., & Gruenberg, J. (2006). Intra-endosomal membrane traffic. *Trends Cell Biol, 16*(10), 514-521. doi:10.1016/j.tcb.2006.08.003

van Niel, G., Charrin, S., Simoes, S., Romao, M., Rochin, L., Saftig, P., . . . Raposo, G. (2011). The tetraspanin CD63 regulates ESCRT-independent and -dependent endosomal sorting during melanogenesis. *Dev Cell, 21*(4), 708-721. doi:10.1016/j.devcel.2011.08.019

van Niel, G., D'Angelo, G., & Raposo, G. (2018). Shedding light on the cell biology of extracellular vesicles. *Nat Rev Mol Cell Biol, 19*(4), 213-228. doi:10.1038/nrm.2017.125

Vance, J. E. (2015). Phospholipid synthesis and transport in mammalian cells. *Traffic, 16*(1), 1-18. doi:10.1111/tra.12230

Vanessa, L.-R., Cristina, P. R. X., Diana, S., Hugo, O., Yehuda, G. A., Raquel, T. L., & M., H. V. (2019). ALIX protein analysis: storage temperature may impair results. *JMCM, 2*(2), 29-34. doi:10.31083/j.jmcm.2019.02.7161

Varkouhi, A. K., Scholte, M., Storm, G., & Haisma, H. J. (2011). Endosomal escape pathways for delivery of biologicals. *J Control Release, 151*(3), 220-228. doi:10.1016/j.jconrel.2010.11.004

Vietri, M., Radulovic, M., & Stenmark, H. (2020). The many functions of ESCRTs. *Nat Rev Mol Cell Biol, 21*(1), 25-42. doi:10.1038/s41580-019-0177-4

Vito, P., Pellegrini, L., Guiet, C., & D'Adamio, L. (1999). Cloning of AIP1, a novel protein that associates with the apoptosis-linked gene ALG-2 in a Ca2+-dependent reaction. *J Biol Chem, 274*(3), 1533-1540. doi:10.1074/jbc.274.3.1533

Von Bartheld, C. S., & Altick, A. L. (2011). Multivesicular bodies in neurons: distribution, protein content, and trafficking functions. *Prog Neurobiol, 93*(3), 313-340. doi:10.1016/j.pneurobio.2011.01.003

von Kleist, L., Stahlschmidt, W., Bulut, H., Gromova, K., Puchkov, D., Robertson, M. J., . . . Haucke, V. (2011). Role of the clathrin terminal domain in regulating coated pit dynamics revealed by small molecule inhibition. *Cell, 146*(3), 471-484. doi:10.1016/j.cell.2011.06.025

Wang, J., Li, J., Cheng, C., & Liu, S. (2020). Angiotensin-converting enzyme 2 augments the effects of endothelial progenitor cells-exosomes on vascular smooth muscle cell phenotype transition. *Cell Tissue Res, 382*(3), 509-518. doi:10.1007/s00441-020-03259-w

Wang, J. T., Teasdale, R. D., & Liebl, D. (2014). Macropinosome quantitation assay. *MethodsX, 1*, 36-41. doi:10.1016/j.mex.2014.05.002

Wang, Z., Zhu, H., Shi, H., Zhao, H., Gao, R., Weng, X., . . . Ge, J. (2019). Exosomes derived from M1 macrophages aggravate neointimal hyperplasia following carotid artery injuries in mice through miR-222/CDKN1B/CDKN1C pathway. *Cell Death Dis, 10*(6), 422. doi:10.1038/s41419-019-1667-1

Wei, D., Zhan, W., Gao, Y., Huang, L., Gong, R., Wang, W., . . . Kang, T. (2021). RAB31 marks and controls an ESCRT-independent exosome pathway. *Cell Res, 31*(2), 157-177. doi:10.1038/s41422-020-00409-1

Weissenhorn, W., Hinz, A., & Gaudin, Y. (2007). Virus membrane fusion. *FEBS Lett, 581*(11), 2150-2155. doi:10.1016/j.febslet.2007.01.093

White, J., Matlin, K., & Helenius, A. (1981). Cell fusion by Semliki Forest, influenza, and vesicular stomatitis viruses. *J Cell Biol, 89*(3), 674-679. doi:10.1083/jcb.89.3.674

White, J. M., & Whittaker, G. R. (2016). Fusion of Enveloped Viruses in Endosomes. *Traffic, 17*(6), 593-614. doi:10.1111/tra.12389

Whitlock, J. M., & Chernomordik, L. V. (2021). Flagging fusion: Phosphatidylserine signaling in cell-cell fusion. *J Biol Chem, 296*, 100411. doi:10.1016/j.jbc.2021.100411

Willms, E., Johansson, H. J., Mäger, I., Lee, Y., Blomberg, K. E., Sadik, M., . . . Vader, P. (2016). Cells release subpopulations of exosomes with distinct molecular and biological properties. *Sci Rep, 6*, 22519. doi:10.1038/srep22519

Wozniak, A. L., Adams, A., King, K. E., Dunn, W., Christenson, L. K., Hung, W. T., & Weinman, S. A. (2020). The RNA binding protein FMR1 controls selective exosomal miRNA cargo loading during inflammation. *J Cell Biol, 219*(10). doi:10.1083/jcb.201912074

Wozniak, M. A., Modzelewska, K., Kwong, L., & Keely, P. J. (2004). Focal adhesion regulation of cell behavior. *Biochim Biophys Acta, 1692*(2-3), 103-119. doi:10.1016/j.bbamcr.2004.04.007

Wubbolts, R., Leckie, R. S., Veenhuizen, P. T., Schwarzmann, G., Möbius, W., Hoernschemeyer, J., . . . Stoorvogel, W. (2003). Proteomic and biochemical analyses of human B cell-derived exosomes. Potential implications for their function and multivesicular body formation. *J Biol Chem, 278*(13), 10963-10972. doi:10.1074/jbc.M207550200

Xie, F., Zhou, X., Fang, M., Li, H., Su, P., Tu, Y., . . . Zhou, F. (2019). Extracellular Vesicles in Cancer Immune Microenvironment and Cancer Immunotherapy. *Adv Sci (Weinh), 6*(24), 1901779. doi:10.1002/advs.201901779

Xu, J., Wang, Y., Hsu, C. Y., Gao, Y., Meyers, C. A., Chang, L., . . . James, A. W. (2019). Human perivascular stem cell-derived extracellular vesicles mediate bone repair. *Elife, 8*. doi:10.7554/eLife.48191

Xu, W. D., Huang, Q., & Huang, A. F. (2021). Emerging role of galectin family in inflammatory autoimmune diseases. *Autoimmun Rev, 20*(7), 102847. doi:10.1016/j.autrev.2021.102847

Yamada, E. (1955). The fine structure of the gall bladder epithelium of the mouse. *J Biophys Biochem Cytol, 1*(5), 445-458. doi:10.1083/jcb.1.5.445

Yanatori, I., Richardson, D. R., Dhekne, H. S., Toyokuni, S., & Kishi, F. (2021). CD63 is regulated by iron via the IRE-IRP system and is important for ferritin secretion by extracellular vesicles. *Blood, 138*(16), 1490-1503. doi:10.1182/blood.2021010995

Yang, L., Peng, X., Li, Y., Zhang, X., Ma, Y., Wu, C., . . . Liu, J. (2019). Long non-coding RNA HOTAIR promotes exosome secretion by regulating RAB35 and SNAP23 in hepatocellular carcinoma. *Mol Cancer, 18*(1), 78. doi:10.1186/s12943-019-0990-6

Yang, S. T., Kiessling, V., Simmons, J. A., White, J. M., & Tamm, L. K. (2015). HIV gp41-mediated membrane fusion occurs at edges of cholesterol-rich lipid domains. *Nat Chem Biol, 11*(6), 424-431. doi:10.1038/nchembio.1800

Yang, T., Fogarty, B., LaForge, B., Aziz, S., Pham, T., Lai, L., & Bai, S. (2017). Delivery of Small Interfering RNA to Inhibit Vascular Endothelial Growth Factor in Zebrafish Using Natural Brain Endothelia Cell-Secreted Exosome Nanovesicles for the Treatment of Brain Cancer. *Aaps j, 19*(2), 475-486. doi:10.1208/s12248-016-0015-y

Yao, Z., Qiao, Y., Li, X., Chen, J., Ding, J., Bai, L., . . . Yuan, Z. (2018). Exosomes Exploit the Virus Entry Machinery and Pathway To Transmit Alpha Interferon-Induced Antiviral Activity. *J Virol, 92*(24). doi:10.1128/jvi.01578-18

Yokoi, A., Villar-Prados, A., Oliphint, P. A., Zhang, J., Song, X., De Hoff, P., . . . Sood, A. K. (2019). Mechanisms of nuclear content loading to exosomes. *Sci Adv, 5*(11), eaax8849. doi:10.1126/sciadv.aax8849

You, Y., Borgmann, K., Edara, V. V., Stacy, S., Ghorpade, A., & Ikezu, T. (2020). Activated human astrocyte-derived extracellular vesicles modulate neuronal uptake, differentiation and firing. *J Extracell Vesicles, 9*(1), 1706801. doi:10.1080/20013078.2019.1706801

Yuan, D., Zhao, Y., Banks, W. A., Bullock, K. M., Haney, M., Batrakova, E., & Kabanov, A. V. (2017). Macrophage exosomes as natural nanocarriers for protein delivery to inflamed brain. *Biomaterials, 142*, 1-12. doi:10.1016/j.biomaterials.2017.07.011

Zaitseva, E., Yang, S. T., Melikov, K., Pourmal, S., & Chernomordik, L. V. (2010). Dengue virus ensures its fusion in late endosomes using compartment-specific lipids. *PLoS Pathog, 6*(10), e1001131. doi:10.1371/journal.ppat.1001131

Zhan, Q., Yi, K., Li, X., Cui, X., Yang, E., Chen, N., . . . Kang, C. (2021). Phosphatidylcholine-Engineered Exosomes for Enhanced Tumor Cell Uptake and Intracellular Antitumor Drug Delivery. *Macromol Biosci, 21*(8), e2100042. doi:10.1002/mabi.202100042

Zhang, Y., Liu, Y., Liu, H., & Tang, W. H. (2019). Exosomes: biogenesis, biologic function and clinical potential. *Cell Biosci, 9*, 19. doi:10.1186/s13578-019-0282-2

Zhao, Y. G., Codogno, P., & Zhang, H. (2021). Machinery, regulation and pathophysiological implications of autophagosome maturation. *Nat Rev Mol Cell Biol, 22*(11), 733-750. doi:10.1038/s41580-021-00392-4

Zhou, X., Pan, S., Sun, L., Corvera, J., Lee, Y. C., Lin, S. H., & Kuang, J. (2009). The CHMP4b- and Src-docking sites in the Bro1 domain are autoinhibited in the native state of Alix. *Biochem J, 418*(2), 277-284. doi:10.1042/bj20081388